12-2014

DIFFERENTIAL PAX5 LEVELS PROMOTE MCL DISPERSAL AND PROGRESSION AND PREDICT A POOR PROGNOSIS IN ADVANCED MCL PATIENTS

Albert Teo

DIFFERENTIAL PAX5 LEVELS PROMOTE MCL DISPERSAL AND PROGRESSION AND PREDICT A POOR PROGNOSIS IN ADVANCED MCL PATIENTS

by

Albert Eng Keong Teo, B.S.

APPROVED:

_____
Advisory Professor
Nami McCarty, Ph.D.

_____
Zhiqiang An, Ph.D.

_____
R. Eric Davis, M.D.

_____
Shiaw-Yih Lin, Ph.D.

_____
Timothy J. McDonnell, M.D., Ph.D.

APPROVED:

_____
Dean, The University of Texas
Graduate School of Biomedical Sciences at Houston

DIFFERENTIAL PAX5 LEVELS PROMOTE MCL DISPERSAL AND PROGRESSION AND PREDICT A POOR PROGNOSIS IN ADVANCED MCL PATIENTS

A

DISSERTATION

Presented to the Faculty of
The University of Texas
Health Science Center at Houston
and
The University of Texas
MD Anderson Cancer Center
Graduate School of Biomedical Sciences
in Partial Fulfillment

of the Requirements

for the Degree of

DOCTOR OF PHILOSOPHY

By

Albert Eng Keong Teo, B.S.
Houston, Texas

December, 2014

..

Dec 2014

DEDICATION

This dissertational work is dedicated to:

Chris and Im,
parents who always believed in and supported me,
parents who are always proud,
and for being parents who understand.

Noel,
brother, fellow lover of *bola sepak*
and for teaching me that life does not revolve around work.

Irene,
sister, friend and psychologist
who always kept my belly full and an ear open
for her little brother.

AKNOWLEDGEMENTS

I would like to take time and give thanks and appreciation to my mentor Dr. Nami McCarty. I thank her for her willingness in giving me a chance to work in her lab, and for her mentorship over the past two years. For the two years I have been under her tutelage, Dr. McCarty was integral in guiding me as a young researcher. She has thought me on the importance of being more independent, resourceful and, critically, more diligent in scientific planning and experimentation.

Over the six years of graduate school, I have been blessed to be guided by a panel of advisors that were excellent. All provided outstanding scientific support, and were pivotal in molding me into a better scientist. I would like to personally thank Dr. Phoebus Lin; an ever present advisor, who always showed support and was willing to share his knowledge and wisdom with me through my third rotation, qualifiers and defense. A special thanks as well to Dr. Zhiqiang An and Dr. Eric Davis for their time and help through all the committee meetings. Both helped shaped my dissertation project, providing valuable input on experimental methodologies and reasoning. Also special thanks to Dr. Timothy McDonnell, who was my first mentor in the early part of my graduate career. Dr. McDonnell helped forge my nascent career in science, and guided me through my candidacy examination. He has been there from the start, and for that, I thank him.

I would also like to thank Dr. Clifford Stephen and his group for their invaluable assistance in completing the high throughput compound screen at the Center for Translational Cancer Research, Texas A&M Health Science Center Houston. Dr. Stephen, Ms. Mary Sobieski and Goeun Bae showed me the intricacies of a high

throughput screen, and allowed me to be part of every step of the experimental process (I had the experience of using a robot to plate drugs!). I feel this was an experience I significantly benefited from.

I would also like to thank Dr. Roberto Miranda, Sanat David and the MD Anderson Hematopathology Tissue Bank (HTB) for their services in providing relevant clinical samples for the completion of my research. Dr. Miranda was willing to take time out of his busy clinical schedule to meet with me and go over the HTB inventory; discussing and singling out samples that would be beneficial for our study.

Finally, I would be remiss if I did not thank all my former and current lab members – Judy Chen, Eric Pittmann, Jennifer Zhang and Jimmy Lin. All helped the early mornings, long days and late nights go by a bit faster, and their ever presence allowed for a resource to bounce experimental ideas and concerns off.

Differential PAX5 Levels in B Cells Promote MCL Dispersal and Progression and Predict a Poor Prognosis in Advanced MCL Patients.

Albert Eng Keong Teo, B.S.

Advisory Professor: Nami McCarty, Ph.D.

Abstract: Although PAX5 conditional silencing in mice models led to aggressive lymphoma formation, there has been a lack of understanding in the precise functions of PAX5 in human B cell cancers. PAX5 expression is used to diagnose different B cell lymphoma in the clinic including mantle cell lymphoma (MCL), which is one of the most aggressive B cell cancers. PAX5 levels in MCL patients were significantly repressed compared to normal B cells. Surprisingly, we found there were quantitative differences in PAX5 expression levels within MCL patient tissues, which prompted us to silence PAX5 in MCL cell lines to characterize PAX5 functions in MCL disease progression. PAX5 silencing in MCL cells ($PAX5^{-}$) not only increased cell proliferation in vitro and in vivo but also contributed towards retention of quiescent PKH^{+} stem-like cells in xenograft bones. Decreased PAX5 signaling led to deregulation of the cell cycle and increased MCL survival pathways. $PAX5^{-}$ cells also exhibited increased dissemination and adhesion to bone marrow stromal cells. Analyses of clinical MCL cases further revealed that lower PAX5 levels are correlated with MCL dispersal and poorer overall survival in patients. In addition, aggressive blastoid variant MCL demonstrated lower levels of PAX5 compared to non-blastoid types, indicating a decreased PAX5 phenotype promotes MCL dispersal and progression. We also conducted a high

throughput screening (HTS) of 3800 compounds to discover compounds that selectively target the aggressive MCL. The data revealed important properties of PAX5^{-} MCL cells, which are highly drug resistant compared to parental cells. Several novel compounds were discovered through the HTS, which can be new potential therapeutic options for aggressive MCL. Collectively, our data support PAX5 functions as a tumor suppressor-like protein in MCL, and that PAX5 expression can predict advanced MCL patient prognosis.

TABLE OF CONTENTS

LIST OF ILLUSTRATIONS

LIST OF TABLES

RECURRENT ABBREVIATIONS

Pax5	murine PAX5 homolog
PAX5	PAX5 protein
PAX5	PAX5 mRNA
BTZ	Bortezomib
MCL	Mantle Cell Lymphoma
HTS	High Throughput Screen
BM	Bone marrow
CM	Conditioned medium

Chapter 1: GENERAL INTRODUCTION

Mantle Cell Lymphoma

Mantle cell lymphoma (MCL) is categorized as a mature B cell lymphoma of the mantle zone, and was only defined as recently as the 1990s (Banks, Chan et al. 1992, Weisenburger and Armitage 1996). MCL accounts for approximately 6% of all Non-Hodgkin's Lymphomas (NHLs) in the Western world (Zhou, Wang et al. 2008, Sant, Allemani et al. 2010), are heterogeneous tumors that are highly refractory to standard radiation and chemotherapy, contributing to the worst survival rate among NHL patients (Vose 2012). Mantle cell lymphoma has a median diagnoses age of 67, and is typically twice as common in males compared to females (Smedby and Hjalgrim 2011). The median survival of MCL typically ranges from 3-5 years, though current therapy has led to an increase in overall survival (Martin, Chadburn et al. 2008, Herrmann, Hoster et al. 2009).

Pathology of Mantle Cell Lymphoma

A major genomic abnormality in mantle cell lymphoma, which also distinguishes them from low-grade B cell lymphomas, is the t(11:14)(q13:q32) translocation, leading to increased cyclin D1 (CCND1) expression due to the juxtaposition of CCND1 with B-cell IgG heavy chain transcriptional enhancers (Salaverria, Perez-Galan et al. 2006). This increase in CCND1 expression is linked to cell cycle deregulation (Fernandez, Hartmann et al. 2005), and tumor proliferation is the best predictor of survival in MCL (Rosenwald, Wright et al. 2003). Routine use of the Ki-67 cell proliferation index (% of Ki-67-positive lymphomas) in the clinic can serve a strong prognostic factor for overall survival (Tiemann, Schrader et al. 2005).

MCL cells show B cell associated antigens such as CD20, CD79 and the T cell associated antigens CD5. However, MCL cells do not express CD23, a critical receptor for B cell activation and growth (Jares, Colomer et al. 2007). MCL cells bear close topographic and phenotypic similarity to normal CD5-positive B cells, which also colonizes the mantle zone of lymphoid tissue and have the ability to recirculate (Dono, Cerruti et al. 2004).

Mantle Cell Lymphoma Progression and Dissemination

Mantle cell lymphoma is normally disseminated at presentation, with 20% - 30% of patients exhibiting a leukemic (high-grade bone marrow and peripheral blood) compartment (Perez-Galan, Dreyling et al. 2011). MCL has been reported to disseminate to the bone marrow, gastrointestinal tract (GIT), spleen, liver and central nervous system (Campo, Raffeld et al. 1999, Jares, Colomer et al. 2007). MCL xenografts in mice also depict a similar dissemination trend to the bone marrow, spleen, GIT and liver (Wang, Zhang et al. 2008, Chao, Tang et al. 2011, Klanova, Soukup et al. 2014).

Mantle Cell Lymphoma Subtypes

The blastoid variant type of MCL (MCL-BV) is a highly aggressive but a rare form of MCL and demonstrates a worse prognosis than the common forms of MCL (Argatoff, Connors et al. 1997, Bosch, Lopez-Guillermo et al. 1998, Bernard, Gressin et al. 2001). About 17% of diagnosed MCL cases are MCL-BV. MCL-BV has a median survival range of 12-24 months, significantly less than classical MCL (Bosch, López-Guillermo et al. 1998). MCL-BV is also marked with typical t(11:14)(q13:q32) translocation, loss of expression of cell cycle inhibitors (Pinyol, Hernandez et al. 1997) and genomic instability (Ott, Kalla et al. 1998). MCL-BV is often diagnosed at initial

presentation, often with leukemic involvement (Campo, Raffeld et al. 1999). It is rare for classical variants to histologically progress to MCL-BV (Argatoff, Connors et al. 1997).

Such is the heterogeneity of MCL that there have been reports of an indolent form of the disease as well (Nodit, Bahler et al. 2003, Orchard, Garand et al. 2003, Espinet, Sole et al. 2005).

Clinical Management of Mantle Cell Lymphoma

The heterogeneity of mantle cell lymphoma biology poses a significant challenge to define standard therapies (Smith 2011), with frequent disease relapse and progressive resistance reported in the clinic (Dreyling 2011). Complete remission with conventional therapy is achieved in 20 – 80% of cases, but almost all will relapse (Jares, Colomer et al. 2007).

This calls for an approach to understanding the disease biology to better overcome this problem in MCL. For example, the proteasome inhibitor bortezomib has been approved to be used in relapsed MCL patients after a failed first line therapy (Kane, Dagher et al. 2007). Bortezomib functions by disrupting the ubiquitin-proteosome system (Molineaux 2012), thus causing endoplasmic reticulum stress (Pérez-Galán, Mora-Jensen et al. 2011). This occurs due to the accumulation of undegraded poly-ubiquitinated proteins, and apoptosis is induced in MCL through upregulation of Noxa (Perez-Galan, Roue et al. 2006). However, there are reported cases where second line therapy of bortezomib failed to clear the disease (Suh and Goy 2008), hinting to a population of MCL cells that are highly drug resistant. Current use of ibrutinib in the treatment of MCL (Wang, Rule et al. 2013) has improved the outlook of MCL prognosis significantly. However, recent reports (Young and Staudt

2014) suggest that tumor resistance may occur, signifying the need to understand the biology behind this drug resistant cells.

Genomic Deregulation in Mantle Cell Lymphoma

Reciprocal gene translocations involving the immunoglobulin genes are a common pathogenic event in lymphomas (Kuppers 2005). The t(11:14)(q13:q32) translocation observed in MCL leads to increase in CCND1 expression, cell cycle progression and promotes tumorigenesis (Kim and Diehl 2009). It is important to note however, that transgenic mice overexpressing CCND1 in B cells do not develop spontaneous lymphomas, revealing that overexpression of CCND1 by itself is not sufficient to induce MCL and indicating that other genetic pathways are necessary (Bodrug, Warner et al. 1994, Adams, Harris et al. 1999). Often times, gain of CCND1 expression in MCL is synergized with the loss of a tumor suppressor (Bea, Salaverria et al. 2009).

Indeed, MCL exhibit one of the highest degrees of genomic instability in B cell lymphomas (Jares, Colomer et al. 2007) leading to a highly heterogeneous disease. This instability causes loss of tumor suppressor expression or gain in oncogene activation (Bea, Ribas et al. 1999). The origin of this genomic instability is unknown; it is postulated that frequent re-initiation of entry into the S-phase due to CCND1 overexpression leads to chromosomal abnormalities (Kim and Diehl 2009). Chromosomal aberrations of DNA damage checkpoint genes as well as genes related to microtubule dynamics was also discovered in MCL (Vater, Wagner et al. 2009), signifying that loss of some genes might have a compounding effect as a whole due to genome wide effects.

The Paired Box 5 (PAX5) Protein

Paired box 5 (Pax5) belongs to a family of nine PAX transcription factors which play an important role in early mammalian development (Chi and Epstein 2002). Of the PAX proteins, it is the only one expressed within the hematopoietic system. Like other PAX family members, Pax5 has a conserved 'paired' domain, which functions as a bipartite DNA-binding region consisting of N- and C-terminal sub-domains (Czerny, Schaffner et al. 1993). This bipartite domain interacts with degenerate Pax5 consensus-binding DNA sequences, and multiple sequence variants can increase the affinity of one half-site while decreasing affinity at the other half-site (Dorfler and Busslinger 1996). This enables Pax5 to affect a variety of genes, both in an activating or repressive manner (Delogu, Schebesta et al. 2006). This is achieved by recruitment of chromosomal remodeling and basal transcription factor complexes to the target loci (McManus, Ebert et al. 2011).

PAX5 is a B Cell Transcription Factor

Pax5 is a transcription factor that plays central roles in restricting the differentiation of lymphoid progenitors toward the B cell lineage (Hagman and Lukin 2006). Pax5 is expressed throughout B cell development; from the pro-B cell stage, Pax5 is uniformly expressed until it is downregulation during plasma cell differentiation (Barberis, Widenhorn et al. 1990, Adams, Dorfler et al. 1992, Nutt, Heavey et al. 1999, Cobaleda, Schebesta et al. 2007) . Plasma cells and mature B cells differ significantly in their transcriptional program, and Pax5 expression is a key factor in the change. During this physiological down-regulation of Pax5, many Pax5-repressed genes are re-expressed and B cell-specific genes are altered (Mikkola, Heavey et al. 2002, Delogu, Schebesta et al. 2006)

Precursor cells from Pax5 deficient ($Pax5^{-/-}$) mice are blocked at the pro-B cell stage (Mikkola, Heavey et al. 2002), and these cells can differentiate into functional macrophages, granulocytes, dendritic cells, osteoclasts and natural killer cells in vivo (Mikkola, Heavey et al. 2002, Schaniel, Bruno et al. 2002). In vitro, $Pax5^{-/-}$ pro-B cells differentiate into functional T cells in the presence of OP9 stromal cells expressing the Notch ligand Delta-like 1 (DL1) (Hoflinger, Kesavan et al. 2004). These highlights PAX5 function as a master regulator for B cell identity, by fulfilling a dual role of activating B cell specific and concomitantly repressing lineage inappropriate genes (Revilla, Bilic et al. 2012).

PAX5 in B Cell Lymphomas

Despite its established roles as a determinant in normal B cell lineage commitment, how PAX5 regulates development and progression of human B cell cancers is controversial. For example, in some lymphomas PAX5 has been implicated as an oncogene via gain-of-function mutations (Morrison, Jager et al. 1998). These mutations are often fusion mutations that retain DNA-binding specificity, that act in a dominant manner to repress wild type PAX5 function (Kawamata, Pennella et al. 2012, Fortschegger, Anderl et al. 2014).

In contrast, human B-progenitor acute lymphoblastic leukemias contain monoallelic mutations resulting in reduced PAX5 protein expression (Mullighan, Goorha et al. 2007) and a loss of wild type function. This was further corroborated when ablation of the Pax5 gene in mice B cells led to spontaneous B cell malignancies (Cobaleda, Jochum et al. 2007), which supports roles for PAX5 as a potential tumor suppressor. Indeed, recent evidence suggests that PAX5 loss is critical in gain of pluripotency in mature B cells (Hanna, Markoulaki et al. 2008), a trait similar to other

tumor suppressors (Hong, Takahashi et al. 2009). Mechanisms for PAX5 upstream regulation in B cell neoplasms are widely unknown, with PAX5 deregulation often due to genomic instability of cells (Mullighan, Goorha et al. 2007, Nebral, Denk et al. 2008, Familiades, Bousquet et al. 2009, Fortschegger, Anderl et al. 2014). Hence, exact roles for PAX5 in human lymphoma initiation and progression remain enigmatic.

Chapter 2: MATERIALS AND METHODOLOGY

Cell lines and culture conditions

The human mantle cell lymphoma cell lines SP53 and Jeko; human Burkitt's lymphoma cell line Raji; human pre B-cell acute lymphocytic leukemia cell line Reh; human acute T-cell leukemia cell line Jurkat and human embryonic kidney cell line 293FT were obtained from the American Type Culture Collection (Manassas, VA). HS5 bone marrow stromal cells (BMSCs) was a kind gift from Dr. B. Torok-Storb (Fred Hutchinson Cancer Research Center, Seattle, WA). Cells were maintained under standard conditions (5% CO2, 37°C) and cultured in complete RPMI1640 medium (Cellgro, Manassas VA) supplemented with 10% FBS, 2mM L-glutamine, 100≤µg/mL streptomycin and 100 U.I. /mL penicillin.

Human MCL samples

Frozen blood or bone marrow specimens from MCL patients were obtained after informed consent, as approved by MDACC as well as by the University of Texas-Health Science Center Institutional Review Boards. Blood or bone marrow samples from non-malignant donors were also obtained from MDACC. Mononuclear cells were isolated from all primary patient PBMC and normal PBMC using standard Ficoll (Pittsburgh, PA) gradient separation methods.

RNA analysis

Total RNA was extracted using a RNeasy Mini Kit (Qiagen, Valencia, CA) and cDNA synthesized using oligo dT-primers and SuperScript II Reverse Transcriptase (Invitrogen, Carlsbad, CA). cDNA was diluted 1:5 in DEPC-treated water prior to PCR amplification. Primers were designed using NCBI's PrimerBLAST tool kit (http://www.ncbi.nlm.nih.gov/tools/primer-blast/).

Quantitative real time-PCR

qRT-PCR was performed using SYBR Green MasterMix Plus (Qiagen, Valencia, CA) on an ABI-7000 (Applied Biosystems, Foster City, CA) for 40 cycles. 1µL of diluted cDNA template was used in 20µL of reaction volume. β-actin or *GAPDH* expression served as the endogenous control for all qRT results.

Semi-quantitative reverse transcriptase PCR

Semi-quantitative RT-PCR was performed using the Qiagen HotStarTaq (Qiagen, Valencia, CA), and the products viewed on a 1.2% agarose gel. Terminal PCR was carried out on a BioRad thermocycler for 30 cycles, with varying annealing temperatures depending on each primer set. 2µL of diluted cDNA template was used in 20µL of reaction volume. *GAPDH* served as the endogenous control for all RT results.

Lentivirus generation and infection

293FT cells were transfected with either shRNA specific for human PAX5 (Open Biosystem; Oligo ID: V2LHS-135477) or a lentivirus plasmid containing a scramble RNA (controls) or the ORF for human PAX5 (Open biosystem; Oligo ID: PLOHS-100061597). Lentiviruses were then collected 48 hours post transfection followed by infection in the cells using polybrene (9 µg/mL). Media containing lentiviral particles were replaced with complete media 24 hours post infection and the cells were sorted at 96 hours post infection for GFP expression. GFP^+ cells were then selected using increasing amounts of puromycin (4 µg/mL *starting*) or blasticidin (2 µg/mL *starting*) to generate stable cell lines.

PKH staining and analysis

B-cell lymphoma cell lines were stained with the membrane dye PKH26 (Sigma, St. Louis, MO) according to the manufacturer's protocol. Briefly, up to 1 x 10^7 of lymphoma cells were washed in serum free media, then suspended in 1 mL Diluent C and the PKH26 dye were added at a ratio of 1:250. The cells were stained with the dye mixture for 5 minutes at room temperature. The staining process was quenched with addition of 1 volume of 100% serum for 1 minute. The cells were then washed twice with complete medium. PKH staining intensity was measured in multiple ways: using a LSR-II flow cytometer (BD Biosciences, San Jose, CA), an Infinite®M1000 (TECAN, Morrisville, NC) plate reader or using an Eclipse TE200-E (Nikon, Melville, NY) microscope.

Fluorescence-activated cell sorting (FACS) and flow cytometry

Cells were prepared using standard tissue culture protocols and suspended in 2% FBS in PBS on ice before FACS. FACS was performed on a BD FACS Aria II system. Results were analyzed using the provided FACS Diva software.

Apoptosis assay

Cells were checked for apoptosis using the PE-Annexin V and 7-AAD staining kit (BD Pharmingen, San Jose, CA). Cells were stained and promptly run through a LSR-II flow cytometer (BD Biosciences, San Jose, CA) to determine the apoptotic index of cell populations.

Cell cycle analysis

Cells were harvested after cycling for at least 48 hours, and resuspened as single cell suspension. Cells were fixed in cold 70% ethanol, added drop wise to the pellet while vortexing. Cells were fixed on ice for 30 minutes, treated with ribonucleases

(RNAse A) and stained with 300µl propidium iodide (50 µg/ml). When analyzing the cell cycles, cell clumps and duplets were omitted, with only single cells analyzed.

CD45/GFP/PKH26 detection

Cells were stained with anti-CD45-APC (BD Pharmingen, San Jose, CA), or PKH26, and resuspended in FACS wash buffer prior to analysis.

MethoCult™ colony assay

Approximately 5 x 10^3 MCL cells were suspended in 1 mL of complete MethoCult™ medium and plated onto 35mm petri dishes. Colonies were maintained at 37°C with 5% CO_2 and 95% humidity for 7 days. Colonies were counted and scored at day 7 and pictures taken using an Eclipse TE200-E microscope (Nikon, Melville, NY). Only colonies consisting of 50 or more cells were considered for analysis.

In vitro adhesion assay

24-well variant

HS5 human BMSCs were seeded at a density of 5 x 10^4 cells/well in a 24-well plate and allowed to form a monolayer over 48-72 hours. MCL cell lines were stained with the membrane dye PKH26 (Sigma, St. Louis MO) according to the manufacturer's protocol. Cells (5 x 10^5) suspended in 200µL of complete medium were then plated onto the pre-established monolayer of HS5 cells and allowed to adhere for 1 hour at 37°C. After washing with 1 x PBS twice, PKH26 dye intensity was measured using an Infinite®M1000 (TECAN, Morrisville NC) fluorescent plate reader. Wells containing just MCL cells with no wash step served as 100% adhesion controls, while wells containing just the monolayer of HS5 cells served as 0% adhesion controls.

96-well variant

Similar to the 24-well variant, but with HS5 human BMSCs seeded at a density of 1 x 10^4 cells/well in a 96-well plate and allowed to form a monolayer over 24-48 hours. MCL cells (1 x 10^5) suspended in 100µL of complete medium.

Immunoblotting

Whole cell lysates were prepared using RIPA buffer (Boston BioProducts, Ashland, MA) containing phosphatase and protease inhibitors (Sigma, St. Louis, MO). Protein concentration was measured using a Bradford assay kit (Biorad, Hercules, CA) and 5 - 30 µg of whole cell lysate were run through either 10% - 15 % SDS gel. Proteins were transferred to methanol activated PVDF membranes. Membrane blots were blocked in either 5% non-fat milk or 5% animal-free blocker (Vector Labs, Burlingame, CA) and washed with 0.1% Tween-20 in TBS. Primary antibody incubations were done overnight at 4°C, or for two hours at room temperature with a dilution factor of 1:1000 – 1:4000. Secondary antibody incubations were done from 1 – 2 hours, with a dilution factor of 1:2000 – 1:8000. Protein bands were visualized using a HyGLO ECL kit (Denville Scientific, South Plainfield, NJ).

Immunohistochemistry

Tissues were fixed in 2% PFA (paraformaldehyde) in PBS, 30% sucrose before being snap frozen embedded in Optimal Cutting Temperature (OCT) compound prior to being sectioned. Sectioning was done by the IMM Histopathology Service Center (Houston, TX). Slides were stained with anti-CD45-PE (BD Pharmingen, San Jose, CA), for IHC bone marrow analysis. Nuclear staining was done using Draq5, with native GFP from PAX5– MCL being preserved and observed for as well. Slides were analyzed using a Leica TSC SP5 confocal microscope (Buffalo Grove, IL).

Motility assay

Jeko and SP53 cells were stained with the membrane dye PKH26 as described above. 3 x 10^4 cells were suspended in 100 µL complete RPMI1640 were then plated onto empty 96-well plates. Cells were allowed to rest for 2-3 hours at 37°C before having their motions recorded using time lapse microscopy. Time lapse images were acquired with an Andor IXon3 885 EMCCD camera (Andor, Belfast, NIR) on an Olympus IX-81 (Olympus, Center Valley, PA) microscope fitted with a microscope enclosure (Precision Plastics, Rochester, NY) maintained at 37°C with 5% CO2. Images were analyzed using Amira® (FEI Visualization Sciences Group, Burlington, MA) as an analysis tool, with PKH26 labeled cells tracked over a 24 hour window.

NOD/SCID Xenograft assays and tumor evaluation

Immunodeficient NOD/SCID mice were purchased from the Jackson Laboratory (Bar Harbor, ME) and bred and maintained under barrier conditions at the University of Texas Health Science Center. For all in vivo studies, mice were maintained until they exhibited signs of distress that required euthanasia as designated by the protocol.

PKH retention and engraftment assay

Jeko and SP53 PAX5– MCL or control cells were stained with PKH26. PKH labeling was confirmed to be 100% by flow cytometry. The stained cells (1 x 10^6) were transplanted into NOD/SCID mice via intravenous injection (I.V) and mice were sacrificed 48 hours post injection. Cells from the spleen, vascular niche and osteoblastic niche were isolated and collected for analysis as reported. Briefly For our studies, the vascular and osteoblastic niches were combined to form the bone marrow sample.

In vivo intravenous (engraftment) xenograft studies

Jeko and SP53 PAX5– MCL or control cells were injected into NOD/SCID mice via I.V. Mice injected with 1 and 5 x 10^6 cells were sacrificed 8 weeks post injection, with predicted organ dissemination sites collected for analysis. Mice used for survival analysis were injected with 2.5 and 5 x 10^6 cells and monitored every two days post injection for signs of morbidity and tumor burden. Human MCL cell engraftment in various xenograft tissues were analyzed using anti-CD45 staining and GFP by flow cytometry and immunohistochemistry.

In vivo subcutaneous (dissemination) xenograft studies

SP53 cells (3 x 10^6) were injected into the subcutaneous neck fold of NOD/SCID mice and SP53 cells (1.5 x 10^6) via I.V.. Xenografts were sacrificed 6 weeks post injection and PAX5 transcript levels determined from xenograft tumors. Subcutaneous tumor size was determined as previously described (Euhus, Hudd et al. 1986, Tomayko and Reynolds 1989) with tumor volume calculated by the modified ellipsoidal formula: Tumor volume = ½ (length x width^2), where length is the longest longitudinal diameter and width is the greatest transverse diameter.

Use of ^{18}F-FDG was employed to detect dissemination of tumor cells to distant sites. Host mice with subcutaneous xenografts at 4 weeks were injected with ^{18}F-FDG 2.5 hours before being image, sacrificed and having select tissues measured using a γ counter. The results were expressed as a percentage of the injected dose per gram of tissue (%ID/g) relative to muscle controls which served as a baseline for glucose absorption.

CellTiter-Blue® cytotoxicity assay

Cytotoxicity was assessed with Fluorimetric cell viability assay using CellTiter-Blue® (Promega, Madison, WI). Briefly, cells were incubated in 96-well plates for the

indicated times at 37 °C with determined doses of drugs. After the indicated incubation time, 20µl of CellTiter-Blue® reagents was added to suspended cells. Cells were further incubated for 2 – 4 hours at 37 °C. The fluorescent signal was measured at 560Ex/590Em using a fluorescence plate reader equipped with SoftMax Pro software (Molecular Devices, Sunnyvale, CA), and the level of fluorescent resorufin was calculated. Dose-response curves were calculated based on the cell viability assay of cells treated with each chemotherapeutic drug. Cell viability was assessed based on the value of fluorescent signal of live cells with no drug treatments. Viability of drug treated cells was calculated based on a ratio of the fluorescent signal to that of the non-treated control (DMSO). Blank media only readouts were used as baseline controls.

High throughput screening (HTS)

A high-throughput drug screening was carried out in collaboration with Dr. Clifford Stephen from the Center for Translational Cancer Research, Texas A&M University (Houston, TX). PAX5– MCL (Jeko and SP53) and scramble RNA control MCL cells were used to screen chemical compounds from the NCI Oncology/Custom Clinical, Prestwick and NCI libraries, a total of 3864 compounds.

Conditions for the HTS

Prior to the start of the screen, screening conditions (cell growth curve, positive inhibition control and final readout) were optimized to determine the best way to measure the inhibitory effects of the screened compounds. Cells at varying densities and cell numbers were measured over three or four days either by the MTT assays (CellTiterBlue™ Promega, Madison, WI) or by direct imaging of cells stained with nucleic acid (data not shown). Six compounds were selected as positive controls– paclitaxel, anisomysin, CCCP, etoposide, doxorubicin and doxetaxel. Three of the

compounds were analyzed further for consistency in inhibition across all cell lines. Finally, reproducibility assays were conducted with the one positive control (doxorubicin) in order to have a clear distinction between signals (positive controls, positive hits) and noise (negative controls, negative hits) during HTS screening.

Procedure for the HTS

The following screening protocol was used: 2000 cells were suspended in complete RPMI1640 medium (Cellgro, Manassas, VA) containing no penicillin/streptomycin and plated onto 384-well plates (Corning, Corning, NY) using a Multidrop® Combi Dispenser (Thermo Scientific, Waltham, MA). Compound addition to multiwell plates was performed using a Beckman Biomek FX robotic platform (Beckman Coulter, Brea, CA) equipped with a multichannel pod to ensure repeatability from experiment to experiment. Briefly, 50 nL of each compound was diluted into a well containing 50µL of cells, yielding a final 10 µM working concentration for each screened compound. Each assay was repeated twice, with CellTiterBlue® readouts taken using an Infinite®M1000 (TECAN, Morrisville, NC) plate reader.

Compound analysis for the HTS

Data gathered from our HTS of 3864 compounds was analyzed using the following protocol:

Replicates (n=2) were averaged and the mean fluorescent intensity for proliferation for each compound tested was recorded. Any replicate with standard deviations (S.D.)> 20% (meaning a 40% difference in replicates) were omitted from further analysis. The cleaned data set was then analyzed in two different ways:

Overall drug resistance: Compounds with <40% inhibition of our positive control (doxorubicin) was omitted. Differences of less than 5% between control and $PAX5^{-}$

cells were also omitted. Thus, only compounds that inhibited cell proliferation by 40%, and with at least a 5% difference between control and PAX5^{-} cells were recorded for drug resistance statistics.

Significant differences between control and PAX5^{-} cells: Compounds with differences between PAX5^{-} and control cells that are less than the sum of the two S.D. for each cell type were omitted. For example: Compound A with a difference of proliferation of 20% was omitted as the S.D. for the two types of cells were 12% and 18% each. This method of filtering results yielded a robust list of compounds that had proliferative differences that accounted for replication errors.

Doxorubicin- and DMSO-treated cells served as positive and negative controls for cell inhibition respectively. Candidate compounds were chosen using the following criteria: (1) fluorescence level of at least 40% (40% inhibition) of corresponding doxorubicin control samples or (2) a ≥10%- 20% fluorescence level difference between PAX5 knockdown and control cells.

Reagents

Compounds and drugs

The following chemical compounds were used for cell cytotoxicity studies: Bortezomib, doxorubicin and dexamethasone were acquired from the MD Anderson Cancer Center (MDACC) drug repository.

Antibodies

Anti-CD45-APC (BD Pharmingen, San Jose, CA), anti-CD45-PE (BD Pharmingen, San Jose, CA), anti-CD19-PE (BD Pharmingen, San Jose, CA), anti-CD11a-PE (Biolegend, San Diego, CA; HI111), anti-CD18-APC (Biolegend, San Diego, CA; TS1/18) and anti-gp130-APC (R&D Systems, Minneapolis, MN) were used for

FACs analysis. The following antibodies were used for protein blots: anti-phosphop44/42 MAPK (Cell Signaling, Danvers, MA), anti-phosphoAKT (Cell Signaling, Danvers, MA), anti-phosphop38 MAPK (Cell Signaling, Danvers, MA), anti-phosphoSTAT3 (Cell Signaling, Danvers, MA), anti-phosphoSrc family (Cell Signaling, Danvers, MA), anti-PAX5 (AbCam, Cambridge, MA; 3852-1), anti- β-actin (Santa Cruz, Dallas, TX; C4), anti-STAT3 (Santa Cruz, Dallas, TX; K-15), anti-IL6 (Milipore, Billerica, MA), anti IRF4, anti CCND1 (Santa Cruz, Dallas, TX), anti p21 (Milipore, Billerica, MA), anti p27 (Milipore, Billerica, MA), anti p53 (Santa Cruz, Dallas, TX), anti pmTOR (Cell Signaling, Danvers, MA) and anti mTOR (Milipore, Billerica, MA).

HS5 conditioned medium

HS5-conditioned media (HS5-CM) was generated by incubating a monolayer of HS5 cells with fresh complete RPMI1640 medium for 3 days. The aspirated conditioned medium was collected and centrifuged at 2000 rpm for 5 minutes to remove cellular debris, and stored at -80°C. To obtain a working concentration of HS5-CM, collected HS5-CM was diluted 1:1 with complete RPMI1640 medium. Recombinant human IL6 (R&D Systems, Minneapolis, MN) was diluted in complete RPMI1640 medium to yield a working concentration of 5ng – 50ng/μL.

Statistical analysis

Data reported are expressed as experimental mean ± standard deviations. Statistical significance of differences between control and experimental groups was evaluated by the Student t-test, where $p < 0.05$ was considered statistically significant. All experiments and assays were repeated at least twice and performed in duplicate or triplicate.

IC50 determination

IC50 value (the concentration of a drug that is required for 50% inhibition in vitro) was used to indicate the quantitative measure of the different cell killing effect of drugs. The Hill-Slope logistic model is used to calculate IC50 using CompuSyn software (ComboSyn, NJ, USA).

Chapter 3: LOSS OF PAX5 IN MCL CONTRIBUTES TO AN INCREASE IN CELL PROLIFERATION

INTRODUCTION

The exact role of PAX5 in B cell lymphomagenesis is currently unknown. PAX5 expression has been reported to be loss in 30% of B cell acute lymphoblastic leukemia (B-ALL) cancers, with loss of function reported in over expression mutants. PAX5 deregulation in B cell neoplasm is attributed to genomic instability (Mullighan, Goorha et al. 2007). As mantle cell lymphoma (MCL) exhibit a high degree of genomic instability (Jares, Colomer et al. 2007), we sought to investigate if PAX5 expression is altered in MCL. Mantle cell lymphoma is a disease marked with increased tumor burden and cell proliferation. Lymphnode tissue sections of MCL patients often exhibit increased proliferation markers, such as Ki-67, and increased proliferation is often times a marker for overall survival in MCL (Rosenwald, Wright et al. 2003). Since PAX5 has been reported to exhibit properties of a tumor suppressor gene (Cobaleda, Jochum et al. 2007), we decided to examine PAX5's role in mantle cell lymphoma. As previously outlined, MCL cells display a high proliferative index and MCL disease is marked with progressive tumor burden. Here, we examined PAX5's expression in the clinic, possible role in cellular proliferation and tumorigenesis in vitro and in vivo.

RESULTS

PAX5 is downregulated in MCL cell lines and CD19$^+$ cells from MCL patients

To investigate *PAX5* expression in mantle cell lymphoma (MCL), we performed a preliminary screen comparing *PAX5* mRNA expression levels found in normal B cells with that from three primary MCL patients as well as two MCL cell lines, SP53 and Jeko. Two other non-MCL B cell lymphoma cell lines, Raji and Reh were also analyzed

for PAX5 mRNA levels. Jurkat, a T cell lymphoma cell line, does not express *PAX5* mRNA and served as a negative control. *PAX5* mRNA was significantly reduced in all (MCL and non-MCL) B cell cell lines (**Figure 1A**), as well as in 3 MCL primary patient samples (**Figure 1B**). Interestingly, Jeko, a cell line derived from blastoid MCL (Alinari, White et al. 2009), exhibited significantly less *PAX5* than SP53, a classical MCL variant.

To further expand on the clinical relevance of our findings, we determined *PAX5* levels in more MCL patients. PAX5 immunostaining is often used to identify B cells or B cell derived lymphomas in the clinic, however, no studies have quantitatively compared PAX5 levels in distinct cell populations. Moreover, most studies performed used whole tissue biopsy extracts which contain different immune and stromal cells, which make interpretation of these data difficult. We conducted comprehensive *PAX5* level analyses on 39 different primary MCL samples, consisting of 31 peripheral blood and 8 bone marrow biopsies (**Table 1**). *PAX5* expression from MCL samples were compared to peripheral blood or bone marrow from health donors. Analyses were performed in a blind manner without knowledge of the disease prognosis or sites of collection, which were only traced back after completion of the study. In all screens, only $CD19^+$ cells were analyzed, which were isolated by positive selection.

Compared to normal bloods or normal bone marrows, *PAX5* levels in $CD19^+$ cells from MCL patient samples were highly reduced (**Figure 1C and D**), indicating PAX5 play a role as a tumor suppressor-like protein. Further analysis found that *PAX5* expression within MCL patients could be subdivided further into different groups from the same data set (for example, within the peripheral blood data set) suggesting that there potentially exists a differential PAX5 expression gradient in B cell lymphomas.

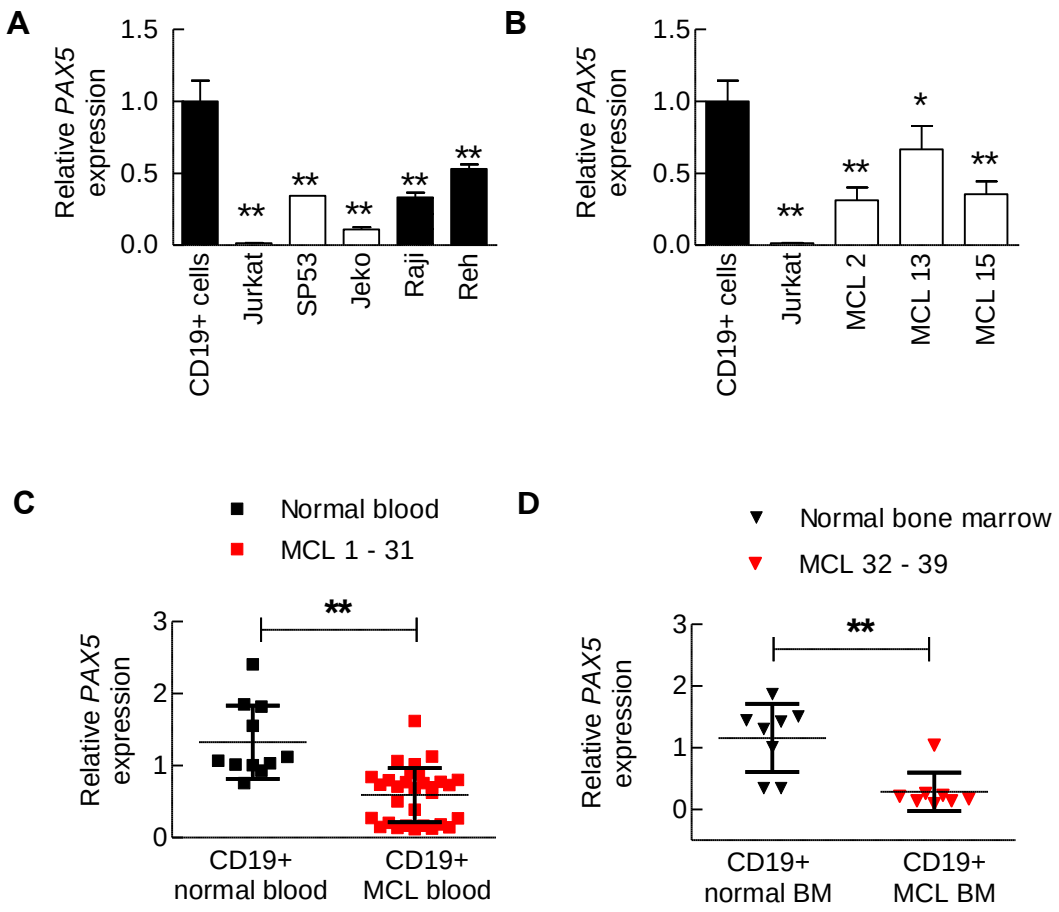

Figure 1: PAX5 is Downregulated in Mantle Cell Lymphoma. qRT-PCR analysis of *PAX5* transcript levels in (A) 2 MCL cell lines, SP53 and Jeko, and 2 non-MCL, B cell tumors, Raji and Reh and (B) 3 $CD19^+$ MCL patient peripheral blood. (C) $CD19^+$ B cells were isolated from MCL blood or apharesis samples (n=31) or normal blood patients (n=10) and (D) $CD19^+$ cells were purified from bone marrows of normal persons (n=8) or MCL patients (n=8) and *PAX5* mRNA levels determined via qRT-PCR. Each replicate was run in triplicate with values normalized to *GAPDH*. * $p < 0.05$ (vs. $PAX5^{control}$; Student's t-test); ** $p < 0.005$ (vs. $PAX5^{control}$; Student's t-test).

Table 1: *PAX5* Analysis: List of 31 MCL Patient Samples. MCL patient samples (n=39) were evaluated for *PAX5* levels. A total of 31 peripheral blood and 8 bone marrow samples were used. All cases were stage IV with extranodal diseases. All data were recorded and collected at the UT MD Anderson Cancer Center.

Patient number	Sex	Age (yr)	Extranodal involvement	Morphologic variant[1]	Treatment status[2]	Tissue collection[3]
MCL1	M	64	Bone marrow, other	Blastoid	Untreated	PB
MCL2	F	64	Bone marrow	Blastoid	Treated	PB
MCL3	M	70	Bone marrow	Blastoid	Untreated	PB
MCL4	F	66	Bone marrow	Blastoid	Untreated	PB
MCL5	M	61	Bone marrow, other	Blastoid	Treated	PB
MCL6	F	83	Bone marrow, other	Blastoid	Treated	PB
MCL7	M	68	Bone marrow, other	Blastoid	Treated	PB
MCL8	M	63	Bone marrow	Blastoid	Treated	PB
MCL9	M	62	Bone marrow	Blastoid	Untreated	PB
MCL10	M	64	Bone marrow	Blastoid	Treated	PB
MCL11	M	53	Bone marrow, other	Blastoid	Treated	PB
MCL12	Unk.	Unk.	Bone marrow, other	Blastoid	Treated	PB
MCL13	M	51	Bone marrow	Classical	Treated	PB
MCL14	M	80	Bone marrow	Classical	Treated	PB
MCL15	M	62	Bone marrow	Classical	Untreated	PB
MCL16	F	70	Bone marrow	Classical	Untreated	PB
MCL17	M	58	Bone marrow	Classical	Untreated	PB
MCL18	M	78	Bone marrow	Classical	Treated	PB
MCL19	M	65	Bone marrow	Classical	Treated	PB
MCL20	M	53	Bone marrow, other	Classical	Treated	PB
MCL21	M	35	Bone marrow, other	Classical	Treated	PB
MCL22	M.	53	Unk.	Classical	Treated	PB
MCL23	Unk.	Unk.	Unk.	Classical	Unk.	PB
MCL24	Unk.	Unk.	Unk.	Classical	Unk.	PB
MCL25	M.	75	Unk.	Classical	Treated	PB
MCL26	Unk.	Unk.	Unk.	Classical	Unk.	PB
MCL27	Unk.	Unk.	Unk.	Classical	Unk.	PB
MCL28	Unk.	Unk.	Unk.	Classical	Unk.	PB
MCL29	Unk.	Unk.	Unk.	Classical	Unk.	PB
MCL30	Unk.	Unk.	Unk.	Classical	Unk.	PB
MCL31	Unk.	Unk.	Unk.	Classical	Unk.	PB
MCL32	M	78	Bone marrow	Classical	Treated	BM
MCL33	M	66	Bone marrow, other	Classical	Treated	BM
MCL34	F	58	Bone marrow	Classical	Treated	BM
MCL35	M	56	Bone marrow	Classical	Untreated	BM
MCL36	M	64	Bone marrow	Classical	Treated	BM
MCL37	M	63	Bone marrow	Classical	Treated	BM
MCL38	M	64	Bone marrow, other	Blastoid	Treated	BM
MCL39	M	66	Bone marrow, other	Classical	Treated	BM

[1] Lymphoma staging verified by MD Anderson pathologist

[2] Treatment status of patients upon sample collection

[3] Cells were isolated from either fresh or previously frozen peripheral blood (PB) and bone marrow (BM)
Unk. (Unknown status), PB (Peripheral Blood), BM (Bone marrow)

This highlights (**Figure 1A and B**), and the possible role differential PAX5 expression have in MCL progression.

Generating a relevant model

Our clinical data suggests that further downregulation of PAX5 could potentially contribute to MCL malignancy. To determine the role of PAX5 function in lymphoma, we used two cell line models stably knock down for PAX5: $PAX5^{-}$ Jeko and $PAX5^{-}$ SP53 MCL cells. Our expression vector contained turbo-GFP and an antibiotic resistance cassette, which could be used to select for GFP^{+} cells (**Figure 2**). Lentiviral transduction of PAX5shRNA ($PAX5^{-}$) efficiently silenced PAX5 expression in GFP^{+} SP53 and Jeko cells (**Figure 3**), while PAX5ORF ($PAX5^{ORF}$) lentiviral infection generated cells overexpressing PAX5 (**Figure 4**).

Next, we analyzed expression of select genes that are known to be regulated by murine Pax5 using qRT-PCR. Approximately 110 genes are normally repressed by Pax5 in murine B cells (Delogu, Schebesta et al. 2006, Pridans, Holmes et al. 2008). Among those genes, about 20 are not expressed in humans. We selected 13 genes from the list which had been previously reported to be involved in either cancer development or hematopoietic stem cell (HSC) biology (**Table 2**). Among these 13 Pax5 repressed genes, 10 genes were significantly upregulated in $PAX5^{-}$ SP53 cells (**Figure 5A**), and 7 out of 13 Pax5 repressed genes were significantly upregulated in $PAX5^{-}$ Jeko cells (**Figure 5A**). These data suggest that PAX5 control a similar gene repertoire both in human and mouse cells which could contribute to uncontrolled MCL cell proliferation and ‘stem-like’ maintenance.

Additionally, CD47 has been reported to be repressed by PAX5 (Delogu, Schebesta et al. 2006, Pridans, Holmes et al. 2008). CD47 acts as a “do not eat signal”

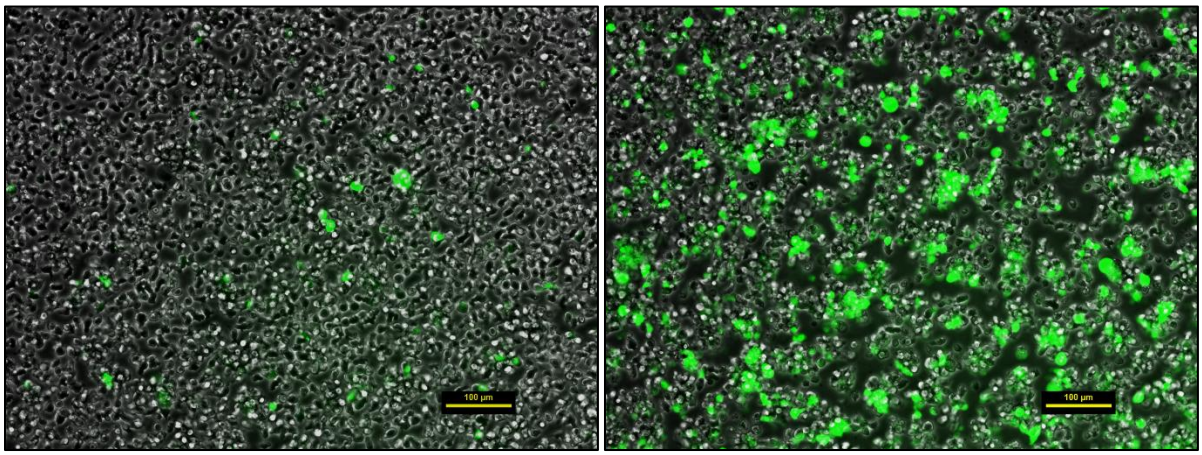

Figure 2: Lentiviral Mediated Knockdown of PAX5 in MCL Cell Lines. PAX5 knockdown and ORF cassettes were transduced into SP53 and Jeko MCL cell lines. Expression vectors contained antibiotic cassettes for either puromycin or blasticidin. (Left) Jeko cells 2 days after transduction, before antibiotic selection. (Right) Jeko cells 10 days post antibiotic selection.

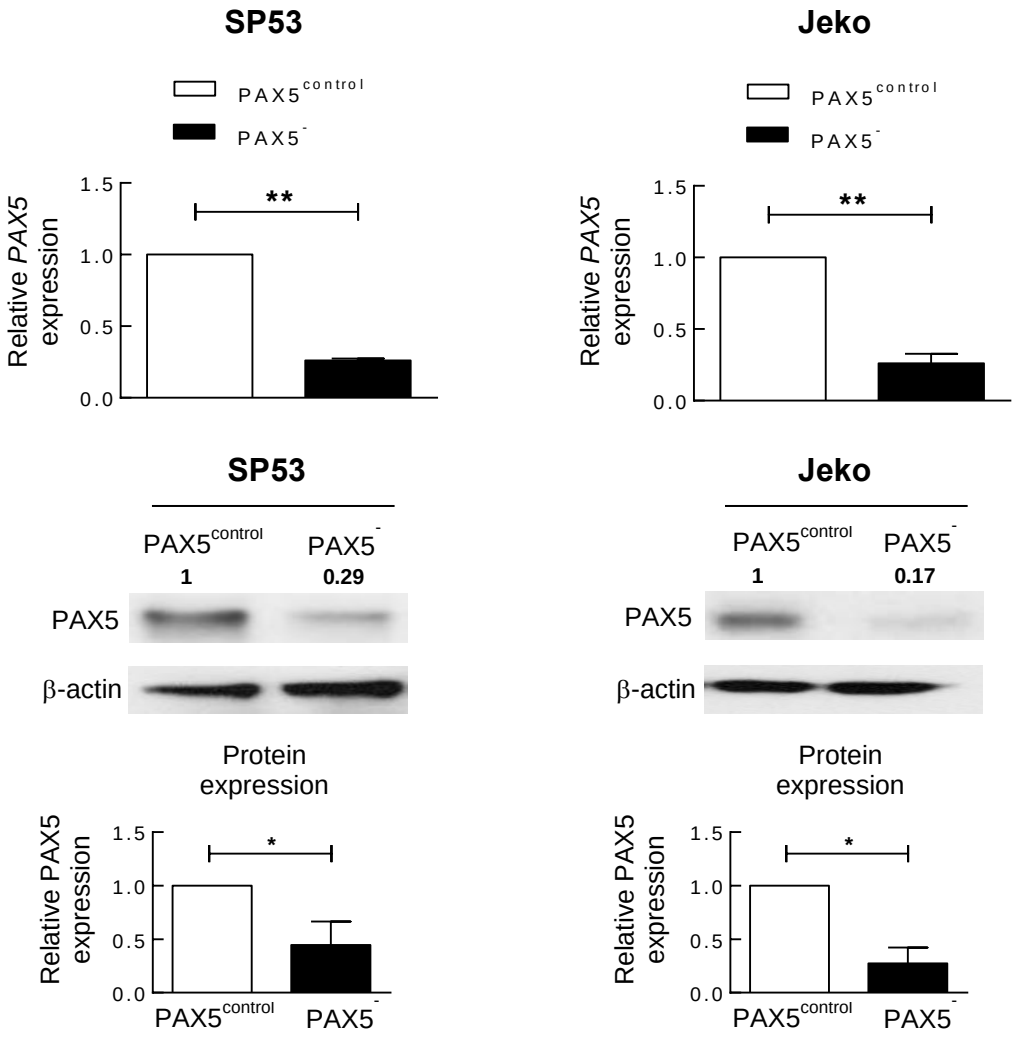

Figure 3: PAX5 Expression is Reduced in PAX5⁻ MCL Cells. PAX5⁻ MCL cells have decreased *PAX5* mRNA (top) and protein (bottom) levels. Numbers above the immunoblots show densitometric values normalized to β-actin protein, with the average values from 2 immunoblots. * $p < 0.05$ (vs. $PAX5^{control}$; Student's t-test); ** $p < 0.005$ (vs. $PAX5^{control}$; Student's t-test).

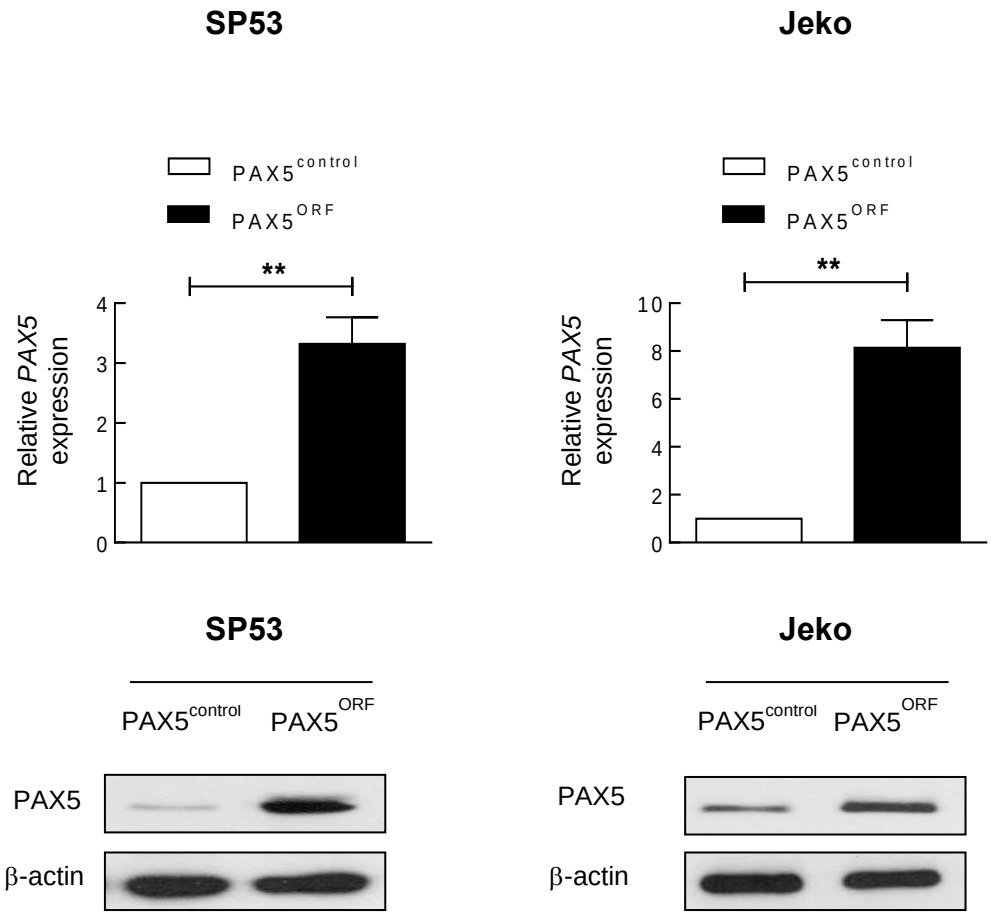

Figure 4: PAX5 is overexpressed in PAX5^{ORF} MCL cells. PAX5^{ORF} cells have increased PAX5 expression. qPCR analyses (top) and immunoblots analyses of PAX5 in SP53 and Jeko cells expressing PAX5^{ORF}. Each value represents the mean ± S.D (n=3). * $p < 0.05$ (vs. PAX5^{control}; Student's t-test); **$p < 0.005$ (vs. PAX5^{control}; Student's t-test).

Table 2: List of Selected Genes Repressed By Murine Pax5. List of selected genes that were previously reported to be repressed by murine Pax5. These genes are also involved in HSC biology or tumorigenesis.

Gene	Implications in HSC maintenance, distribution and differentiation	Implications in tumorigenesis
LMO2	Yamada Y *et al* (1998)[1]	Nam CH *et al* (2006)[2]
CST7	Halfon S *et al* (1998)[3]	
FXYD5		Nam JS *et al* (2007)[4]
CCR2	Si Y *et al* (2010)[5] Kim J *et al* (2014)[6]	Zhang J *et al* (2010)[7]
FLT3	Gilliland DG *et al* (2002)[8] Kikushige Y *et al* (2008)[9]	Kiyoi H *et al* (2002)[10] Gilliland DG *et al* (2002)[8]
VAV3	Vigorito E *et al (*2005)[11]	Colomba A *et al* (2008)[12] Chang KH *et al* (2012)[13]
SATB1	Will B *et al* (2013)[14] Satoh Y *et al* (2013)[15]	Chu SH *et al* (2013)[16]
TTC3	Liu XL (2007)[17]	
LILRB4	Cella M *et al* (1997)[18]	Dobrowolska H *et al* (2013)[19]
CCL3	Cook DN (1996)[20]	Vallet S *et al* (2011)[21] Baba T *et al* (2013)[22]
Notch1	Maillard I (2014)[23]	Grabher C *et al* (2006)[24]
PARP1	Li X *et al* (2014)[25]	Curtin NJ (2005)[26]
IFITM		Andreu P *et al* (2006)[27]

in some cancer cells, which enables escape from immune surveillance (Chao, Weissman et al. 2012), and has been found to regulate metastasis and dissemination in both multiple myeloma and NHL (Kikuchi, Uno et al. 2005, Chao, Alizadeh et al. 2010). PAX5^{-} Jeko MCL cells exhibited increase of *CD47* mRNA expression (**Figure 5B**).

In B cell lymphompoiesis, Pax5 expression is lost when B cells mature into plasma cells (Cobaleda, Schebesta et al. 2007). Knockdown of Pax5 have previously been reported to cause mature B cells to revert to a more plasmacytic like state (Nera, Kohonen et al. 2006), with increase in plasma cell transcription factors and proteins. PAX5^{-} MCL cells upregulated transcription factors that determine plasmacytic differentiation, such as interferon regulatory factor 4 (IRF4) and PR domain zinc finger protein 1 (*BLIMP1*) by qRT-PCR and by immunoblottings (**Figure 6**). It is interesting to note that both our qRT-PCR and protein blots for PAX5^{-} Jeko cells yielded no significance increase in IRF4 expression, an observation consistent with Jeko.BR (bortezomib resistant) sub clones which exhibit plasmacytic characteristics (Pérez-Galán, Mora-Jensen et al. 2011). We also tested PAX5^{-} MCL cells for XBP-1 splicing, as the spliced form of XBP-1 is the isoform that is translated and plays a role in the unfolded protein response during plasma cell development (Shapiro-Shelef and Calame 2004). However, there were no spliced variant present (**Figure 7A**). This is again consistent with what was previously reported, where plasmacytic MCL cell lines did not lead to increased XBP-1 spliced isoforms (Pérez-Galán, Mora-Jensen et al. 2011), suggesting that XBP-1 splicing is a late event of plasmacytic differentiation. In addition, we found the plasma cell marker, CD138, was increased at steady state levels

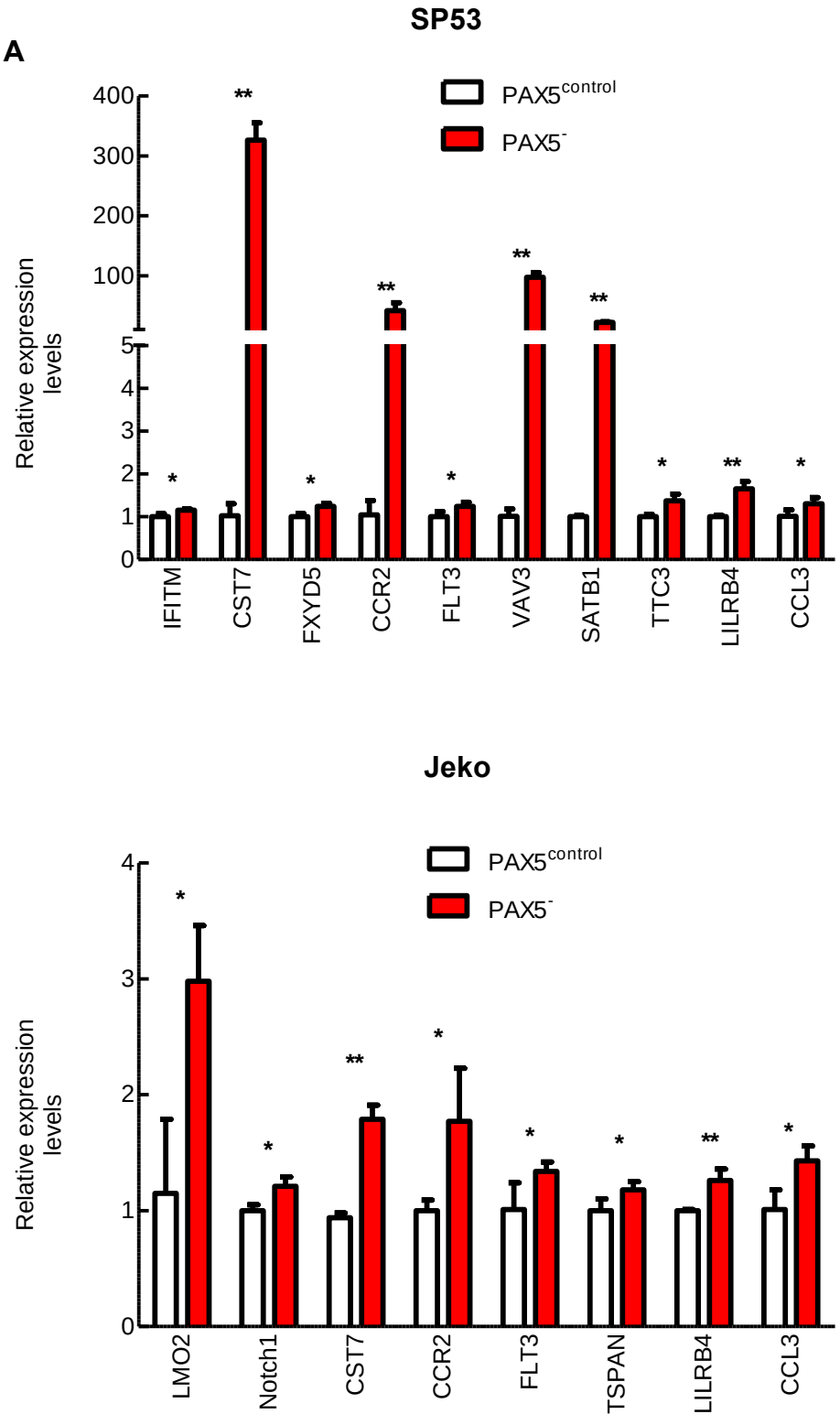
A
SP53
PAX5control
PAX5-
Relative expression levels
400
300
200
100
5
4
3
2
1
0
IFITM
CST7
FXYD5
CCR2
FLT3
VAV3
SATB1
TTC3
LILRB4
CCL3
Jeko
PAX5control
PAX5-
Relative expression levels
4
3
2
1
0
LMO2
Notch1
CST7
CCR2
FLT3
TSPAN
LILRB4
CCL3

B

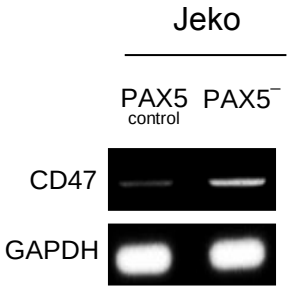

Figure 5: PAX5⁻ MCL Cells Have an Upregulation of Pax5 Repressed Genes. (A) PAX5⁻ cells demonstrate increased expression of PAX5 repressed genes. Gene expression was analyzed by qRT-PCR. Out of the 13 genes that are repressed by murine Pax5, 10 genes (SP53) and 8 genes (Jeko) were upregulated in PAX5⁻ cells. Each value represents the mean ± S.D (n=3). Gene expression was normalized to *ACTB* mRNA levels. (B) RT-PCR analysis of CD47 in Jeko control or PAX5⁻ cells. *GAPDH* served as loading controls. * $p < 0.05$ (vs. $PAX5^{control}$; Student's t-test); ** $p < 0.005$ (vs. $PAX5^{control}$; Student's t-test).

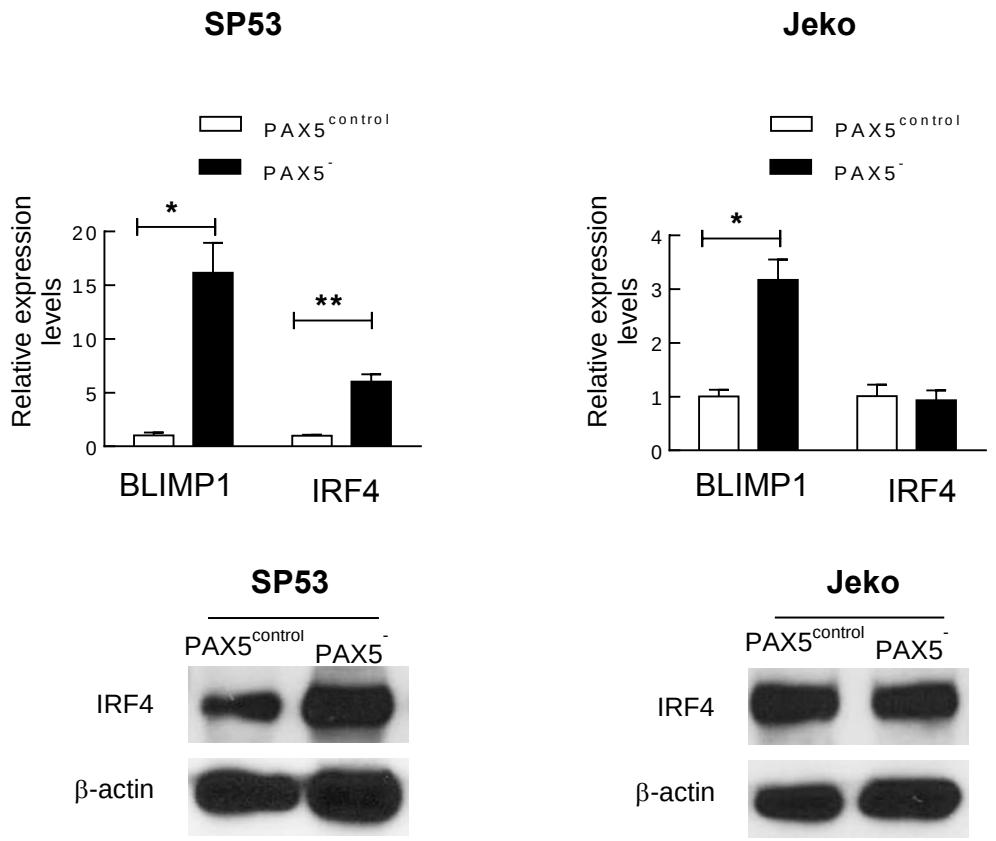

Figure 6: PAX5⁻ MCL Cells Have an Upregulation of IRF4 and BLIMP1. (Top) PAX5⁻ cells have increased levels of BLIMP1 and IRF4 expressions compared to controls. Gene expression was analyzed using qRT-PCR, with results normalized to *GAPDH*. (Bottom) Immunoblot analyses of PAX5⁻ MCL cells for IRF4 with β-actin serving as the loading control. * $p < 0.05$ (vs. $PAX5^{control}$; Student's t-test); ** $p < 0.005$ (vs. $PAX5^{control}$; Student's t-test).

in SP53 PAX5^{-} SP53 cells (**Figure 7B**) and in both PAX5^{-} cells upon bortezomib activation (**Figure 7B**).

PAX5^{-} MCL cells displayed increased tumorigenic traits

Since PAX5 conditional knock out murine B cells increased lineage plasticity by developing T cells upon adoptive transfer into RAG2$^{-/-}$ mice (Cobaleda, Jochum et al. 2007), we analyzed colony-forming abilities of PAX5^{-} MCL cells using phytohemagglutinin leukocyte (PHA-LCM) conditioned medium, which was used to measure stem-like properties in myeloma (Matsui, Huff et al. 2004). PAX5 silencing significantly increased frequency of colony-forming units of MCL cells compared to control cells (**Figure 8**), as well as displaying a larger colony overall (**Figure 8**).

We further analyzed the effect of PAX5 gene silencing on engrafted stem-like cells using PKH dye as described previously (Chen, Orlowski et al. 2014). PKH26 is a fluorescent lipophilic compound that labels the cell membrane, and its fluorescent intensity decreases with each cell division (Parish 1999). Since stem cells are largely quiescent, PKH26 has been used to monitor engraftment of HSC and lymphoid cells (Lanzkron, Collector et al. 1999, Lanzkron, Collector et al. 1999) or to identify cancer stem cells (Mangioni, Fruscio et al. 2012, Xue, Yan et al. 2012).

We allowed 100% PKH26 labelled GFP^{+} MCL cells to undergo cell cycling in vivo for 48 hours and calculated PKH26^{+} recovery rates in different tissues using FACS analyses. Similar to the HSC reported previously (Lanzkron, Collector et al. 1999), the highest amounts of PKH^{+} cells were recovered after 48 hours of in vivo cell cycling (**data not shown**). Therefore, all the following analyses were performed at 48 hours post transplantation. Human cell engraftment was analyzed based on the number of CD45^{+} and PKH26^{+} in each tissue using FACS.

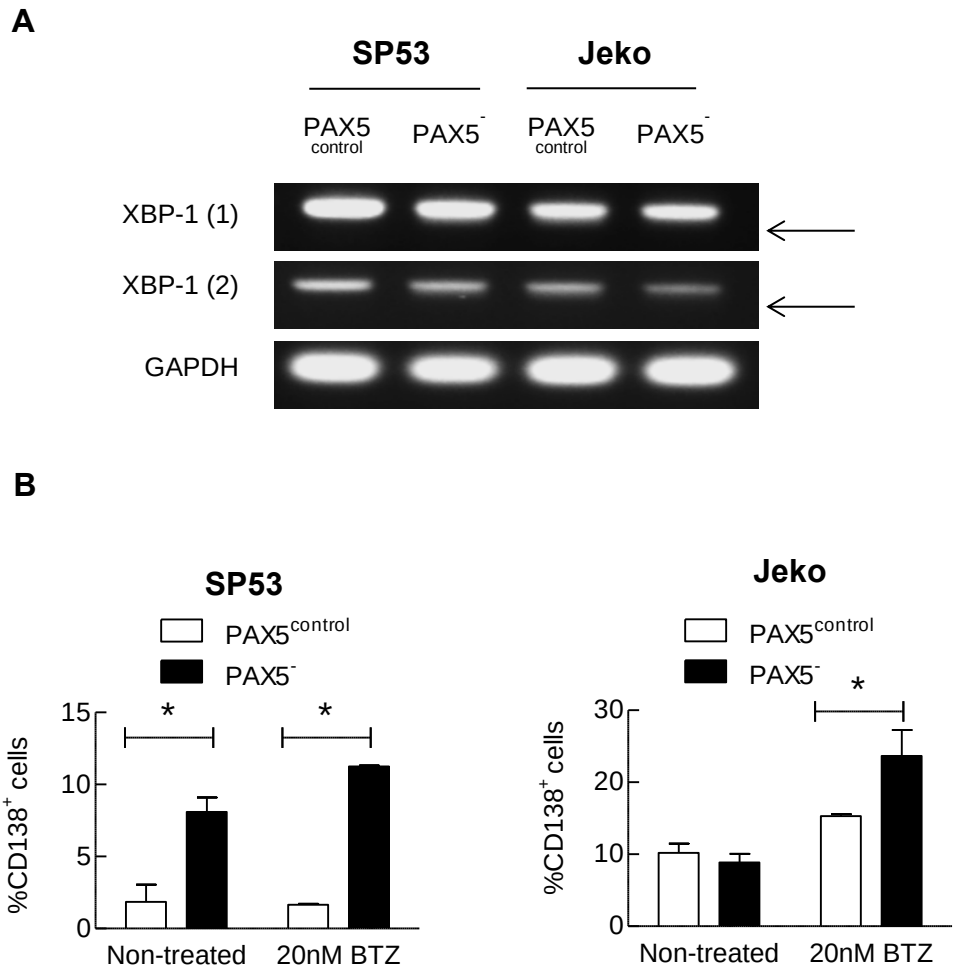

Figure 7: PAX5⁻ MCL Cells Have an Upregulation of CD138 but Do Not Undergo Plasmacytic Differentiation. (A) PAX5⁻ cells do not have spliced XBP-1, an important event for plasmacytic differentiation. Two different XBP-1 primer sets were used to determine the splice variant (shorter isoform). Arrows indicate where splice variant band will show. (B) Marker for plasmacytic differentiation, CD138 expression is increased in PAX5⁻ cells upon bortezomib treatment. FACS analyses were performed at 72 hours post bortezomib treatment (n=2). * $p < 0.05$ (vs. $PAX5^{control}$; Student's t-test); ** $p < 0.005$ (vs. $PAX5^{control}$; Student's t-test).

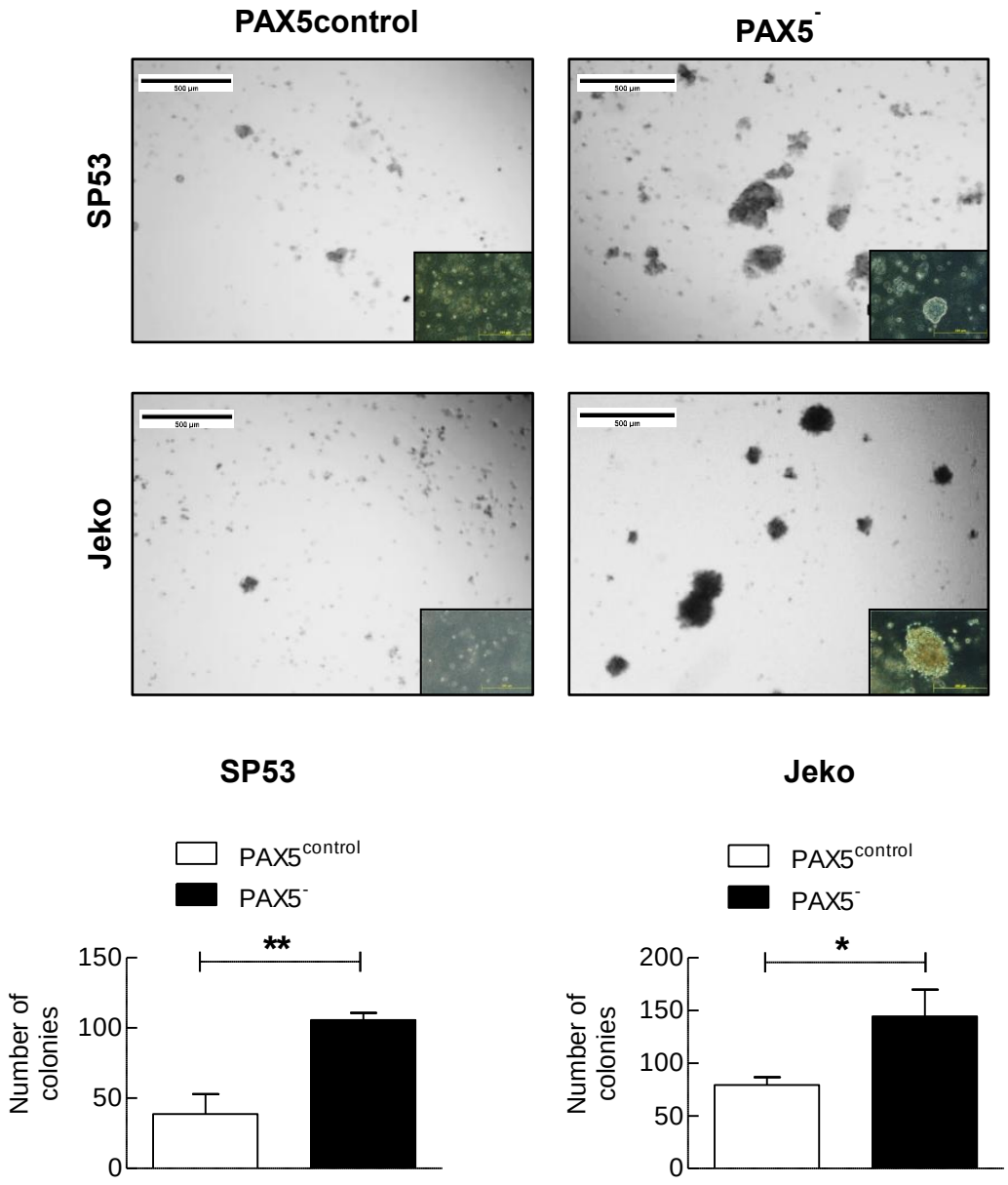

Figure 8: PAX5⁻ Cells Demonstrate Increased Colony Formation. PAX5⁻ cells (5000) were seeded in PHA-LCM and colonies were scored at day 7. Only colonies containing > 50 cells were considered as a positive score. Inset: PAX5⁻ cells also formed larger colonies in PHA-LCM as visualized using a 20 x objective light microscope. Each value represents the mean counted colonies ± S.D (n=3). * $p < 0.05$ (vs. $PAX5^{control}$; Student's t-test); ** $p < 0.005$ (vs. $PAX5^{control}$; Student's t-test).

MCL cell engraftment based on GFP^+ was not different between two cell types after short incubation of 48 hours in vivo. Surprisingly, however, recovery rates of PKH^+ cells population were significantly higher in $PAX5^-$ xenografts compared to control xenografts (**Figure 9**, **Table 3**). After 48 hour in vivo cycling, 21.5% of PKH^+ cells were recovered from the bone marrows of $PAX5^-$ SP53 xenograft mice, compared to just 18.2% of PKH^+ cells recovered from controls, resulting in an 18% increase in engraftment. We also found a similar trend in $PAX5^-$ Jeko xenografts, which had 14% PKH^+ cell recovery vs 10.4% in controls, which is a 35% increase in engraftment (**Table 3**). PKH^+ cell engraftment of $PAX5^-$ cells was also higher in the spleens, however, the levels of increase was less than bone marrows (6.5% in SP53 and 25% in Jeko). This hinted at $PAX5^-$ cells to have a more quiescent like trait, or increase membrane retention. IHC analysis of xenograft mice bones and spleens confirmed the FACS findings (**Figure 10 and 11**), with arrow pointing at $CD45^+$ cells. PKH intensity varies within cells, with $PAX5^-$ cells exhibiting a higher dye-retention.

PAX5 affects cellular proliferation

We then compared the $PAX5^-$ MCL in vitro cell proliferation to control cells. Proliferation was significantly increased in $PAX5^-$ MCL and this trend was repeated in $PAX5^-$ Raji and $PAX5^-$ Reh cells, non-MCL lines (**Figure 12**). On the other hand, PAX5 overexpression led to severely reduced cellular proliferation (**Figure 12**) and increased apoptosis in MCL cells (**Figure 13**) as well as in Raji and Reh (**Figure 14**). Jeko $PAX5^-$ cells were compared to $PAX5^{ORF}$ cells and cell proliferation determined after 6 days in culture.

We then examined cell cycle distribution of the $PAX5^-$ MCL cells. On average, $PAX5^-$ MCL cells had 50-60% more cells in the S-phase compared to control cells,

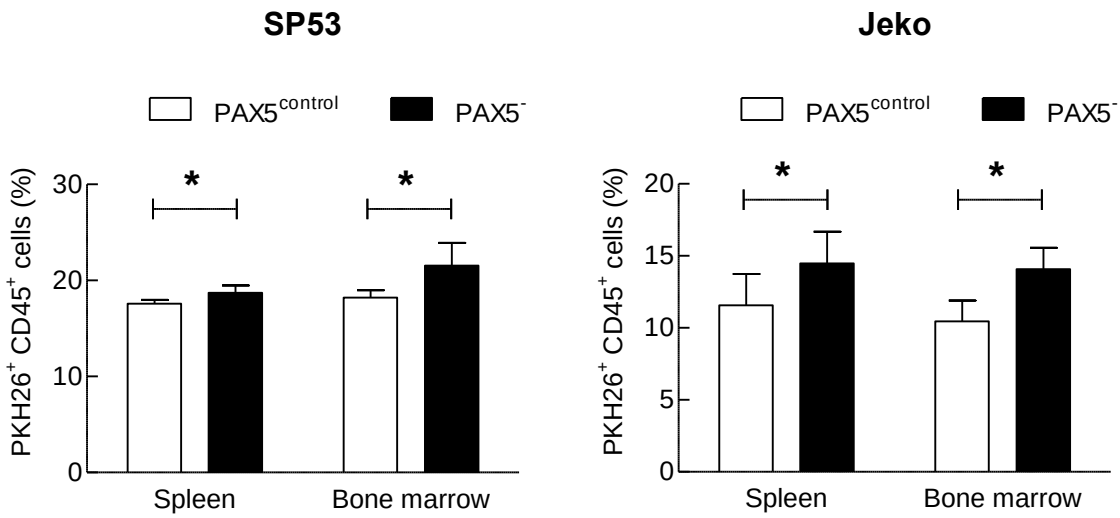

Figure 9: PAX5^{-} Cells Demonstrate Greater PKH26^{+} Cell Retention in Xenograft Mice. (A) PAX5^{-} cells have increased PKH26^{+} cell retention in xenograft mice. PKH26^{+} GFP^{+} PAX5^{-} cells ($1x10^{6}$) cells transferred to NOD/SCID mice. Mice were sacrificed after 48 hours and cells from bone marrows and spleens were collected. FACS analyses are representative of 4 samples. * $p < 0.05$ (vs. PAX5^{control}; Student's t-test); **$p < 0.005$ (vs. PAX5^{control}; Student's t-test).

Table 3: (%) PKH26$^+$ Cell Populations Quantitated from CD45$^+$ Cells. PKH26$^+$ cell populations quantitated from CD45$^+$ cells via flow cytrometry. Cells were isolated from host spleen and bone marrow.

SP53.PAX5^{control}

# of cells injected via tail vein	# of mouse	Tissue Examined	% PKH26$^+$ cells recovered
1 X 10^6	1	Spleen / Bone marrow	17.70 / 17.30
1 X 10^6	1		17.00 / 18.50
1 X 10^6	1		17.60 / 17.95
1 X 10^6	1		18.00 / 19.10
		Average	17.58 / 18.21

SP53.PAX5$^-$

# of cells injected via tail vein	# of mouse	Tissue Examined	% PKH26$^+$ cells recovered
1 X 10^6	1	Spleen / Bone marrow	19.10 / 24.70
1 X 10^6	1		18.30 / 21.15
1 X 10^6	1		17.90 / 21.35
1 X 10^6	1		19.60 / 18.95
		Average	18.73 / 21.53 ↑ 6.5% / 18.2%

Jeko. PAX5^{control}

# of cells injected via tail vein	# of mouse	Tissue Examined	% PKH26$^+$ cells recovered
1 X 10^6	1	Spleen / Bone marrow	11.20 / 8.95
1 X 10^6	1		10.70 / 11.50
1 X 10^6	1		14.70 / 9.50
1 X 10^6	1		9.70 / 11.85
		Average	11.58 / 10.45

Jeko.PAX5$^-$

# of cells injected via tail vein	# of mouse	Tissue Examined	% PKH26$^+$ cells recovered
1 X 10^6	1	Spleen / Bone marrow	13.70 / 13.00
1 X 10^6	1		12.40 / 13.65
1 X 10^6	1		14.10 / 13.95
1 X 10^6	1		14.00 / 13.15
1 X 10^6	1		18.20 / 16.65
		Average	14.48 / 14.08 ↑ 25% / 34.7%

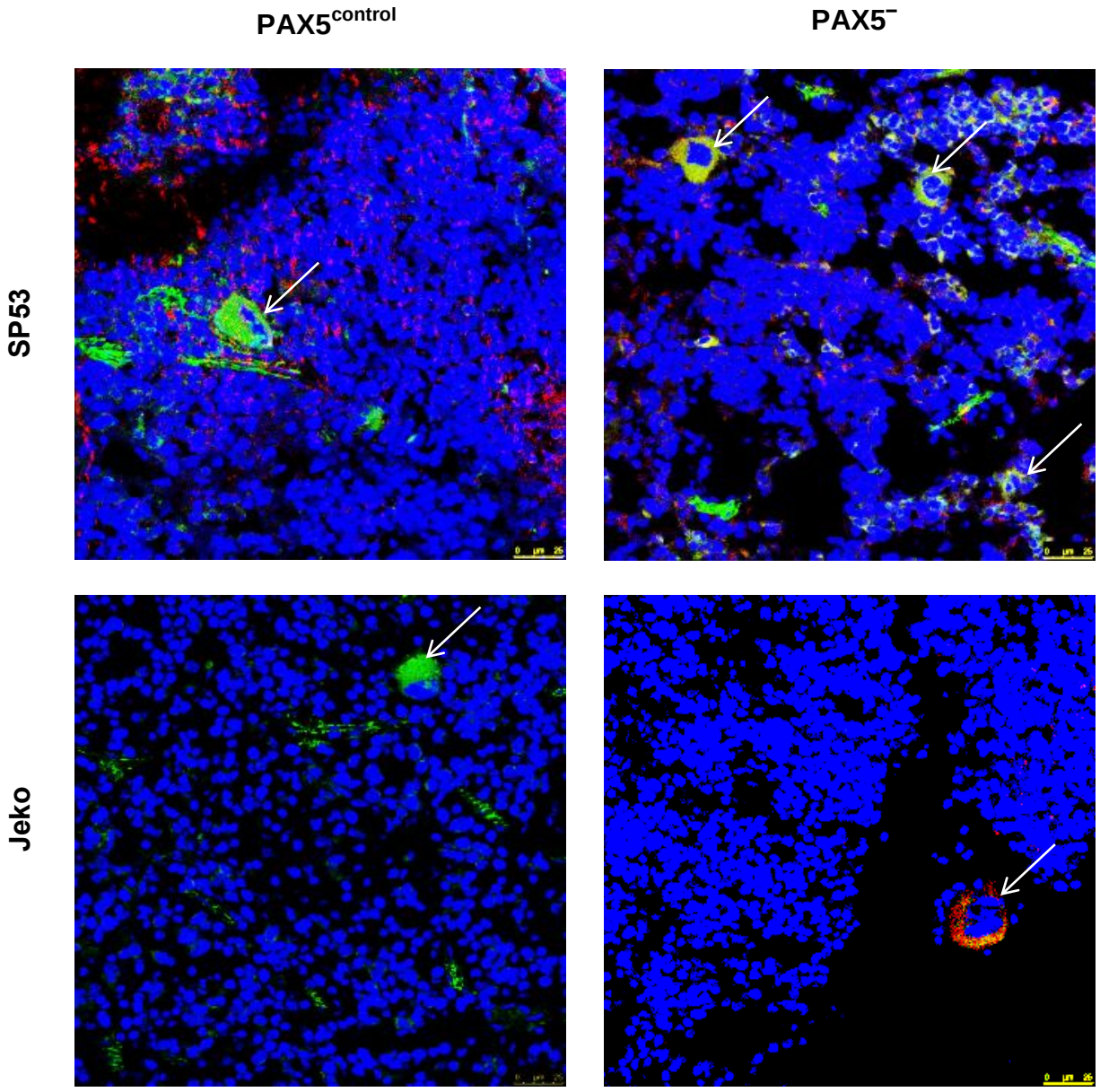

Figure 10: PAX5^{-} Cells Demonstrate Greater PKH26^{+} Cell Retention in Xenograft Mice Spleen. Representative spleen confocal images of GFP- and PKH-positive cells are shown. White arrow points to cells that are GFP positive with PKH26 staining. Scale bar, 25µm.

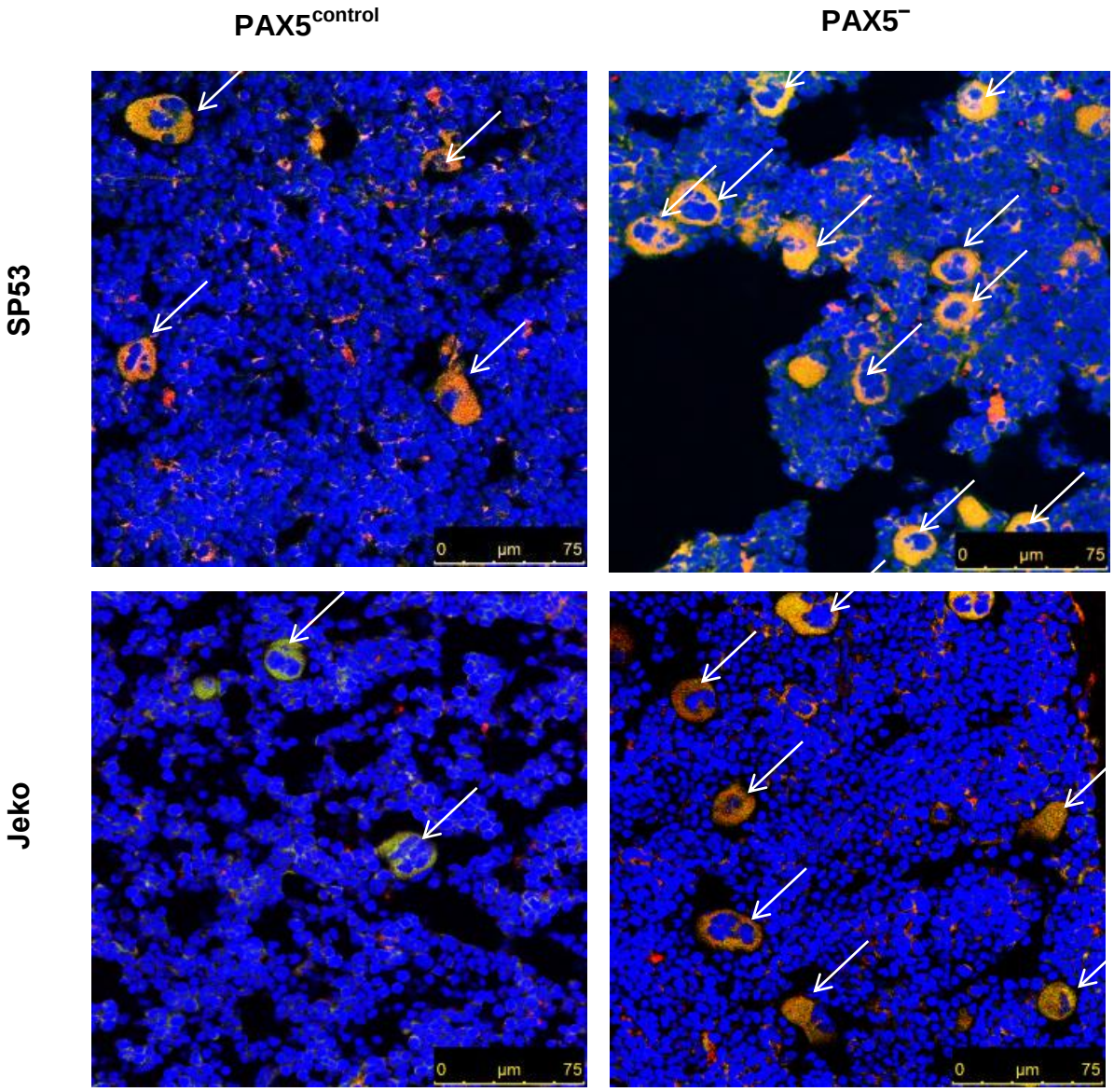

Figure 11: PAX5⁻ Cells Demonstrate Greater PKH26⁺ Cell Retention in Xenograft Mice Bone Marrow. Representative spleen confocal images of GFP- and PKH-positive cells are shown. White arrow points to cells that are GFP positive with PKH26 staining. Scale bar, 75µm.

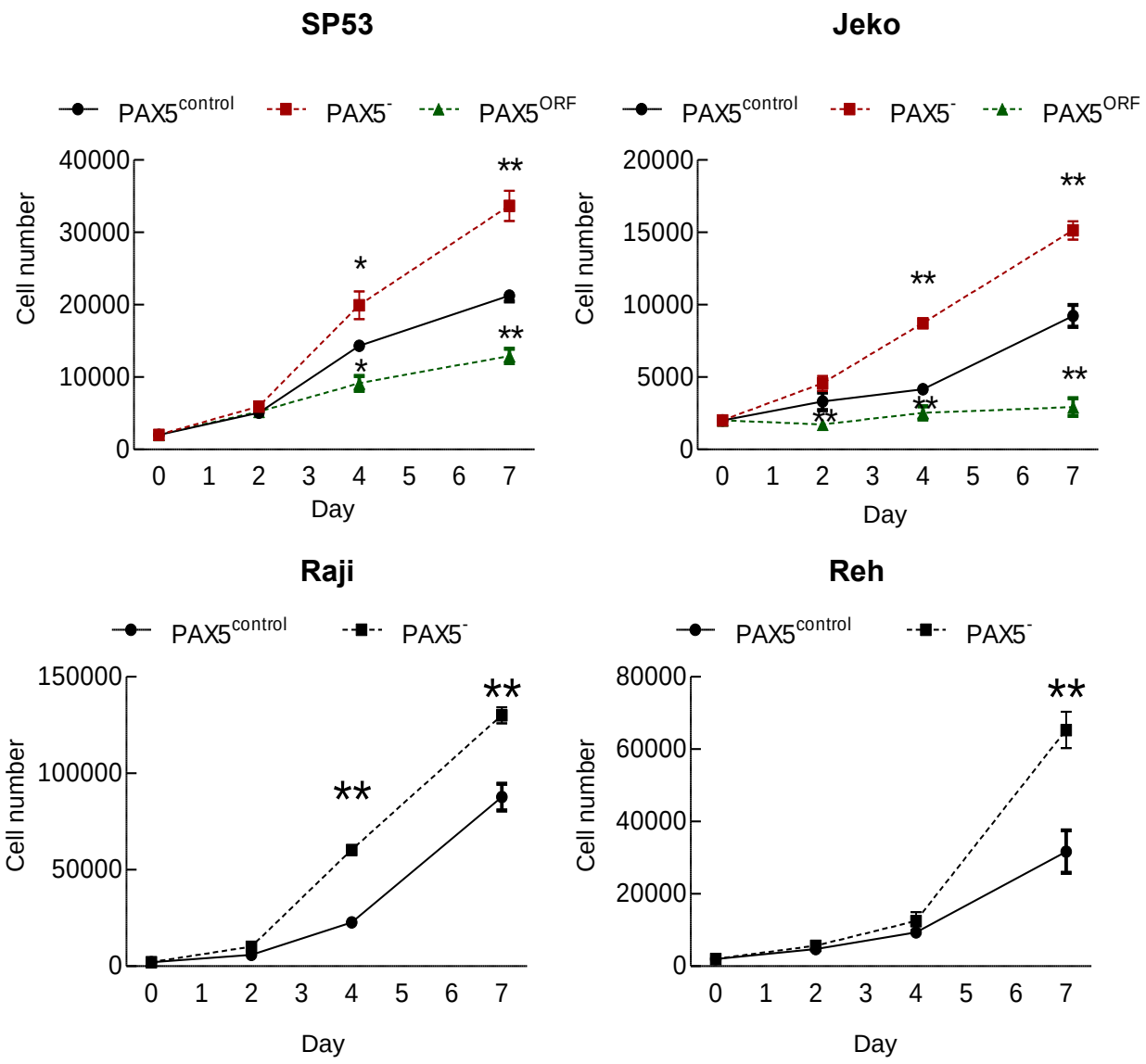

Figure 12: PAX5 Silencing in MCL Leads to Increased Cellular Proliferation.

PAX5^{-} cells were seeded at an initial 2000 cells and allowed to cycle for 7 days. Viable cells were counted using Tryphan Blue at days 0, 2, 4 and 7. Each value represents the mean ± S.D (n=3). * $p < 0.05$ (vs. PAX5^{control}; Student's t-test); **$p < 0.005$ (vs. PAX5^{control}; Student's t-test).

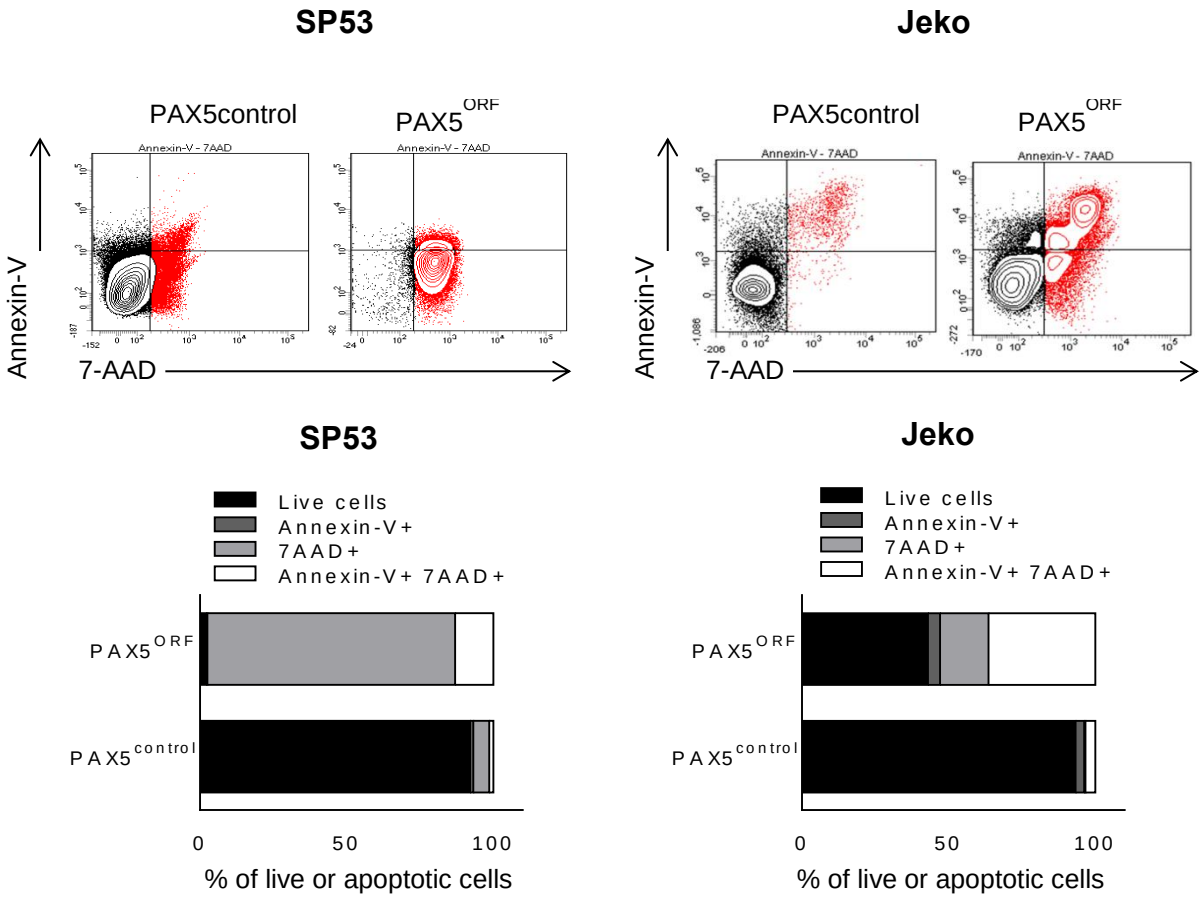

Figure 13: PAX5 Overexpression Leads to Cell Death in MCL Cells. Apoptotic evaluation of SP53 and Jeko cells expressing PAX5^{ORF} using FACS analysis. Cells were cycled in culture for > 1 week before stained with Annexin V and 7AAD. Results are representative of two independent experiments.

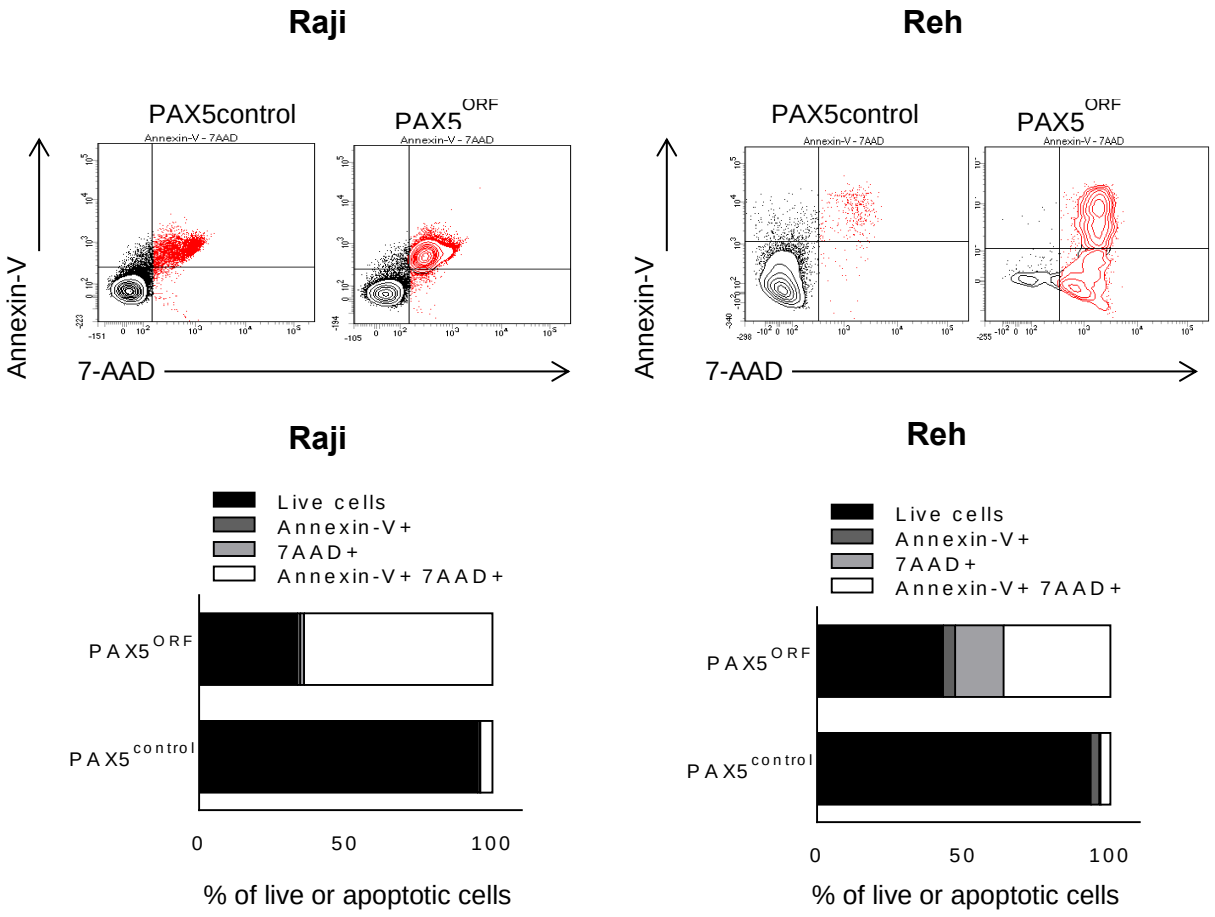

Figure 14: PAX5 Overexpression Leads to Cell Death in non-MCL Cells. Apoptotic evaluation of Raji and Reh cells expressing $PAX5^{ORF}$ using FACS analysis. Cells were cycled in culture for > 1 week before stained with Annexin V and 7AAD. Results are representative of two independent experiments.

while exhibiting less cells in the G0/G1 stage, 30-40% less cells (**Figure 15**). This points to a higher progression of the cell cycle, and corroborates our observations in cell proliferation (**Figure 12**).

To investigate whether PAX5^{-} cells could form a larger tumor (a measure for tumor burden), we transplanted 3 x 10^6 SP53 PAX5^{-} and control cells into the subcutaneous neck fold of NOD/SCID mice. Tumors were measured at week 4 and PAX5^{-} xenografts on average had tumors with larger volumes (**Figure 16A**). Interestingly, we found that PAX5^{-} subcutaneous tumors to have a trend of increased glucose uptake (**Figure 16B**) when hosts were injected with ^{18}F-FDG, though the data was not significant. However, an increased metabolic rate is tied to increased proliferation (Haberkorn, Strauss et al. 1991), suggesting that PAX5^{-} cells causes an increased tumor burden in vivo.

Since PAX5 silencing increased cellular proliferation in vitro and in vivo, we examined expression levels of selected genes that are involved in the cell cycle. Deregulation of cyclin-dependent kinases (CDKs) has been linked with increased cellular proliferation, as well as genomic and chromosomal instability which could lead to acquisition of genetic alterations that can contribute to tumor progression (Kastan and Bartek 2004, Massagué 2004, Malumbres and Barbacid 2005) . Compared to control MCL cells, PAX5^{-} MCL cells demonstrated increased levels of CDK1, CDK2 and CDK6 mRNA, as well as the corresponding cyclins at steady state level (**Figure 17**). CDK1 is a well-studied mitotic CDK with cyclin A or B as its substrate, whereas CDK2 and CDK6 are interphase CDKs which requires cyclin A/E and cyclin D respectively (Malumbres and Barbacid 2005). CDK4 mRNA is increased in SP53 PAX5^{-} cells; however Jeko PAX5^{-} cells had the same amount as control cells (**Figure**

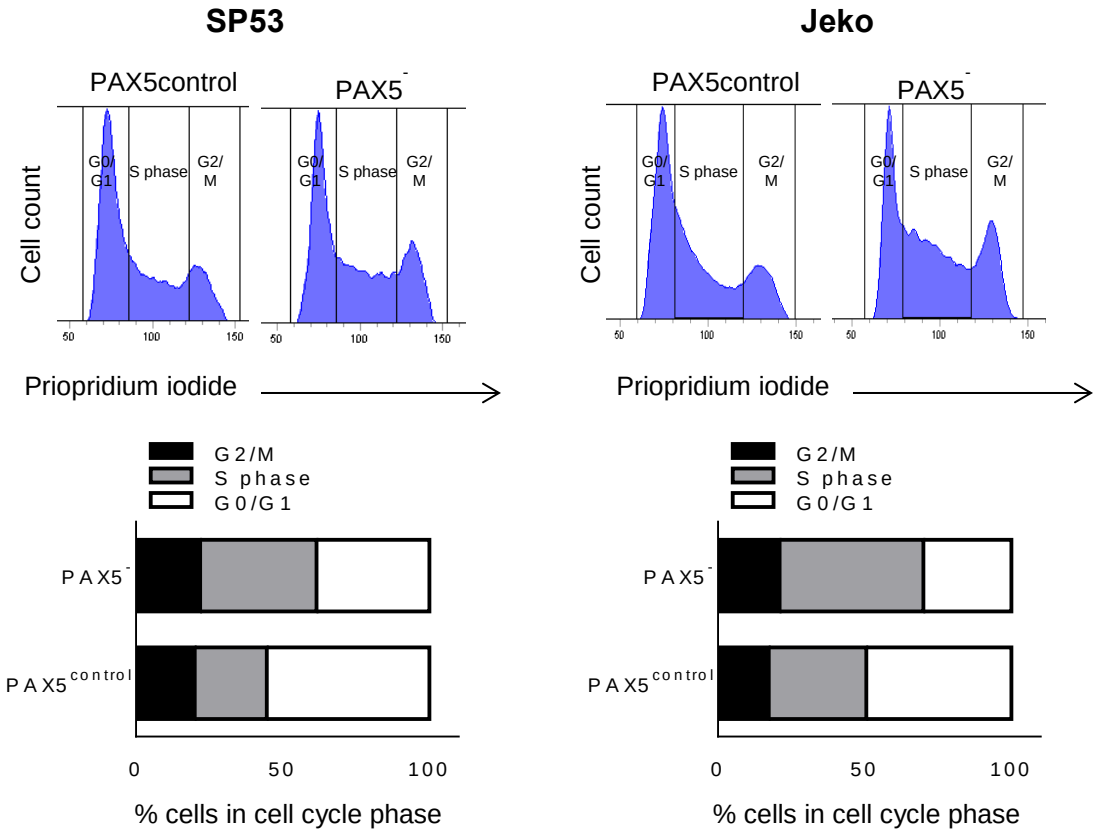

Figure 15: PAX5 Knockdown Leads to an Increase of Cells in the S-Phase.

Propidium iodide staining of cells exhibit a higher % population of cells in the S-phase of the cell cycle in PAX5^{-} cells. Cells were cultured for at least 48 hours before stained.

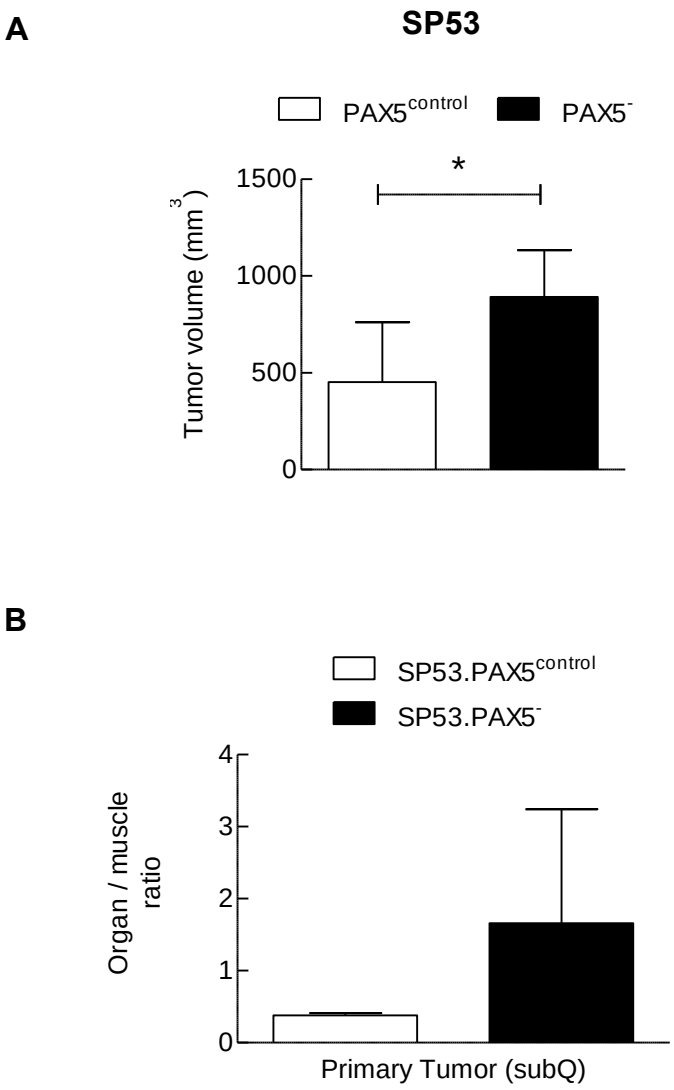

Figure 16: SP53 PAX5⁻ Cells Form Larger Tumors in vivo. (A) A total of 3 x 10^6 PAX5⁻ SP53 cells or control cells were injected into NOD/SCID mice (n=9) via subcutaneous injection and tumor volumes measured with a digital caliper after 4 weeks. (B) ^{18}F-FDG counts of subcutaneous primary tumor and muscle tissue harvested from SP53 PAX5⁻or control xenografts. (%) ID / g of each target organ was normalized to a standardized control and CPM normalized to weight of each tissue, with tumors than normalized to muscle tissue for glucose baseline absorption. * $p < 0.05$ (vs. PAX5^{control}; Student's t-test); **$p < 0.005$ (vs. PAX5^{control}; Student's t-test).

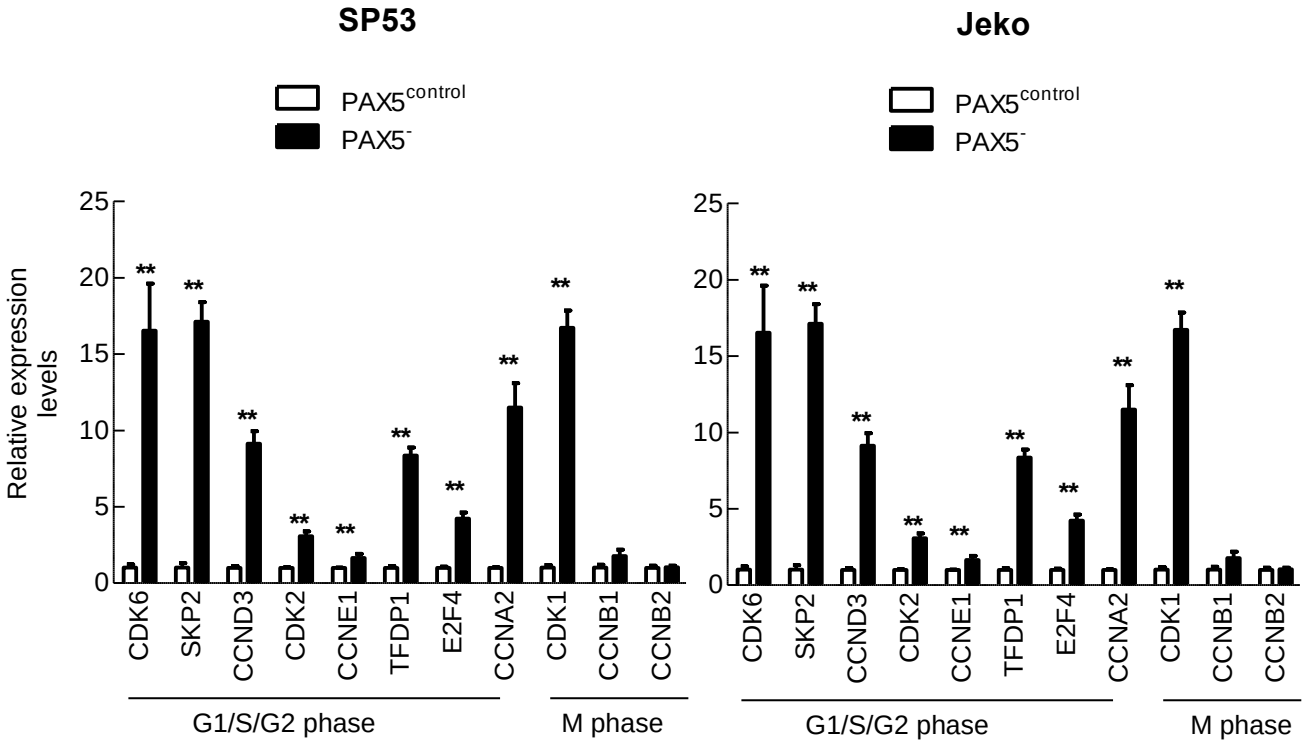

Figure 17: PAX5⁻ Cells Overexpress Cell Cycle Promoting Genes. qPCR analysis of common cell cycle genes in PAX5⁻ cells. Readouts were normalized to *ACTB*. All cells used in the experiments were selected for GFP^+ and stable cell lines were generated via antibiotic selection. * $p < 0.05$ (vs. $PAX5^{control}$; Student's t-test); ** $p < 0.005$ (vs. $PAX5^{control}$; Student's t-test).

18). We also observed an increase in E2F family member 4 and dimerization partner DP1 gene (TFDP1) expression in PAX5¯ MCL cells compared to controls **(Figure 17)**. The E2F family of transcription factors and its binding partners play a critical role in cell cycle development from transition of the G1 to S phase, as complexes negatively regulate RB tumor suppressor pocket proteins retinoblastoma protein (Hagman and Lukin 2006), p107 and p130.

TP53, RB and CDKN1A (p21) are tumor suppressors, with deregulation of these genes and proteins leading to the development of lymphomas (Chilosi, Doglioni et al. 1996, Lee, Cam et al. 2002). We observed that SP53 cells which harbor wild-type p53 (Ding, Whetstine et al. 2001, Drakos, Atsaves et al. 2009) express decreased levels of TP53, CDKN1A and CDKN1B upon PAX5 silencing by semi-quantitative RT-PCR (**Figure 18A**) and by immunoblots (**Figure 18B**). Jeko cells with TP53 deleted mutants (Drakos, Atsaves et al. 2009), exhibited lower levels of retinoblastoma protein (*RB1*) gene transcript as well as *CDKN1A* upon PAX5 silencing (**Figure 18A**), indicating PAX5 silencing affect tumor suppressor gene expression regardless of TP53 mutational status. These collective effects lead to increased MCL cell proliferation.

Serum starvation can be employed as a means to force systemic shock to select for tumorigenic like cell populations (Tavaluc, Hart et al. 2007), and we found PAX5^{-} MCL cells thrived under serum starved conditions; PAX5^{-} MCL cells had significantly increased cell survival in 2% or 5% serum conditions (**Figure 19**) indicating PAX5 silencing promotes MCL cell proliferation not only in normal conditions (10%) but also under stressed cell culture conditions.

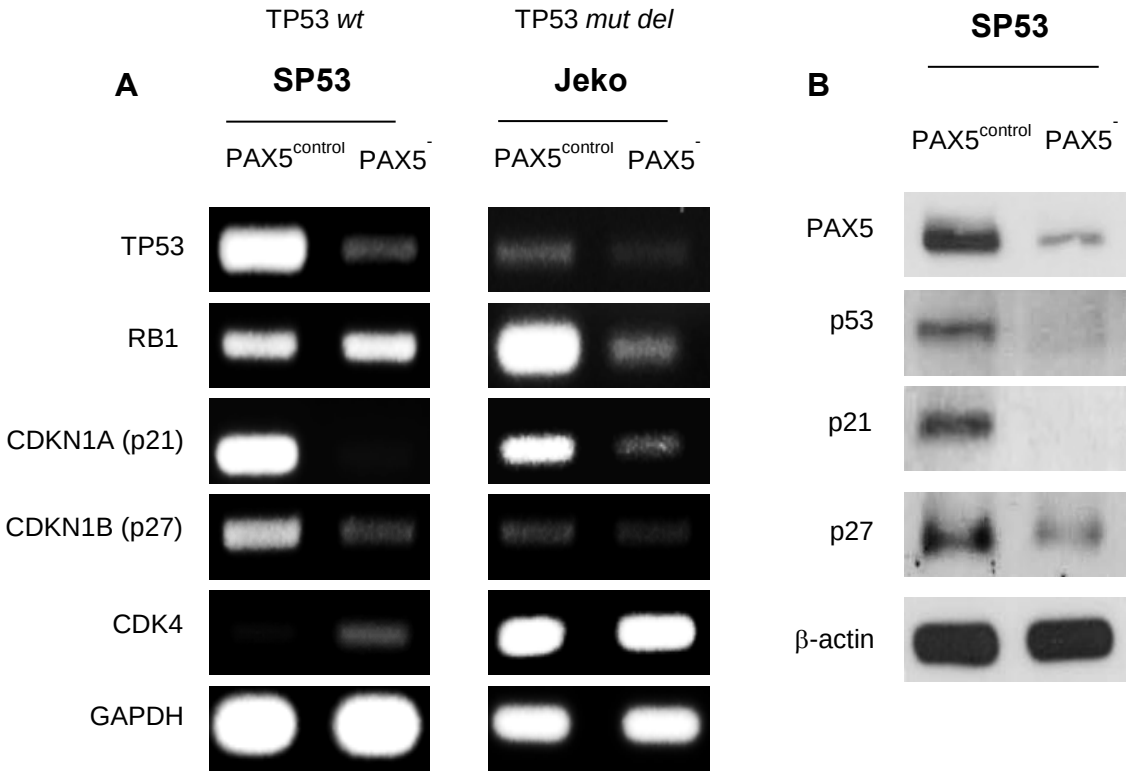

Figure 18: PAX5⁻ Cells Express Decreased Levels of Cell Cycle Regulating Genes. (A) Semi quantitative RT-PCR analysis of potential cell cycle inhibitors deregulated upon PAX5 silencing. SP53 is TP53 wild type and Jeko has TP53 mutant deletion. *GAPDH* serves as a loading control. (B) Immunoblot analyses of cell cycle inhibitors p53, p27 and p21 in PAX5⁻ and control cells, with β-actin serving as the loading control.

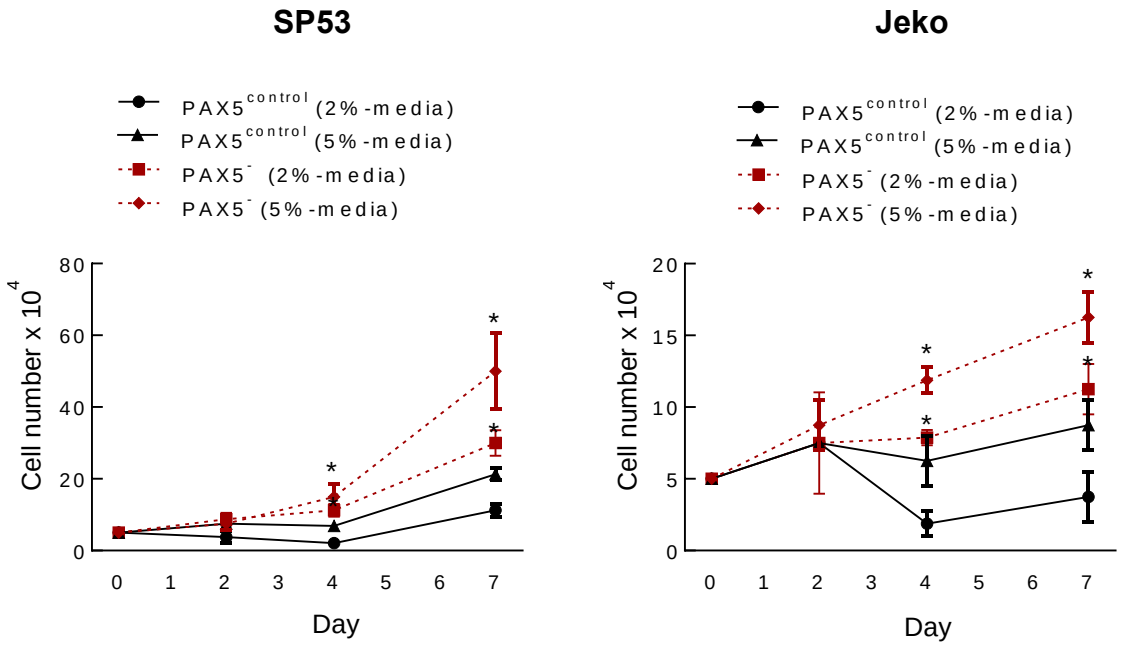

Figure 19: PAX5⁻ Cells Proliferate Faster Under Serum Starved Conditions. (A) A total of 50,000 PAX5⁻ cells were cultured in two different low serum conditions and allowed to cycle for 7 days. Viable cells were counted using Tryphan Blue at days 0, 1, 4 and 7. Each value represents the mean ± S.D (n=3). * $p < 0.05$ (vs. $PAX5^{control}$; Student's t-test); **$p < 0.005$ (vs. $PAX5^{control}$; Student's t-test).

Since PAX5$^-$ MCL cells demonstrated a better survival rate under this stressed condition, we then analyzed several IL-6 related genes upon serum restriction (Zhang, Yang et al. 2012). Compared to control cells, PAX5$^-$ cells showed higher proliferation rate in lower serum conditions (**Figure 19**). A significant increase in cell number was observed at days 4 and 7 of starvation (2% FBS) in PAX5$^-$ cells (**Figure 19**), while these cells have a lower percentage of apoptotic cells at day 3 (**Figure 20**)**.** IL-6, GP80 (IL-6 receptor) and GP130 (IL-6 signal transducer) mRNA were significantly increased in PAX5$^-$ SP53 and Jeko cells compared to controls at day 3 of 2% serum starvation (**Figure 21A**).

BCL-XL and MCL1 are important anti-apoptotic proteins that are involved in the IL-6 signaling cascade (Zushi, Shinomura et al. 1998, Puthier, Bataille et al. 1999), and these proteins are often overexpressed in B cell lymphomas (Agarwal and Naresh 2002, Cho-Vega, Rassidakis et al. 2004). Sphingosine-1-phosphate receptor 1 (S1PR1) is an important marker for MCL diagnosis (Nishimura, Akiyama et al. 2010) as well as a downstream target for IL-6 signaling via STAT3 (Lee, Deng et al. 2010). BCL-XL, MCL1 and S1PR1 mRNA levels were significantly increased after serum restriction in PAX5$^-$ MCL compared to controls (**Figure 21B**).

SP53 cells have previously been reported to secrete autocrine IL-6 (Zhang, Yang et al. 2012). We examined the levels of autocrine IL-6 by ELISA using conditioned media of SP53 PAX5$^-$ MCL. IL-6 levels were significantly increased in conditioned medium PAX5$^-$ MCL compared to controls, with HS5 conditioned medium serving as a positive control (**Figure 22A**). Serum restriction was also reported to induce IL-6 expression (Zhang, Yang et al. 2012), and nutrient restriction resulted in

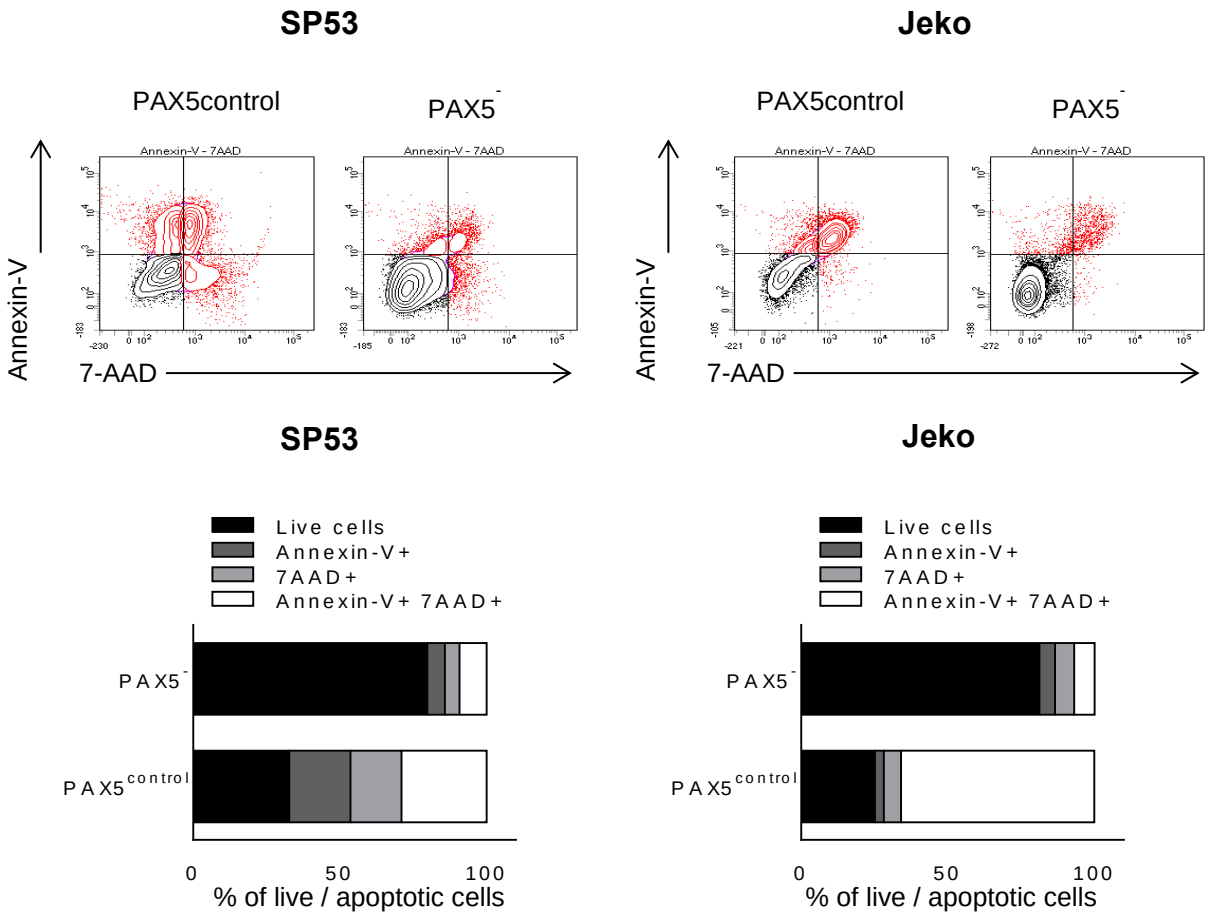

Figure 20: PAX5⁻ Cells Are Less Apoptotic Under Serum Starved Conditions.

PAX5⁻ cells demonstrate reduced cell death in low serum conditions. Apoptotic evaluation of serum starved PAX5⁻ MCL cells using FACS. Cells were cultured in a low serum condition (2% FBS) for 3 days prior to staining with Annexin-V and 7AAD.

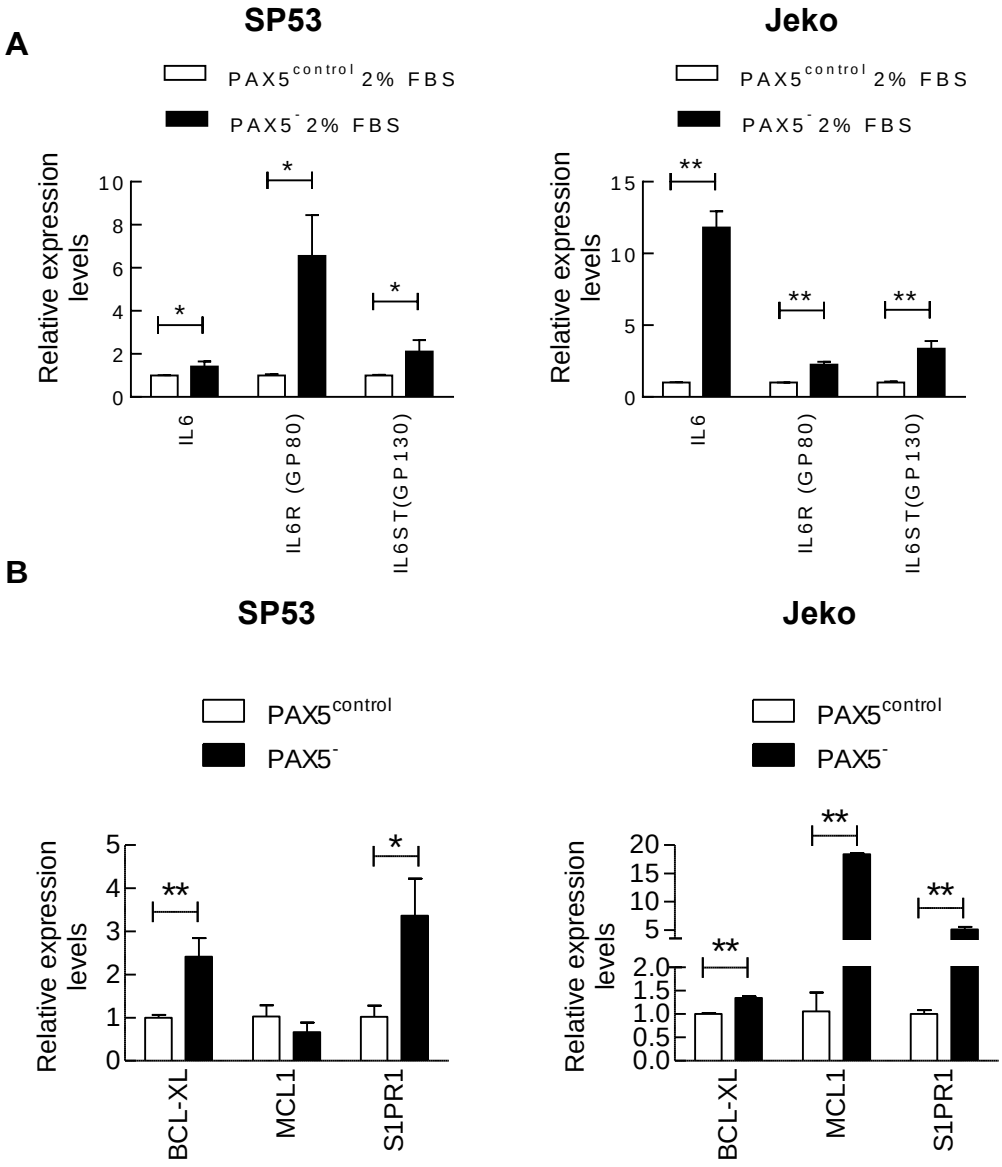

Figure 21: PAX5⁻ Cells Express Increased IL-6 Family and Target Genes. (A) IL-6 signaling components were quantitated using qRT-PCR. Cells were cultured in low serum condition for 3 days prior to mRNA collection, with relative expression normalized to *GAPDH*. (B) *BCL-XL, MCL* and *S1PR1* gene expression are increased in PAX5⁻ cells during culture in 2% RPMI for 3 days. * $p < 0.05$ (vs. PAX5^{control}; Student's t-test); **$p < 0.005$ (vs. PAX5^{control}; Student's t-test).

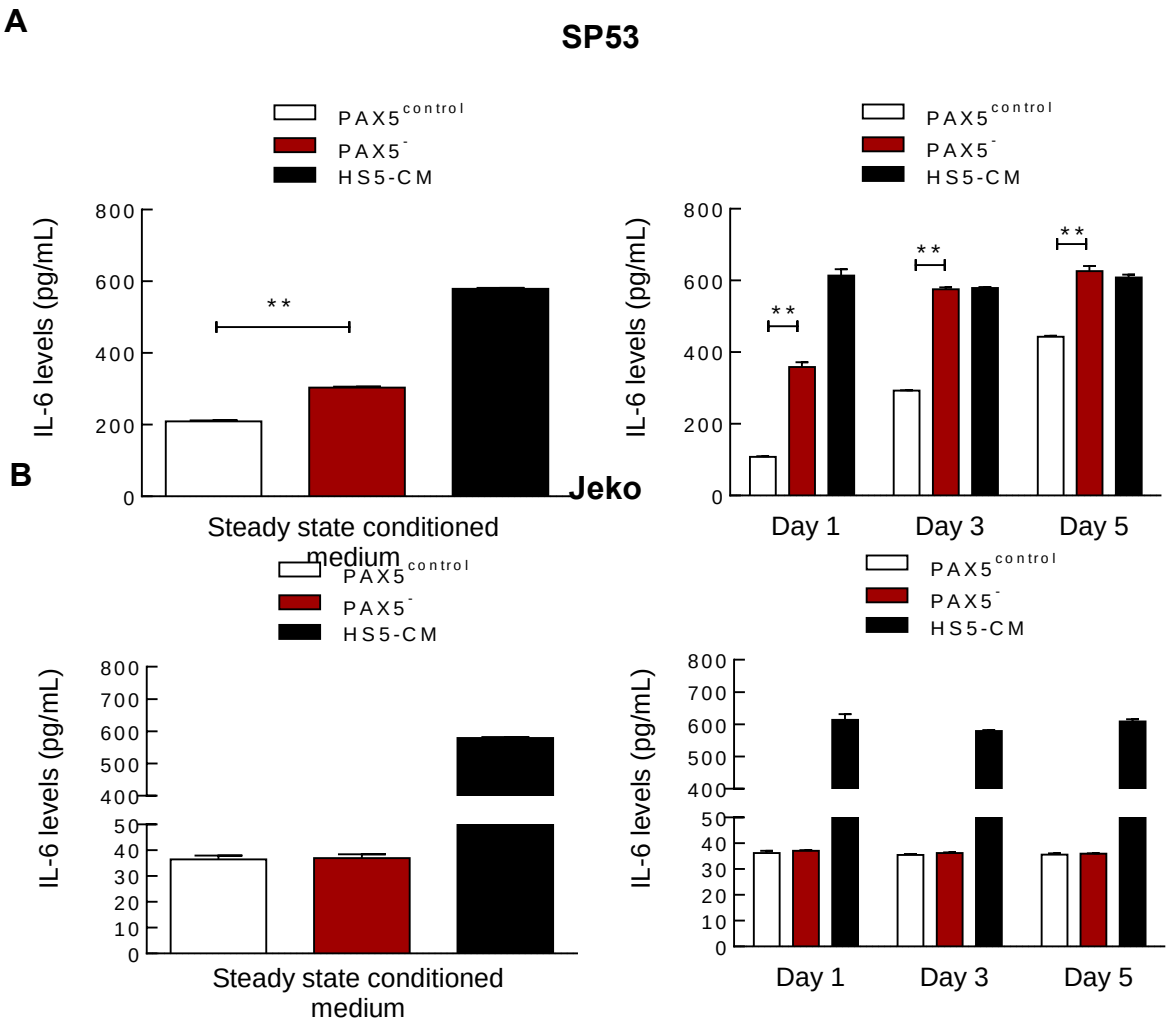

Figure 22: SP53 PAX5⁻ Cells Express Increased IL-6. (A) ELISA analyses of IL-6 using conditioned media from SP53 PAX5⁻ MCL cells or control cells. IL-6 level analyses at steady state levels (left) and during serum withdrawal (right). HS5 conditioned media used as a positive control, which is enriched for IL-6. (B) ELISA analyses of Jeko PAX5⁻ MCL supernatant. * $p < 0.05$ (vs. $PAX5^{control}$; Student's t-test); **$p < 0.005$ (vs. $PAX5^{control}$; Student's t-test).

markedly increased IL-6 secretion in SP53 PAX5^{-} cells compared to control cells (**Figure 22A**). However, Jeko, which do not produce autocrine IL-6 (Zhang, Yang et al. 2012), did not show increased IL-6 secretion upon PAX5 silencing or serum starvation (**Figure 22B**).

SUMMARY

In summary, we discovered that *PAX5* is downregulated in MCL patients, and PAX5^{-} MCL cells have a significant proliferative advantage in vitro and in vivo. This is significant, as MCL disease prognosis is heavily dependent on disease proliferation. We find that PAX5^{-} MCL cells have a similar gene repertoire as Pax5 knockdown murine cells, and to exhibit early expression of plasmacytic differentiation genes. This deregulation of genes is the possible cause of an increased tumorigenic phenotype seen in PAX5^{-} MCL cells.

Chapter 4: LOSS OF PAX5 LEADS TO AN INCREASE IN MANTLE CELL LYMPHOMA DISSEMINATION AND PROGRESSION

INTRODUCTION

Since there was a significant difference between normal and mantle cell lymphoma (MCL) PAX5 expression in patients, we postulated if PAX5 epxression might affect disease dissemination. Mantle cell lymphoma is characterized as a late stage disease, with patients often presenting with stage IV extranodal involvement. MCL can disseminate to the bone marrow, gastrointestinal tract, liver and neural tissue (Perez-Galan, Dreyling et al. 2011). About 30% of MCL patients also present with a leukemic phase. Thus, we sought to investigate if differential levels of PAX5 can affect MCL dissemination.

There is clinical evidence regarding the blastoid phenotype of mantle cell lymphoma. The blastoid form is said to be rarer, with about 15% of cases being reported to be blastoid. Patients exhibiting the blastoid phenotype have significantly poorer overall outcome (Bernard, Gressin et al. 2001, Perez-Galan, Dreyling et al. 2011), and a higher proliferation index leading to a worse prognosis. The blastoid variant has also been reported to be drug resistant is characterized by decreased TP53 expression and a constitutive AKT signaling axis. Both classical and blastoid MCL have been implicated in the latter (Rizzatti, Falcao et al. 2005), implicating the importance of B cell survival pathways in MCL.

RESULTS

Loss of PAX5 causes greater bone marrow engraftment

Similar to multiple myeloma, MCL cells originated from lymph nodes are frequently disseminated to the bone marrow compartments (Salaverria, Perez-Galan et

al. 2006).We evaluated the tumorigenic engraftment capacity of PAX5$^-$ MCL cells using an intravenous (I.V.) xenograft mouse model. We first transplanted 1 x 10^6 and 5 x 10^6 PAX5$^-$ MCL cells or control cells into NOD/SCID mice. After 6-8 weeks, organs were isolated from each mouse and evaluated for tumor engraftment by FACS analyses using human CD45 and GFP as markers. Statistically higher numbers of CD45$^+$ and GFP$^+$ cells were recovered in the PAX5$^-$ MCL xenograft mice compared to controls (**Figure 23**). Especially, cell engraftment to the bone marrows was significantly higher compared to controls regardless of cell transplant dosage (**Figure 23, Figure 24**). Immunohistochemistry analyses of frozen tissue sections also displayed increased numbers of CD45$^+$ cells in PAX5$^-$ xenograft bones. Increased dispersal of PAX5$^-$ MCL cells was found in the bone marrows compared to control SP53 cells (**Figure 25**) and Jeko cells (**Figure 26**).

Since we found an increased engraftment and dissemination of PAX5$^-$ MCL cells in the xenograft bones, we further investigated effects of PAX5 silencing on cell adhesion using HS5 human bone marrow stromal cells (BMSCs). GFP$^+$ PAX5$^-$ MCL cells were labeled with PKH26 red fluorescence dyes in order to easily track the cells (**Figure 27, Figure 28**). Since the adhesion assay was performed in one hour, it did not affect levels of PKH intensity in vitro (**data not shown**). Compared to control cells, PAX5$^-$ MCL cells demonstrated markedly increased cell adhesion to the HS5 BMSC monolayer (**Figure 29**).

PAX5 loss causes greater MCL dissemination

While observing PAX5 silenced and control cells in culture, we discovered an interesting phenomenon regarding cellular motility. PAX5$^-$ cells were more motile compared to control cells. We quantitatively measured distances travelled by MCL

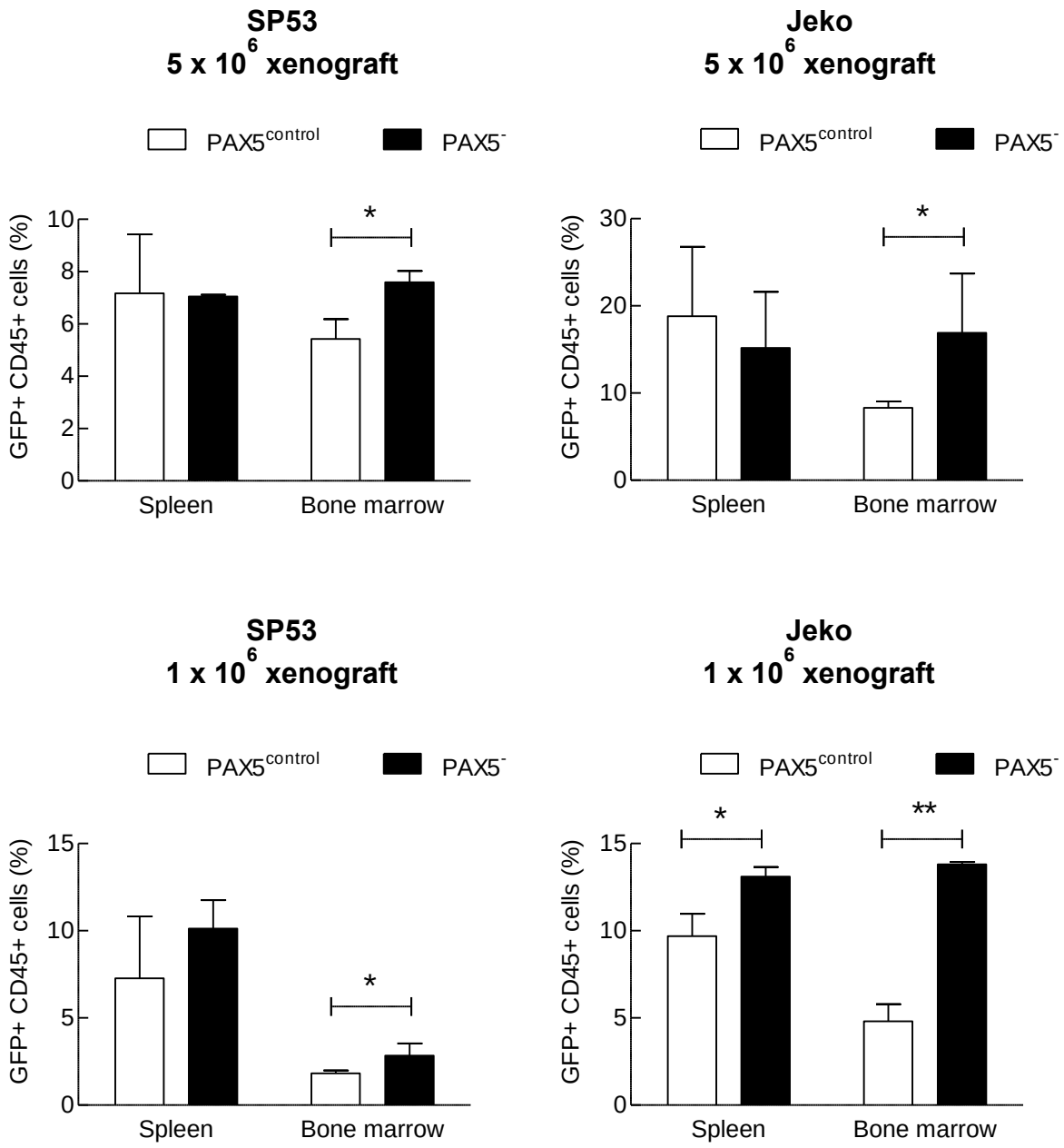

Figure 23: PAX5⁻ Cells Have Higher Bone Marrow Engraftment in vivo. PAX5⁻ MCL cells or control cells were injected into NOD/SCID mice (n=22) via I.V. injection at two different dosages (1 x 10^6 and 5 x 10^6). After 8 weeks, xenograft mice were sacrificed. Bone marrows (from femurs and tibias) and spleens were collected and stained for human leukocyte cells using anti-CD45 antibody. * $p < 0.05$ (vs. $PAX5^{control}$; Student's t-test); **$p < 0.005$ (vs. $PAX5^{control}$; Student's t-test).

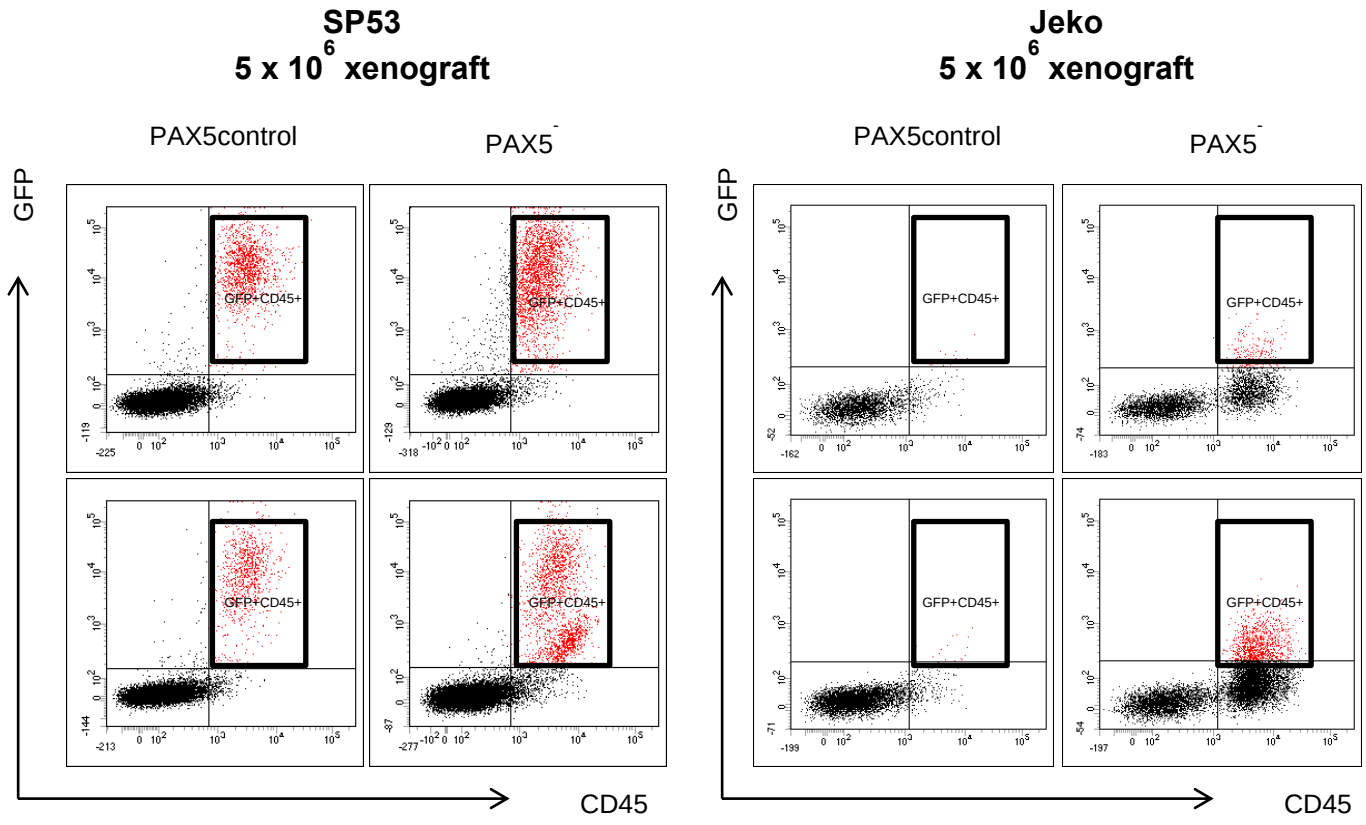

Figure 24: PAX5⁻ Cells Engraft More To the Bone Marrow. Representation of FACS analyses of bone marrow cells from PAX5⁻ MCL ($5x10^6$) injected xenograft mice. Higher numbers of GFP^+CD45^+ cells are noted in PAX5⁻ xenografts compared to controls. Both PAX5⁻ and control mice were sacrificed at the same time.

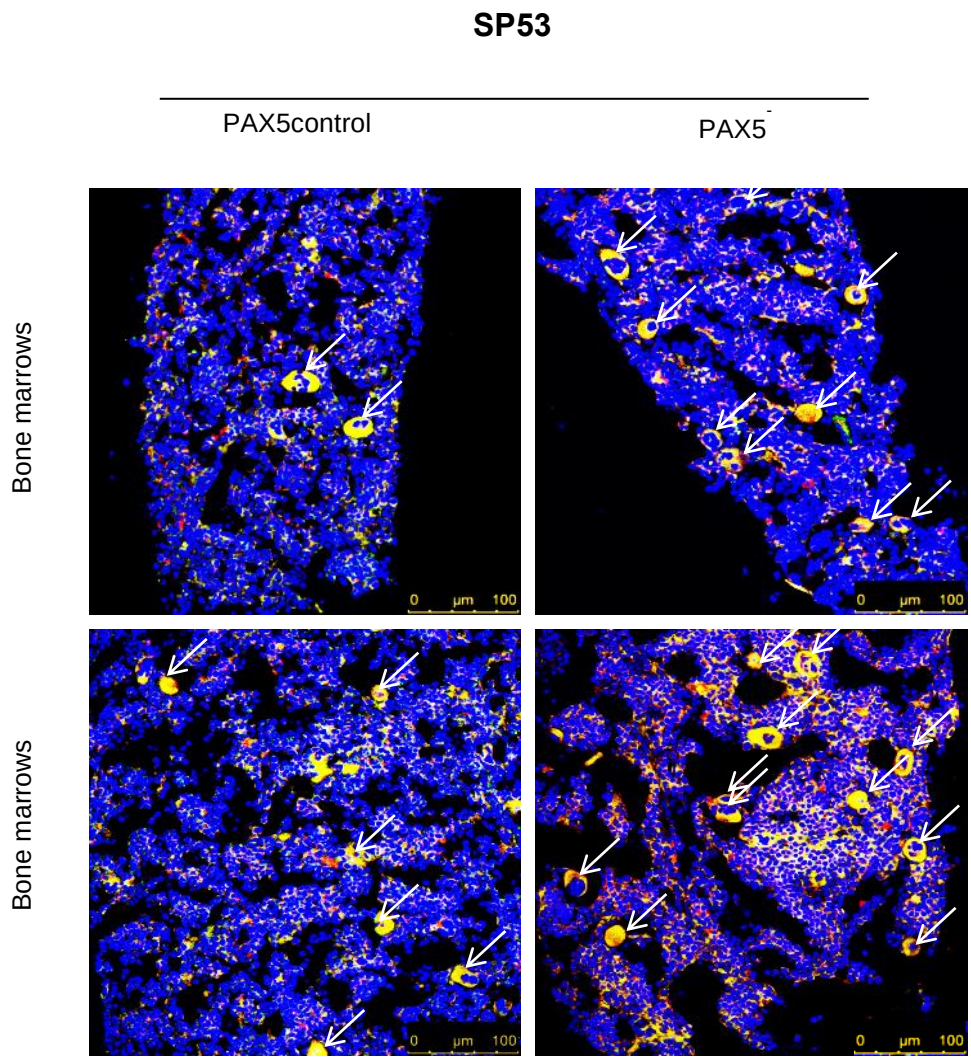

Figure 25: Increased Tumor Cell Engraftment in SP53 PAX5¯ Xenograft Mice.

Representative confocal images of the bone sections of xenograft mice. Increased CD45 and GFP positive cells in host tissue (bone marrow). Arrows indicate CD45 and GFP positive cells. Scale bar, 100µm.

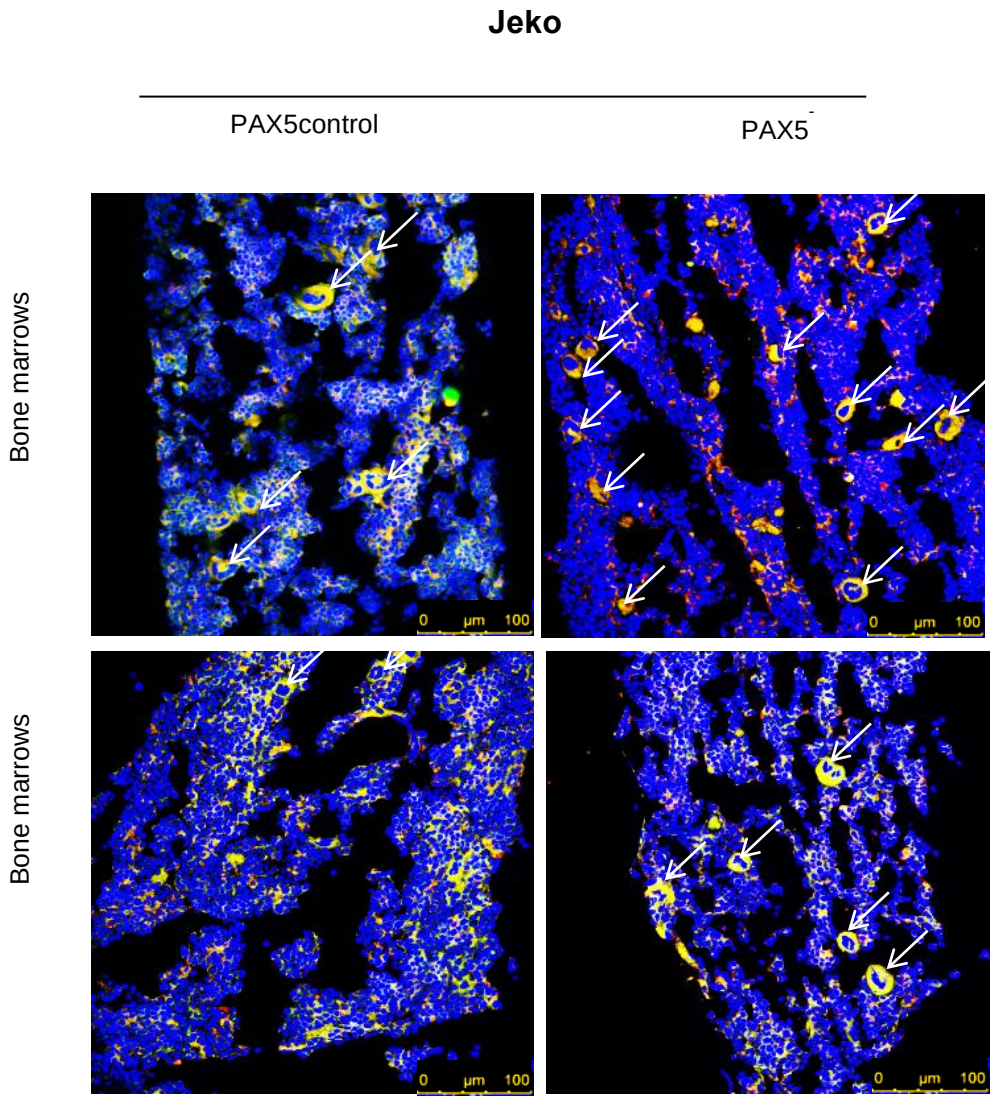

Figure 26: Increased Tumor Cell Engraftment in Jeko PAX5⁻ Xenograft Mice.

Representative confocal images of the bone sections of xenograft mice. Increased CD45 and GFP positive cells in host tissue (bone marrow). Arrows indicate CD45 and GFP positive cells. Scale bar, 100µm.

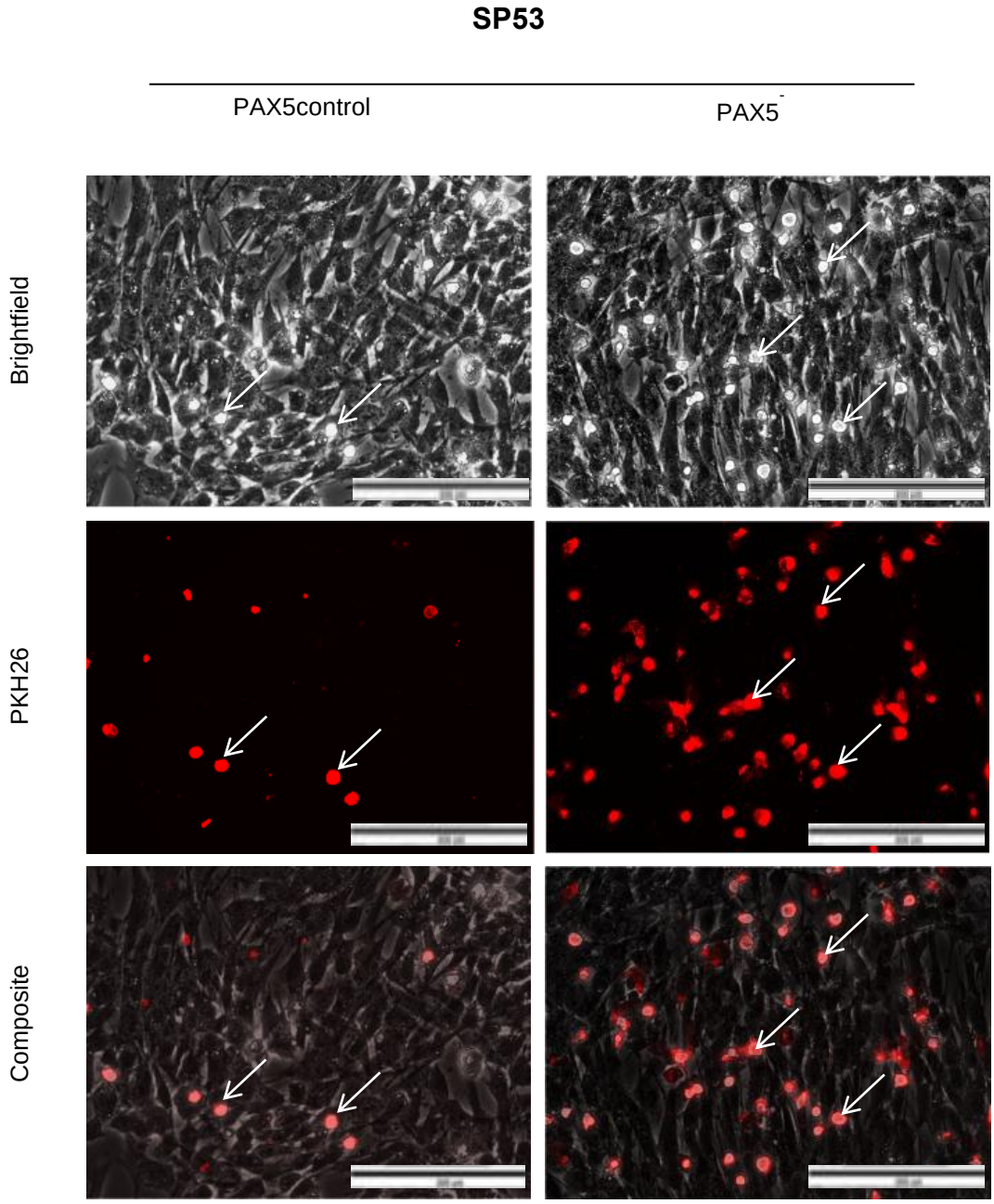

Figure 27: SP53 PAX5⁻ Cells Exhibit Increased Bone Marrow Adhesion. Control or PAX5⁻ SP53 cells were stained with PKH26 and subsequently seeded onto a pre-established monolayer of HS5 bone marrow stromal cells. Arrows point to PKH26$^+$ cells. Scale bar, 200µm.

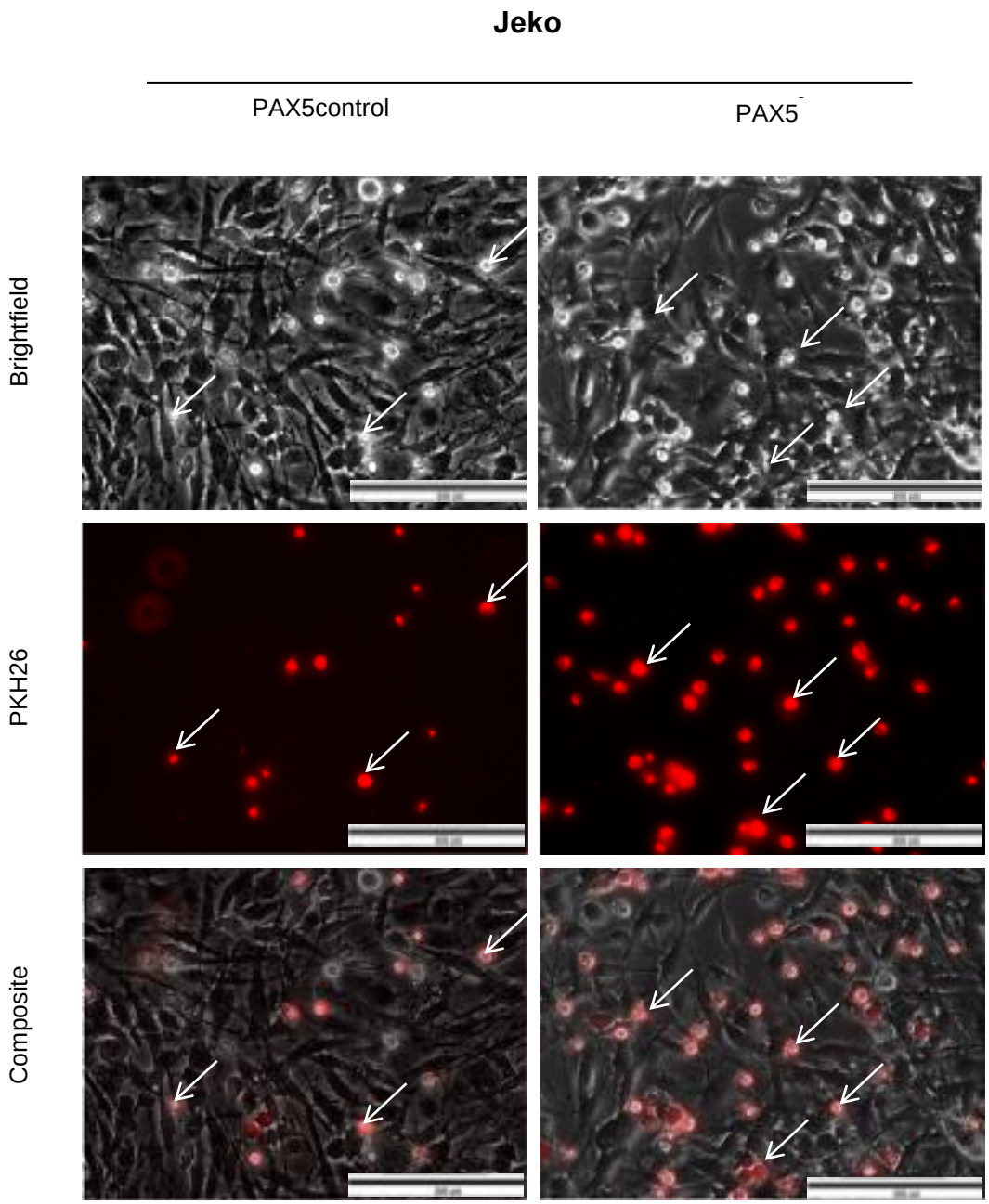

Figure 28: Jeko PAX5⁻ Cells Exhibit Increased Bone Marrow Adhesion. Control or PAX5⁻ Jeko cells were stained with PKH26 and subsequently seeded onto a pre-established monolayer of HS5 bone marrow stromal cells. Arrows point to $PKH26^{+}$ cells. Scale bar, 200µm.

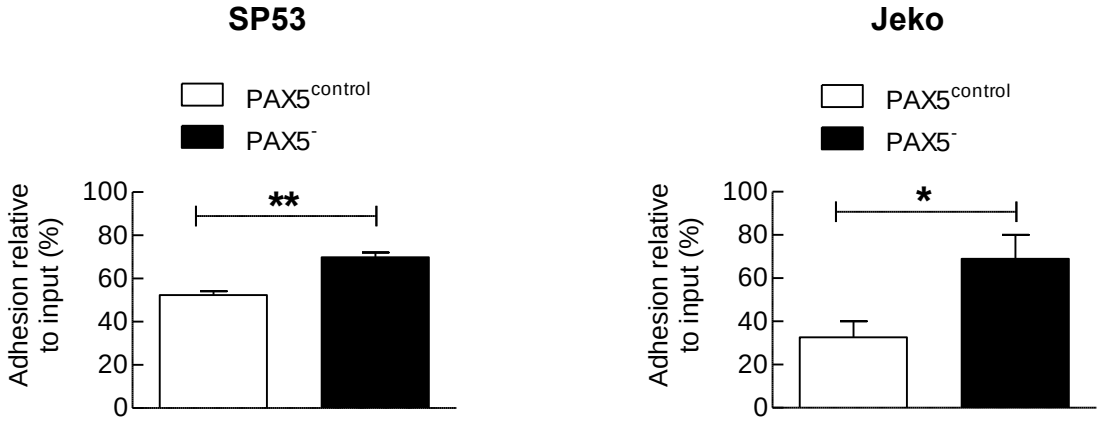

Figure 29: Increased Bone Marrow Adhesion in PAX5⁻ Cells. In vitro adhesion of lymphoma cells to HS5 BMSCs was calculated by measuring PKH26 dye intensity relative to fluorescent reading of inputs. Each value represents the mean ± S.D (n=6).

* $p < 0.05$ (vs. $PAX5^{control}$; Student's t-test); **$p < 0.005$ (vs. $PAX5^{control}$; Student's t-test).

PAX5$^-$ and control cells over 2 days using time lapse video microscopy. Distances (μm) traveled by PAX5 silenced SP53 and Jeko cells, which were averaged of results from 18 different wells, were far greater compared to control cells (**Figure 30**). PAX5$^-$ MCL cells also displayed a greater sense of motility overall – on average PAX5$^-$ MCL cells were significantly faster than control cells (**Figure 31**). When analyzing for the maxima (replicate with highest motility) and minima (replicate with lowest motility) of speed, we find that PAX5$^-$ MCL cells have greater amplitudes for velocity than control cells, suggesting a greater rate of motility (**Figure 31**).

To investigate the role PAX5 has in dissemination in vivo, we transplanted SP53 cells via subcutaneous injection into NOD/SCID hosts. As observed, PAX5$^-$ SP53 xenograft mice developed larger tumors compared to controls (**Figure 16A**). Using ^{18}F-FDG uptake, we successfully determined PAX5$^-$ xenografts having more dissemination sites infiltrated with tumor cells (**Figure 32**). All PAX5$^-$ xenografts had tumor cell infiltration of the thymus, bone marrow or spleen. We also analyzed gastrointestinal track (GIT) harvested organs from SP53 PAX5$^-$ xenografts for tumor cell infiltration. PAX5$^-$ xenografts had significantly higher counts than control xenografts (**Figure 33A**). Interestingly, we noticed that 5 patients reported to have GIT involvement have significantly lower levels of *PAX5* transcript (**Figure 33B**) as well, implying that downregulation of PAX5 expression might be an important event in MCL dissemination.

Within MCL samples, PAX5 levels in CD19$^+$ cells from bone marrows were significantly decreased compared to blood samples (**Figure 34**). This supports our observation that PAX5$^-$ MCL cells have increased bone marrow engraftment in vivo. When we compared paired (blood and bone marrow) MCL samples from two patients,

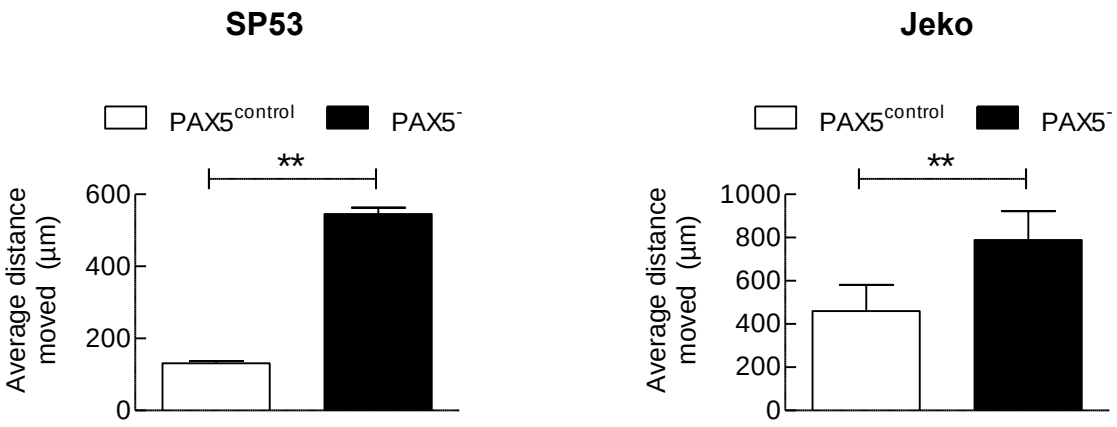

Figure 30: PAX5⁻ Cells Have Increased Motility in Vitro. PAX5⁻ MCL cells were stained with PKH26 and subsequently tracked over 24 hours using time lapse video microscopy. Total average distance moved for PAX5⁻ and control MCL cells was measured, with PAX5⁻ cells moving further on average. Movement of single cells (n=18) were tracked using the Amira software. * $p < 0.05$ (vs. $PAX5^{control}$; Student's t-test); ** $p < 0.005$ (vs. $PAX5^{control}$; Student's t-test).

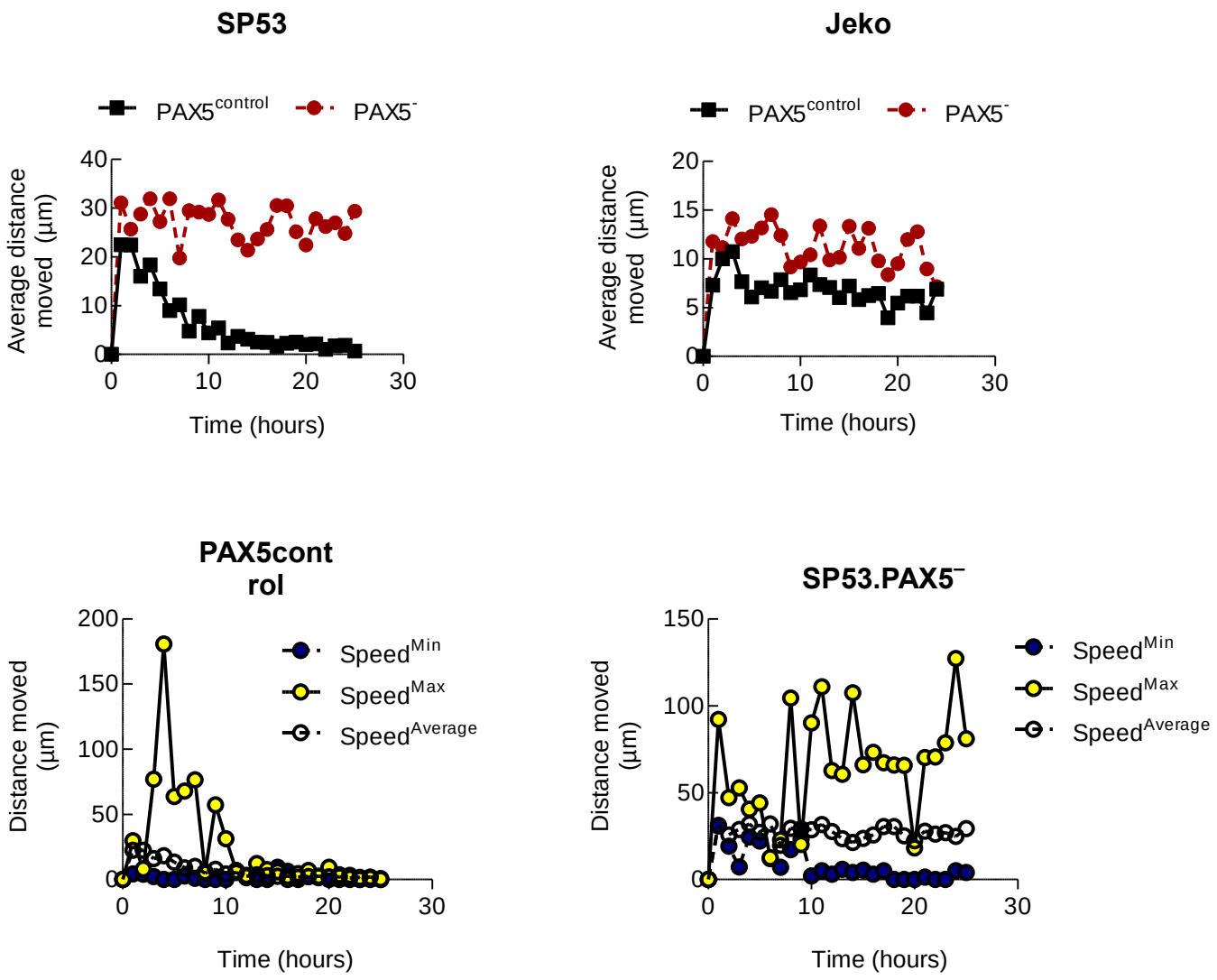

Figure 31: PAX5⁻ Cells Have Greater Maximum Velocity in vitro. (Top) Average distance moved for PAX5⁻ and control MCL over time. (Bottom) The fastest moving replicate ($Speed^{Max}$), slowest moving replicate ($Speed^{Min}$) and average ($Speed^{Average}$) was compared between SP53 PAX5⁻ and control MCL cells. Distance moved was plotted against time.

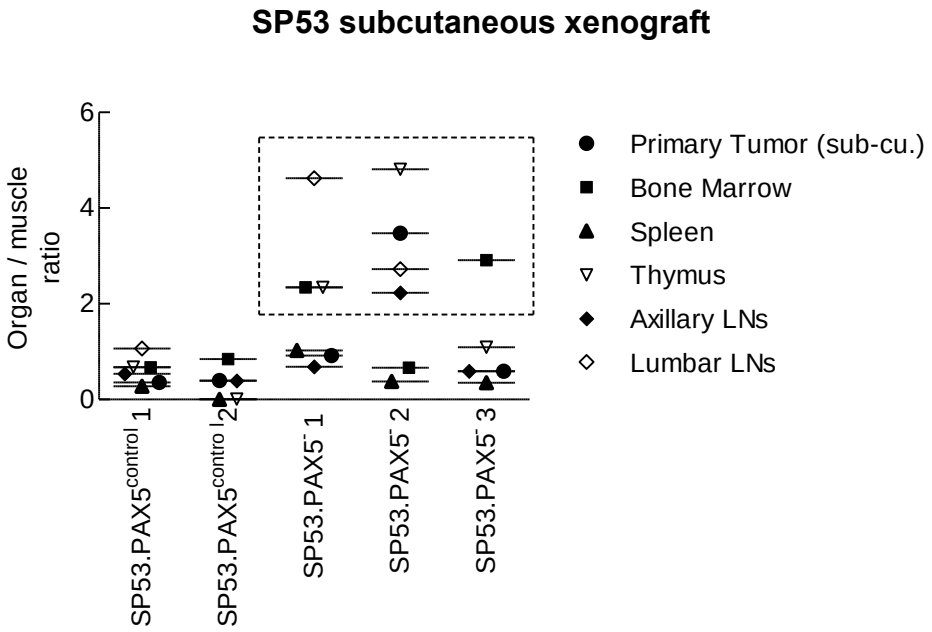

Figure 32: Increased Tumor Cell Dissemination in SP53 PAX5⁻ xenograft mice.

^{18}F-FDG counts of common MCL dissemination organ sites from SP53 PAX5⁻ or control subcutaneous xenografts. (%) ID / g of each target organ was normalized to (%) ID / g of muscle tissue. ID/g = injected dose / gram, LN = lymph node. Dotted box highlights target organs with at least twice the amount of muscle ^{18}F-FDG uptake. Sub-cu = subcutaneous, LN = lymphnode.

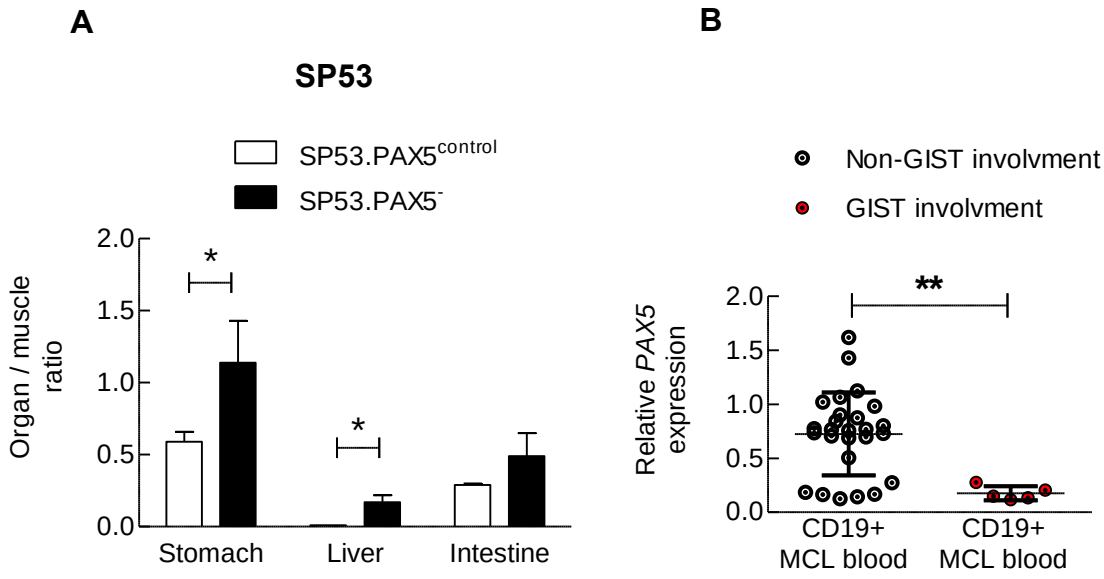

Figure 33: Increased GIT Dissemination in SP53 PAX5⁻ Xenograft Mice. (A) ^{18}F-FDG counts of GIT harvested organs from SP53 PAX5⁻ or control subcutaneous xenografts. (%) ID / g of each target organ was normalized to (%) ID / g of muscle tissue. ID/g = injected dose / gram (B) CD19^{+} cells isolated from MCL GIT-involved patients (n=5) contained lower levels of PAX5 mRNA compared to CD19^{+} cells from MCL non-GIT patients (n=26). Each group represents the mean ± S.D. * $p < 0.05$ (vs. PAX5^{control}; Student's t-test); **$p < 0.005$ (vs. PAX5^{control}; Student's t-test).

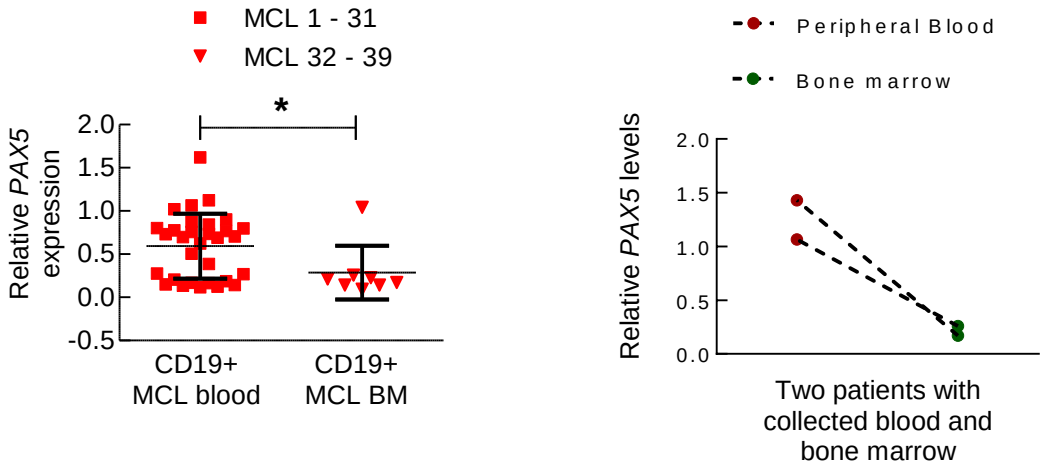

Figure 34: Decreased PAX5 Levels in CD19^{+} Bone Marrow MCL Cells. (Left) CD19^{+} B cells were isolated from MCL blood or apharesis samples (n=31) or from bone marrows of or MCL patients (n=8) and PAX5 mRNA levels determined via qRT-PCR. Each replicate was run in triplicate with values normalized to *GAPDH*. (Right) Two patients with paired peripheral blood and bone marrow were analyzed for PAX5 mRNA levels. CD19^{+} bone marrow cells had less PAX5 transcript compared to peripheral blood when comparing within the same patient. * $p < 0.05$ (vs. PAX5^{control}; Student's t-test); **$p < 0.005$ (vs. PAX5^{control}; Student's t-test).

we find that PAX5 expression of $CD19^+$ cells from the bone marrow was significantly reduced compared to PAX5 expression of peripheral blood in both patients (**Figure 34**).

In order to find relevancy in xenograft models, we transplanted unmanipulated (parental) SP53 MCL cells into mouse xenograft host via subcutaneous injection and evaluated PAX5 levels of dispersed human cells harvested from the spleen or bone marrows of xenograft mice. PAX5 levels are significantly lower in human cells isolated from the spleen and bone marrows, when compared to the parental subcutaneous tumors (**Figure 35**). This again points to PAX5 downregulation being an important event in MCL dissemination. Overall, our data implicates loss of PAX5 expression involvement in MCL organ dissemination.

PAX5 expression as a predictor for aggressive MCL

The median survival of MCL ranges from 3-5 years. The blastoid variant type of MCL is a highly aggressive but a rare form of MCL and demonstrates a worse prognosis than the common forms of MCL (Argatoff, Connors et al. 1997, Bosch, López-Guillermo et al. 1998, Bernard, Gressin et al. 2001). Analysis of samples revealed that blastoid types contained significant reduced levels of *PAX5* compared to non-blastoid cases (**Figure 36**). We found that overall survival of patients with $PAX5^{low}$ was significantly lower than survival of patients with $PAX5^{high}$ (**Figure 37**), even when stratifying for *PAX5* levels in two different manners; $PAX5^{low}$ were either classified as bottom 25% or 50%. $PAX5^{low}$ patients exhibited survival rates very similar to that of verified blastoid survival cases within our data set (**Figure 38**), suggesting *PAX5* levels can be used to predict survival within advanced MCL patients. Collectively, our data

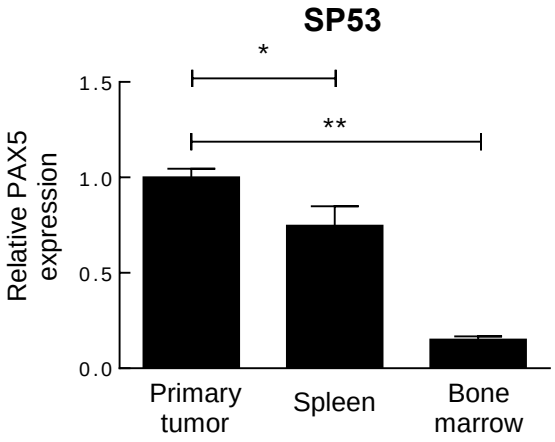

Figure 35: *PAX5* Is Downregulated in Disseminated Cells. A total of 3x 10^6 unmanipulated SP53 parental cells were injected subcutaneously into host xenografts and *PAX5* mRNA expression determined from isolated human cells 6 weeks post injection. Human cells were isolated from the host tumor, spleen and bone marrow with *PAX5* mRNA levels were determined via qRT-PCR. Each replicate was run in triplicate with values normalized to *GAPDH*. * $p < 0.05$ (vs. $PAX5^{control}$; Student's t-test); ** $p < 0.005$ (vs. $PAX5^{control}$; Student's t-test).

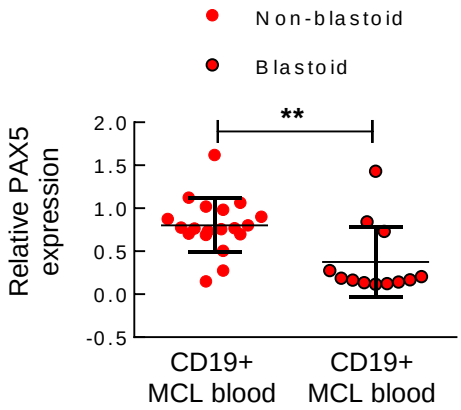

Figure 36: MCL Blastoid Variants Have Significantly Reduced *PAX5* expression. $CD19^+$ cells isolated from MCL blastoid patients (n=12) contained lower levels of *PAX5* mRNA compared to $CD19^+$ cells from MCL non-blastoid patients (n=19). Each group represents the mean ± S.D. * $p < 0.05$ (vs. $PAX5^{control}$; Student's t-test); **$p < 0.005$ (vs. $PAX5^{control}$; Student's t-test). * $p < 0.05$ (vs. $PAX5^{control}$; Student's t-test); **$p < 0.005$ (vs. $PAX5^{control}$; Student's t-test).

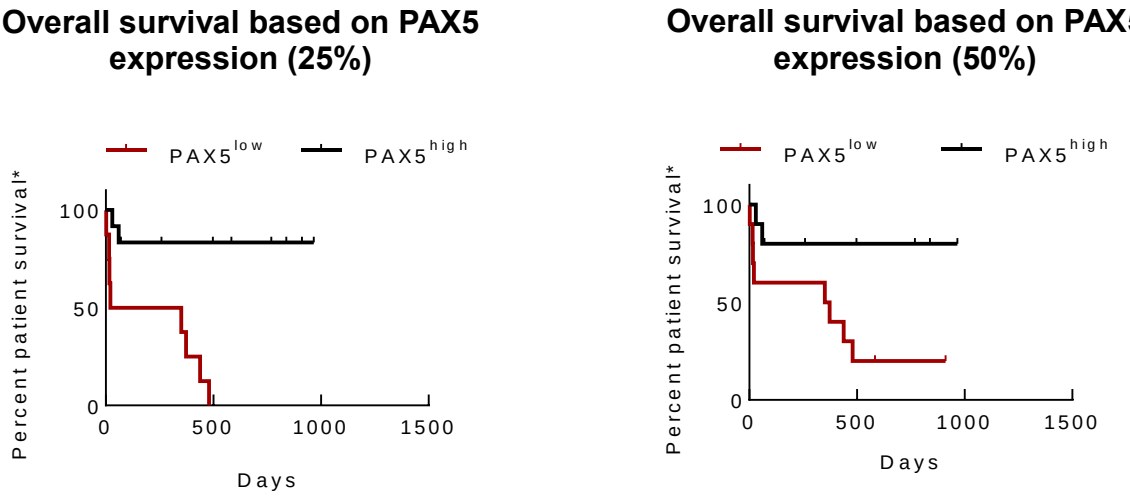

Figure 37: PAX5^{low} MCL Patients Have Significantly Poorer Overall Survival.

Overall survival of MCL patients were significantly decreased in PAX5^{low} populations compared to PAX5^{high} populations. (Left) Samples were stratified to be top 75% = PAX5^{high}, bottom 25% = PAX5^{low}. (Right) Samples were stratified to be top 50% = PAX5^{high}, bottom 50% = PAX5l^{ow}. All analyses were significant (p-value < 0.05 Mantel-Cox curve analysis).

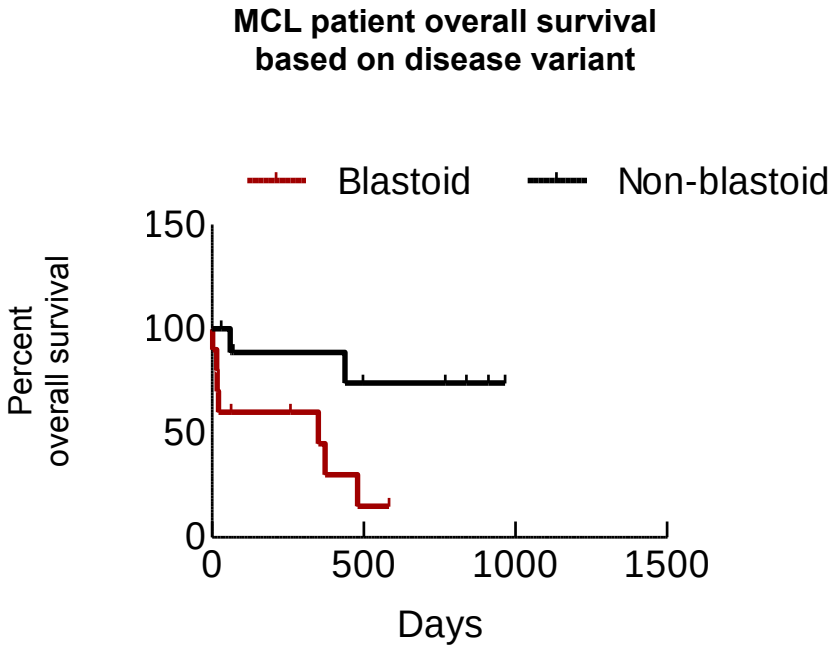

Figure 38: MCL Blastoid Variants Have Significantly Poorer Overall Survival.

Patients with blastoid type MCLs demonstrate a poor overall survival compared to patients with non-blastoid MCL. A total 20 patients were evaluated, with blastoid (n=10) and classical (n=10) cases analyzed for overall survival. *p-value < 0.05 Mantel-Cox and Gehan-Breslow-Wilcoxon.

support PAX5 down-regulation is an important signaling event in MCL that contribute to increased progression and dispersal.

PAX5⁻ have increased AKT, ERK and pSTAT3 signaling

PAX5⁻ MCL cells expressed increased levels of positive cell cycle regulators such as CDKs and cyclins, and decreased levels of negative cell cycle regulators such as TP53 and CDKN1A (**Figure 18**). In order to find molecular pathways that contribute to the growth of PAX5⁻ MCL, we first examined pathways that have been known to be expressed in different hematological malignancies such as the PI3K/AKT/mTOR signaling axis and MAPK/ERK pathway (Dal Col, Zancai et al. 2008, Psyrri, Papageorgiou et al. 2009, Wang, Atayar et al. 2009, Dennison, Shanmugam et al. 2010, Carlo-Stella, Locatelli et al. 2013). Immunoblots showed highly activated signaling components involved in AKT/mTOR pathways such as pmTOR, p-p70 and pAKT, which could account for an increase in proliferation exhibited by PAX5– MCL cells (**Figure 39**). pERK and pMAPK have been implicated in cell survival, adhesion to the microenvironment as well as motility (Kolch 2005), and we also observed an increase of these proteins in PAX5⁻ MCL cells (**Figure 39**). Cyclin D1, a genetic hallmark for MCL, was also upregulated in PAX5⁻ MCL cells (**Figure 39**) (Bea, Salaverria et al. 2009). *CCND3*, which encodes for cyclin D3, has been previously reported to be critical in B cell lymphopoiesis (Cooper, Sawai et al. 2006), and has been implicated in compensating for loss of cyclin D1 function in MCL (Rosenwald, Wright et al. 2003). Here, we report that PAX5⁻ MCL and non-MCL B cell cells express increased *CCND3* transcripts (**Figure 40**).

Since we observed an increase of PAX5⁻ cells engraftment to the bone marrow, we determined if PAX5 expression can affect MCL response to the bone marrow

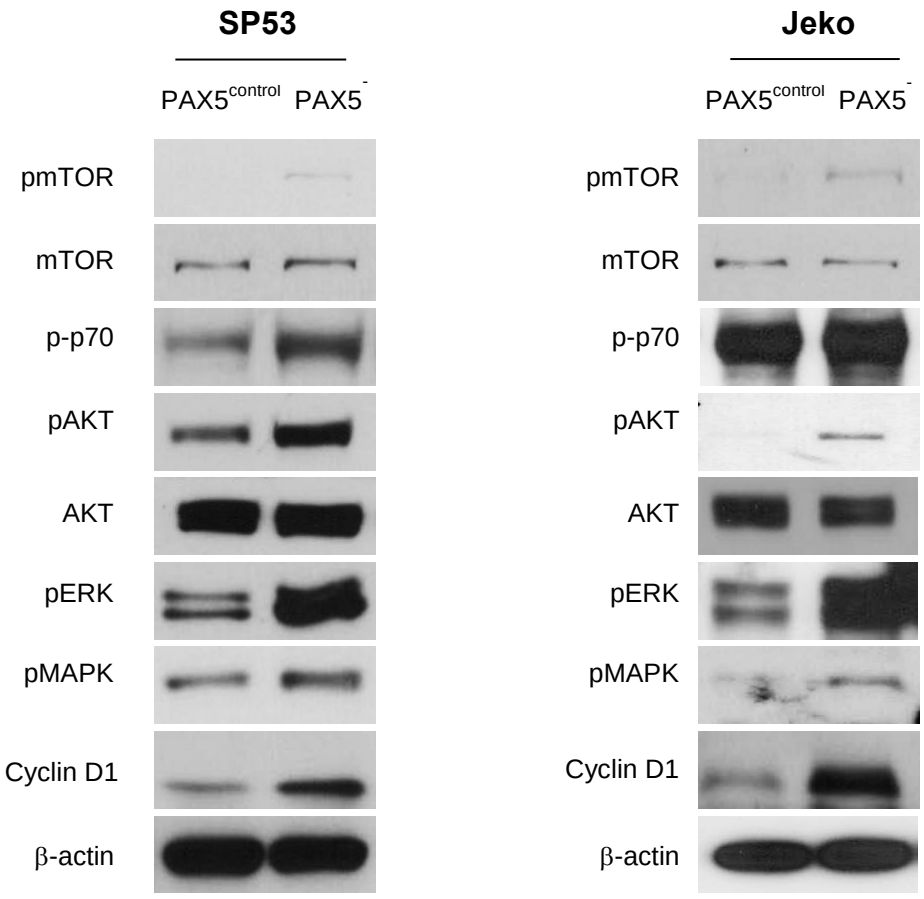

Figure 39: Increased MCL Signaling Pathway Proteins PAX5⁻ cells. Immunoblot analyses of pmTOR, p-p70, p-AKT, pERK (p42/44) and pMAPK (p38) in control and PAX5⁻ MCL cells with β-actin serving as the loading control.

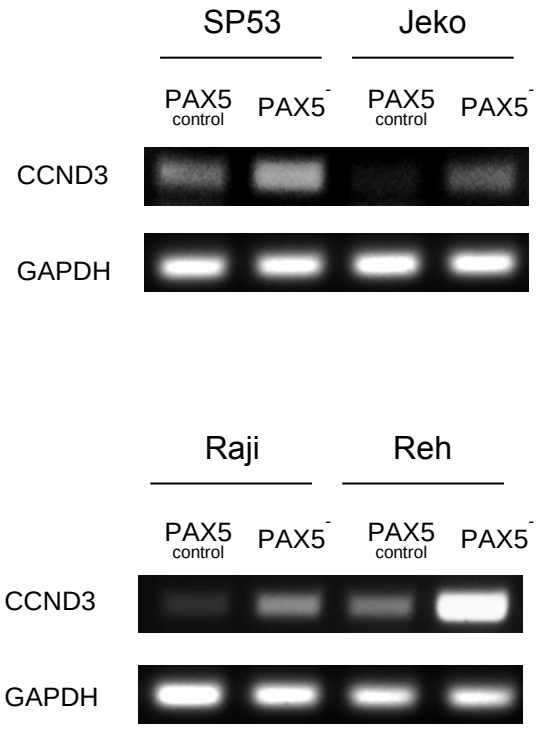

Figure 40: PAX5⁻ Cells Express Increased Amounts of CCND3. Semi quantitative RT-PCR analysis *CCND3* upon PAX5 silencing in MCL and non MCL B cells. *GAPDH* serves as a loading control.

microenvironment. We used conditioned media from HS5 human BMSCs which are enriched for IL-6 (Delk and Farach-Carson 2012), an alternative source of paracrine IL-6. HS5-conditioned medium was supplemented to growth media and the cells allowed to grow in culture for 3 days. At steady state (0 hours), PAX5^{-} MCL constitutively expressed higher levels of phosphorylated STAT3 which was largely increased upon HS5 addition compared to controls (**Figure 41**), suggesting PAX5^{-} cells exhibit a phenotype that is more sensitive to bone marrow microenvironmental cues.

SUMMARY

In summary, we found PAX5^{-} cells significantly engraft more to the bone marrow, while displaying increased adhesion to human BMSCs in vitro. *PAX5* was also found to be downregulated in MCL patient bone marrow compared to peripheral blood. This was corroborated by our finding that PAX5^{-} xenografts have greater tumor infiltration of the bone marrow and that PAX5 downregulation is an important step in in vivo MCL dissemination. Critically, we also report that *PAX5* expression is a predictor for the blastoid phenotype, and that its expression could be used as a means for survival prognosis.

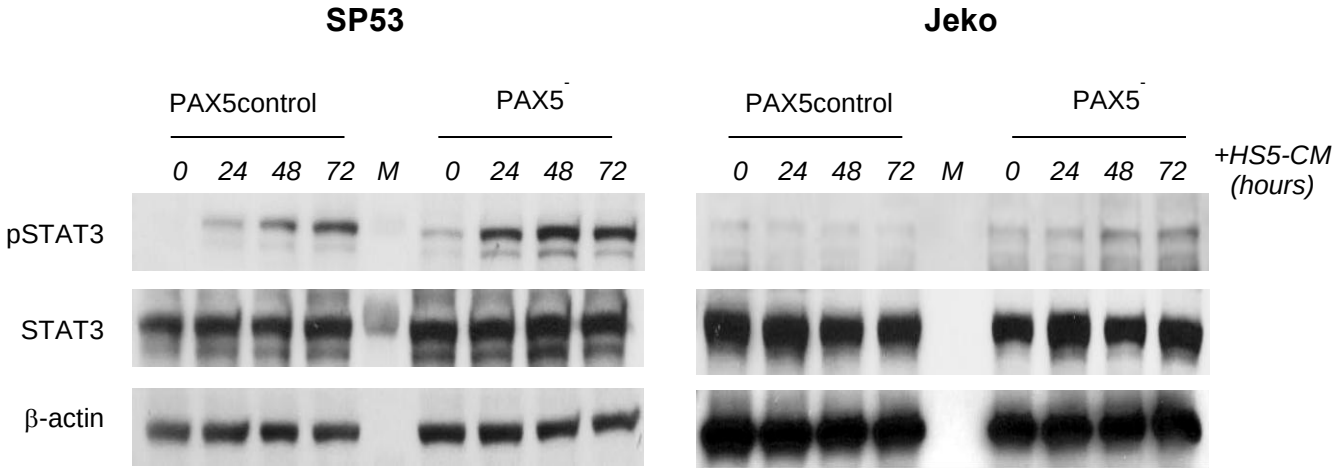

Figure 41: PAX5¯ Cells Have Increased pSTAT3 Signaling in BM Conditioned Media. Immunoblot analyses of pSTAT3 expression in PAX5¯ and control MCL cells upon incubation with HS5 conditioned medium during culture. HS5-CM was added to culture for up to 3 days prior to protein collection. Total STAT3 and β-actin served as loading controls.

Chapter 5: PAX5 EXPRESSION AFFECTS MANTLE CELL LYMPHOMA DRUG SENSITIVITY

INTRODUCTION

Mantle cell lymphoma is a disease marked with increased therapeutic resistance. MCL patients often present with advanced disease, and 20-80% achieves complete remission. However, a high majority of patients suffer relapse, pointing to MCLs harboring a subpopulation of cells that are drug resistant clones that have the ability to reconstitute the disease over time (Jung, Chen et al. 2011).

Bortezomib is a proteasome inhibitor that has found clinical success in multiple myeloma and in mantle cell lymphoma (O'Connor, Moskowitz et al. 2009) is used as a second line treatment option in patients that have failed the first course of treatment. Bortezomib functions by eliciting the unfolded protein response (UPR) in cells, thus leading to cell apoptosis via NOXA upregulation (Perez-Galan, Roue et al. 2006). However, there are reported cases where second line therapy of bortezomib failed to clear the disease (Suh and Goy 2008), hinting again to a population of MCL cells that are highly drug resistant.

To further decipher the drug resistance properties of our cells, we performed a high throughput screen (HTS) of 3864 compounds on Jeko and SP53 control and $PAX5^{-}$ MCL cells. This screen was performed to elucidate the role differential PAX5 expression might have in MCL disease resistance, which is a common hallmark of MCL. Critically, there has not been a previous study employing a HTS of clinical and novel compounds in targeting MCL cells. As such, much was garnered regarding MCL biology and physiology through this HTS.

RESULTS

PAX5 affects drug resistance in vitro

Doxorubicin and etoposide are chemotherapeutic agents that can induce p53 derived cell damage responses (Karpinich, Tafani et al. 2002, Manna, Gangadharan et al. 2012). When SP53 was treated with doxorubicin, an impaired response in TP53 transcription was observed in PAX5$^-$ MCL cells (**Figure 42A**) (Dai, Tang et al. 2011). TP53 transcript levels increased significantly within 24 hours of doxorubicin treatment in control cells (**Figure 42A**). RT-PCR analyses also showed that after 6 and 12 hours of etoposide treatment PAX5$^-$ cells have lower levels of *TP53* transcript (**Figure 42B**). As predicted from *TP53* expression responses after drug treatment, PAX5$^-$ SP53 cells were more resistant to treatment of doxorubicin (**Figure 43**).

Since PAX5$^-$ MCL cells showed increased resistance compared to controls (**Figure 42 and 43**), we further investigated roles of PAX5 in drug resistance of MCL using a clinically relevant reagent, bortezomib. Bortezomib inhibits proteasome activities and is widely used to treat MCL, albeit with varying clinical efficacy due to drug-resistant tumor cells (Suh and Goy 2008). PAX5$^-$ MCL cells showed increased resistance to bortezomib and bortezomib contained regimens (**Figure 44**). A recent study showed that MCL cell lines and unfractionated primary MCL cells differentiate into plasma-like cells after exposure to bortezomib (Pérez-Galán, Mora-Jensen et al. 2011). These bortezomib-resistant cells show elevated expression of CD138, CD38 and BLIMP1, and lack CD19. PAX5$^-$ cells have increased CD138 and *BLIMP1* expression (**Figure 6 and 7**). PAX5 normally represses BLIMP1 expression and promotes CD19 expression during normal B cell development (Johnson, Shapiro-Shelef et al. 2005), suggesting

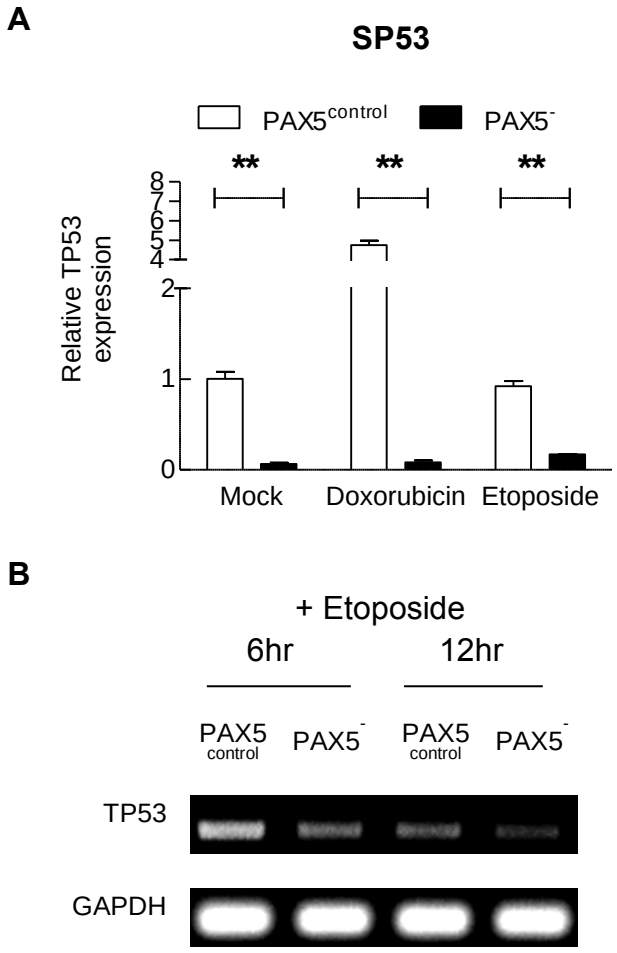

Figure 42: PAX5⁻ SP53 Cells Have a Delayed TP53 Response to DNA Damage. (A) Delayed *TP53* upregulation in PAX5⁻ MCL cells in response to DNA damaging agents. PAX5⁻ MCL cells were treated with doxorubicin (500nM) and etoposide (200nM) for 24 hours and *TP53* mRNA expression was evaluated by qRT-PCR. *GAPDH* served as a loading controls for PCR experiments. (B) *TP53* expression in response to etoposide**.** Cells were treated with etoposide (200nM) for 6 and 12 hours and *TP53* expression was evaluated by semi-quantitative RT-PCR. * $p < 0.05$ (vs. $PAX5^{control}$; Student's t-test); ** $p < 0.005$ (vs. $PAX5^{control}$; Student's t-test).

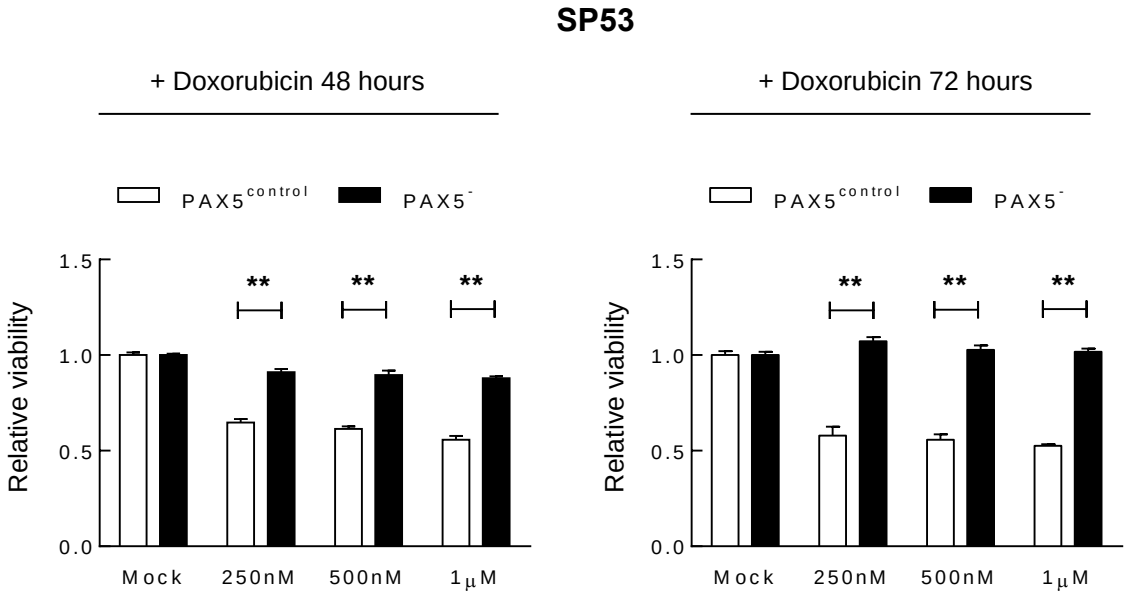

Figure 43: PAX5⁻ SP53 Cells Are More Resistant to Doxorubicin. PAX5⁻ cells are more resistant to doxorubicin. Cells were treated with doxorubicin for 48 to 96 hours and cell viability was analyzed using CTB® assays. Each value represents the mean ± S.D (n=3). * $p < 0.05$ (vs. $PAX5^{control}$; Student's t-test); ** $p < 0.005$ (vs. $PAX5^{control}$; Student's t-test).

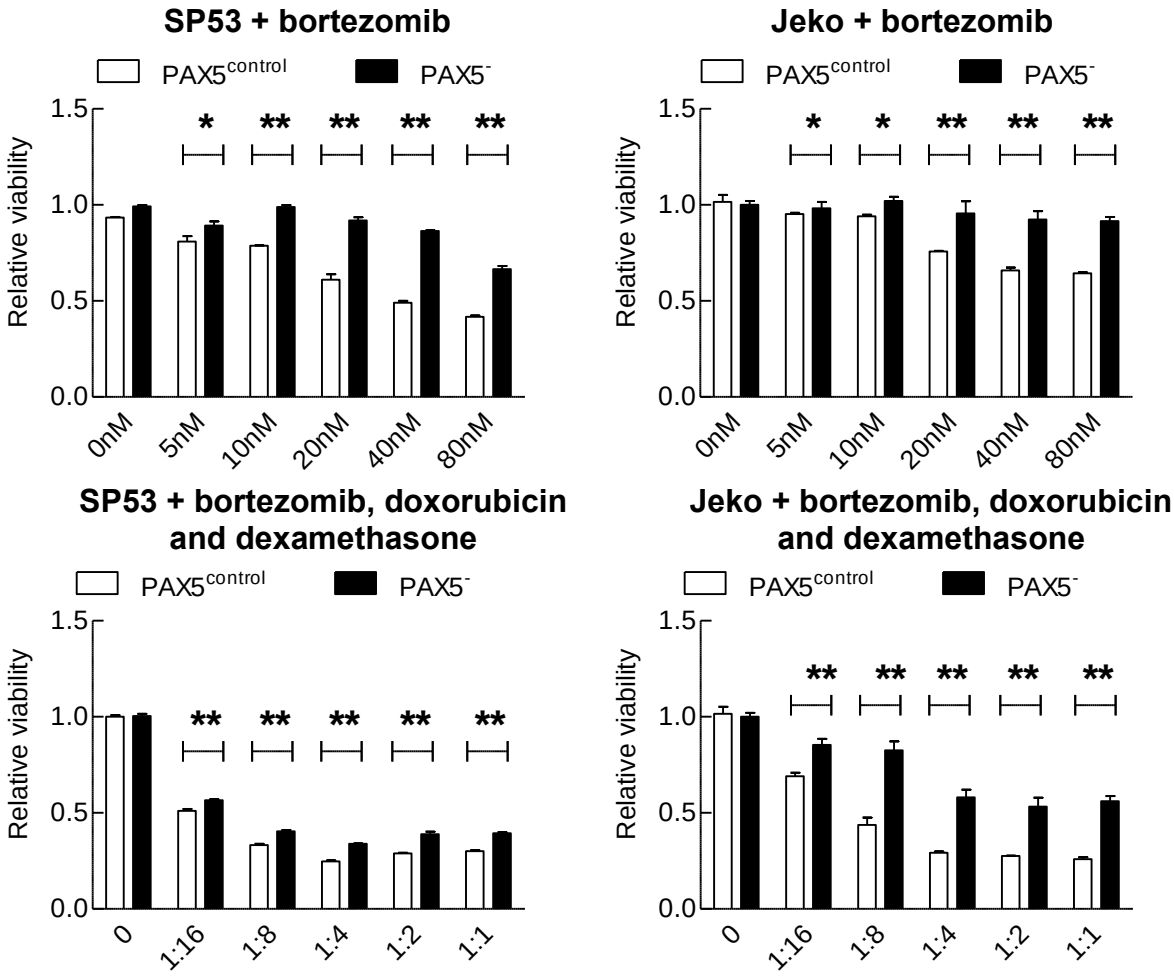

Figure 44: PAX5⁻ Cells Are More Resistant to Bortezomib. PAX5⁻ and control MCL cells were treated either with bortezomib or a bortezomib combined regiment (80nM bortezomib, 4µg/mL doxorubicin and 40µg/mL dexamethasone) for 24 hours. Cellular viability was measured using CellTiterBlue™. Each value represents the mean ± S.D (n=3). * $p < 0.05$ (vs. $PAX5^{control}$; Student's t-test); ** $p < 0.005$ (vs. $PAX5^{control}$; Student's t-test).

that PAX5 down-regulation may be an important event for bortezomib resistance in MCL.

High-throughput screen of 3864 compounds

To profile for functional therapeutic targets against our highly aggressive PAX5^{-} populations, a high-throughput screen (HTS) of 3864 compounds was performed using the two MCL cell lines (SP53 and Jeko). Prior to the start of the screen, growth conditions for each cell line used were measured to ensure optimization of our HTS, where differences in compound toxicity could be replicated with high reproducibility and sensitivity**.** Cells were seeded at varying densities and cell number measured over three or four days either through the use of proliferative assays (CellTiterBlue™ PROMEGA) or through direct imaging of cells stained with nucleic acid dyes (**data not shown**). As we plan to use a robotic platform to facilitate our HTS, a positive control to ensure consistent compound transfer from stock to assay plates needed to be determined.

Six compounds were chosen for their use in general cell cytotoxicity – paclitaxel, anisomysin, carbonyl cyanide m-chlorophenyl hydrazine (CCCP), etoposide, doxorubicin and doxetaxel **(Figure 45)**. All compounds are common cell cytotoxic inducers and would serve as ideal positive controls for our HTS. Three of the compounds were further analyzed for consistency in inhibition across all cell lines (**Figure 46**). Finally, reproducibility assays were conducted with our chosen positive control (doxorubicin) so that a clear distinction between signals (positive controls, positive hits) and that to noise (negative controls, negative hits) of our HTS could be recorded.

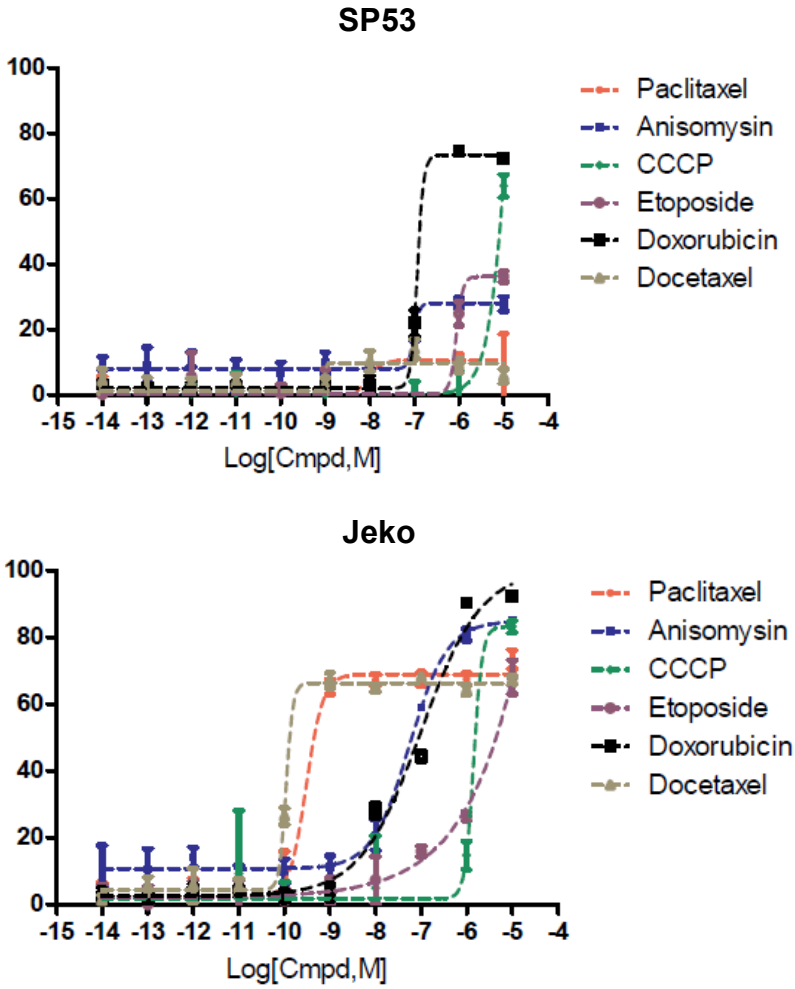

Figure 45: 6-Compounds Evaluation for HTS Positive Control Selection. Cells were incubated with log fold dilutions of paclitaxel, anisomysin, CCCP, etoposide, doxorubicin and doxetaxel to determine a compound that could be used as a general cytotoxic agent in our HTS.

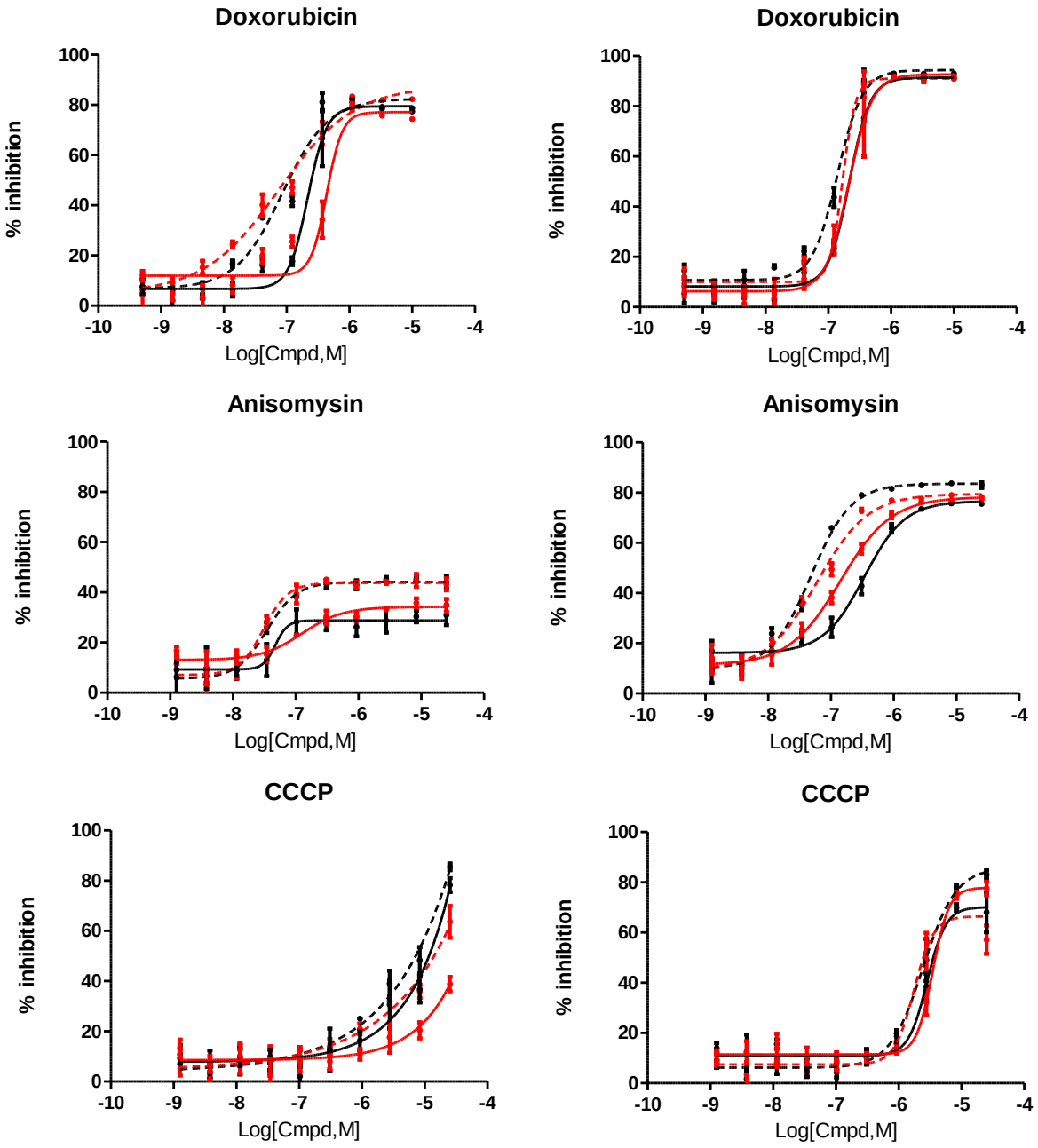

Figure 46: Further Evaluations of Cytotoxic Compounds for the HTS.

Doxorobucin, Anisomycin and CCCP were compared and doxorubicin found to be the best compound to be used as a positive control for the HTS. Red lines are PAX5^{-} replicates, black lines are PAX5control replicates. Solid lines are replicates #1, and dashed lines are replicates #2.

High throughput screening (HTS) has been a tool for novel drug discovery; however, no reported screenings were performed using only MCL cells. In order to understand the drug resistant nature of PAX5 silenced MCL in a comprehensive way, we screened 3864 compounds from three different libraries; a custom made library of clinically relevant compounds (Custom Clinical, 246 compounds), a bioactive library containing FDA approved compounds (Prestwick, 1200 compounds) and an NCI diversity library containing compounds currently in development or clinical trials (NCI Diversity library, 2418 compounds) (**Figure 47**). A consistent Z' score of >0.5 across different screening days indicated that the screen was consistent and reliable. A good separation between signal and noise was achieved in all three libraries screened, with a scatterplot graph for each cell type depicting a clear distinction between control and test compounds (**Figure 48A - C**). Doxorubicin served as positive controls in all our screens, with DMSO serving as the negative control and media only wells serving as blanks (**Figure 48A - C**). Indeed for reproducibility, when we further analyzed for independent replicates we find that compounds were relatively consistent over two across the different libraries. Plotting for values for replicate #1 as the Y-axis, and the values for replicate #2 as the X-axis, we can determine that most compounds follow a linear trend (**Figure 48D, data not shown**), indicating reproducibility over two replicates.

PAX5^{-} MCL cells have increased compound resistance

Compounds that have a difference in efficacy of at least 5% between control and PAX5^{-} MCL were analyzed. After filtering the compounds that have at least a 40% inhibitory effect of doxorubicin (HTS positive control), we were left with a positive compound hit rate of 3.7% - 7.0% for the HTS libraries. Across all three libraries,

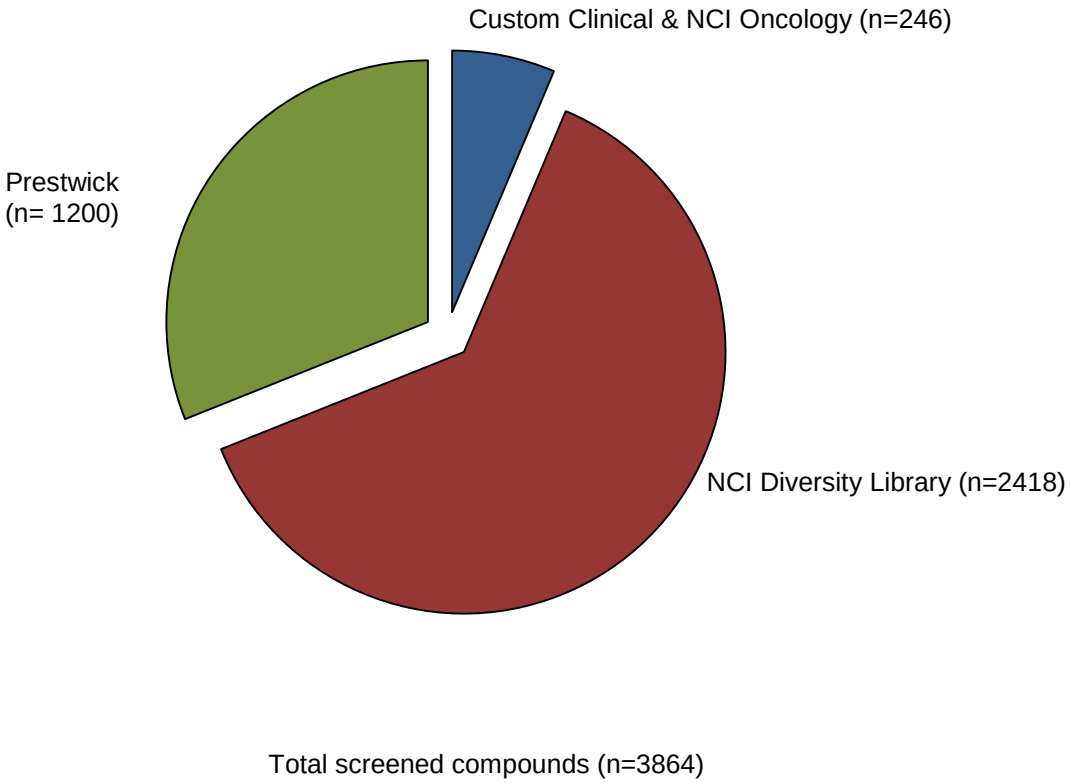

Figure 47: Three Unique Compound Libraries in the HTS. A Pie chart summarizing sources for compounds used in the HTS study comprising of three unique library sets; a custom made library of clinically relevant compounds (Custom Clinical, 246 compounds), a bioactive library containing FDA approved compounds (Prestwick, 1200 compounds) and an NCI diversity library containing compounds currently in development or clinical trials (NCI Diversity library, 2418 compounds).

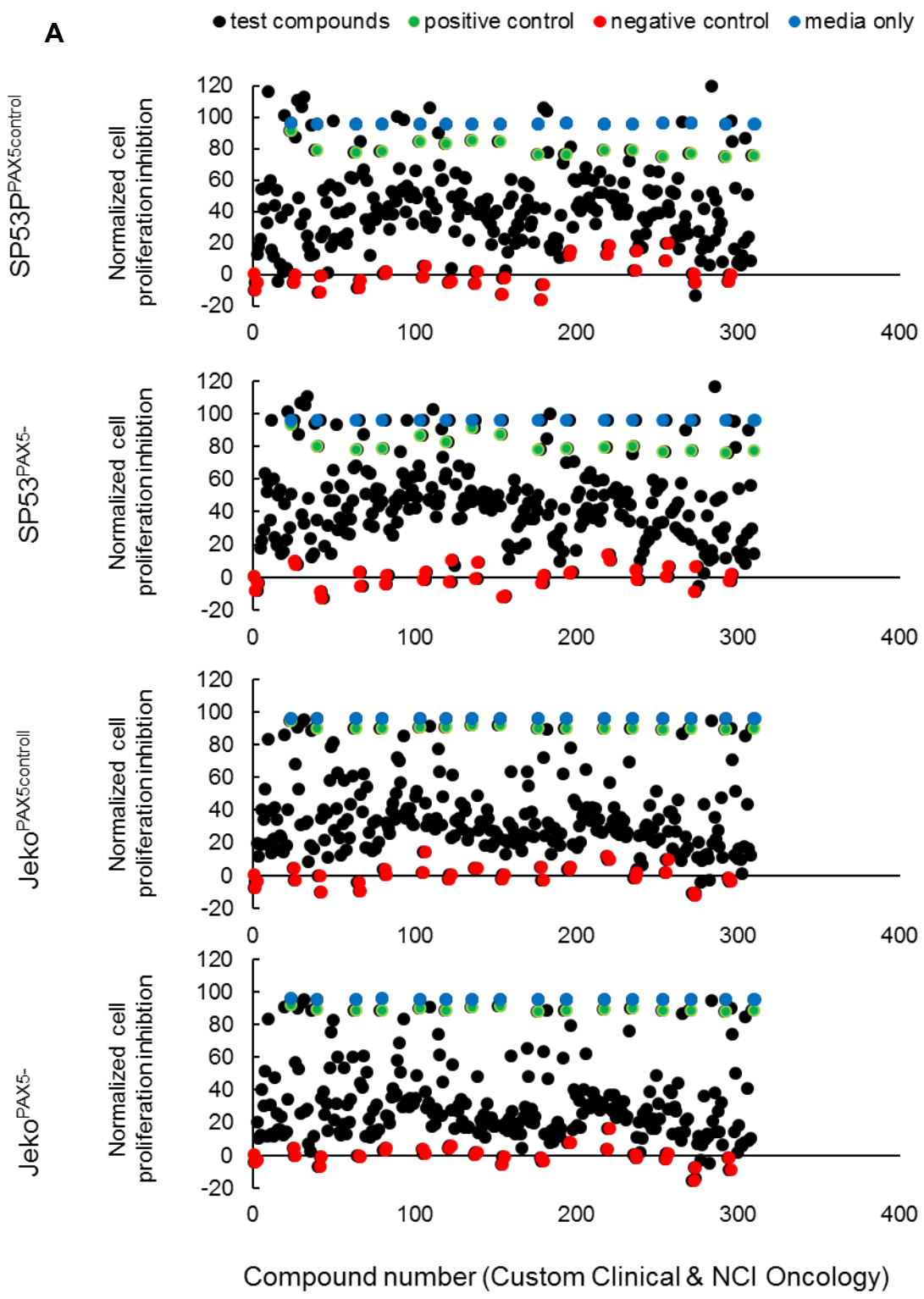
A
test compounds
positive control
negative control
media only
SP53P^PAX5control
SP53^PAX5-
Jeko^PAX5controll
Jeko^PAX5-
Normalized cell proliferation inhibtion
120
100
80
60
40
20
0
-20
0
100
200
300
400
Compound number (Custom Clinical & NCI Oncology)

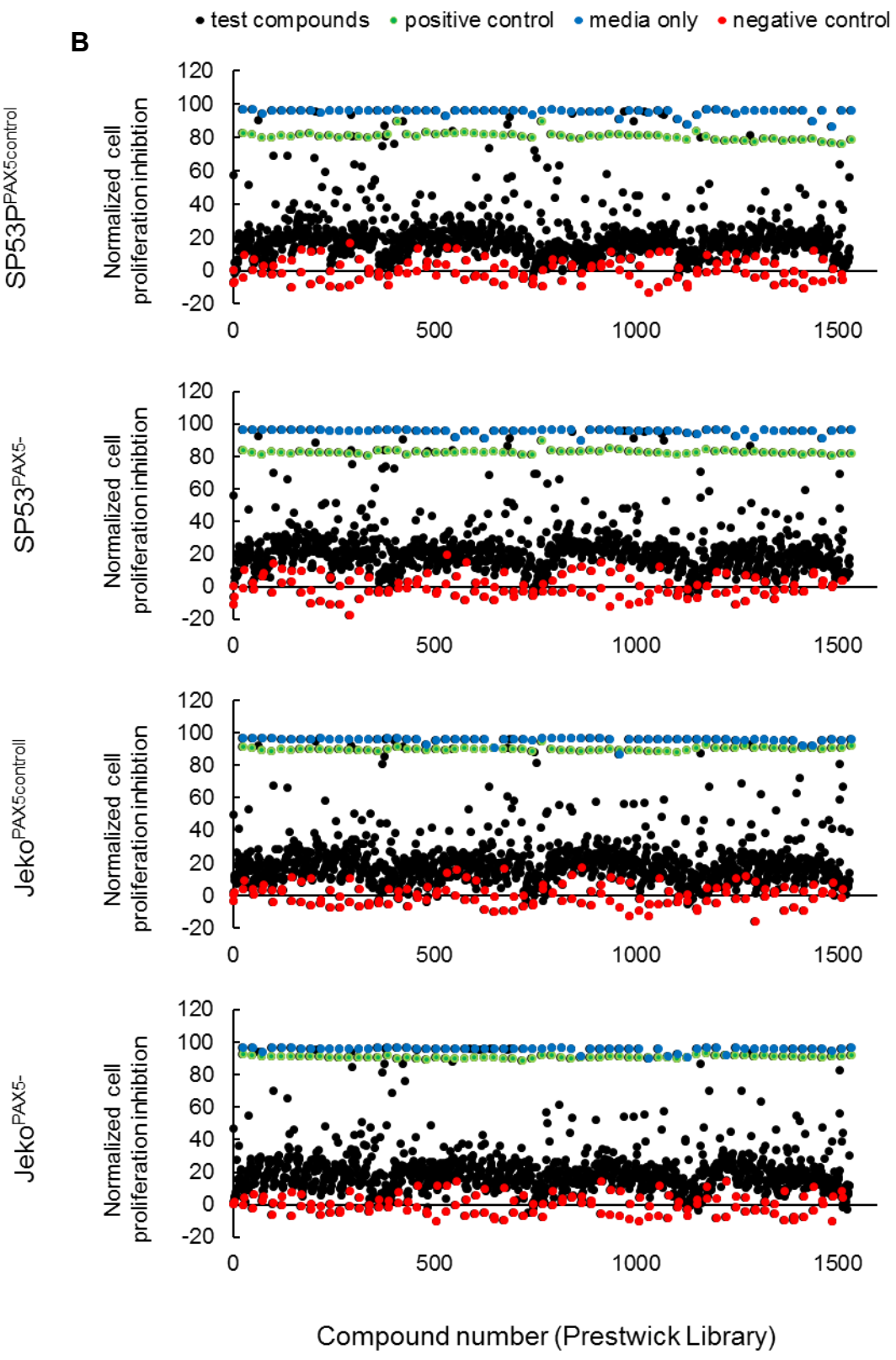
B
test compounds
positive control
media only
negative control
SP53P^PAX5control
SP53^PAX5-
Jeko^PAX5controll
Jeko^PAX5-
Normalized cell proliferation inhibtion
120
100
80
60
40
20
0
-20
0
500
1000
1500
Compound number (Prestwick Library)

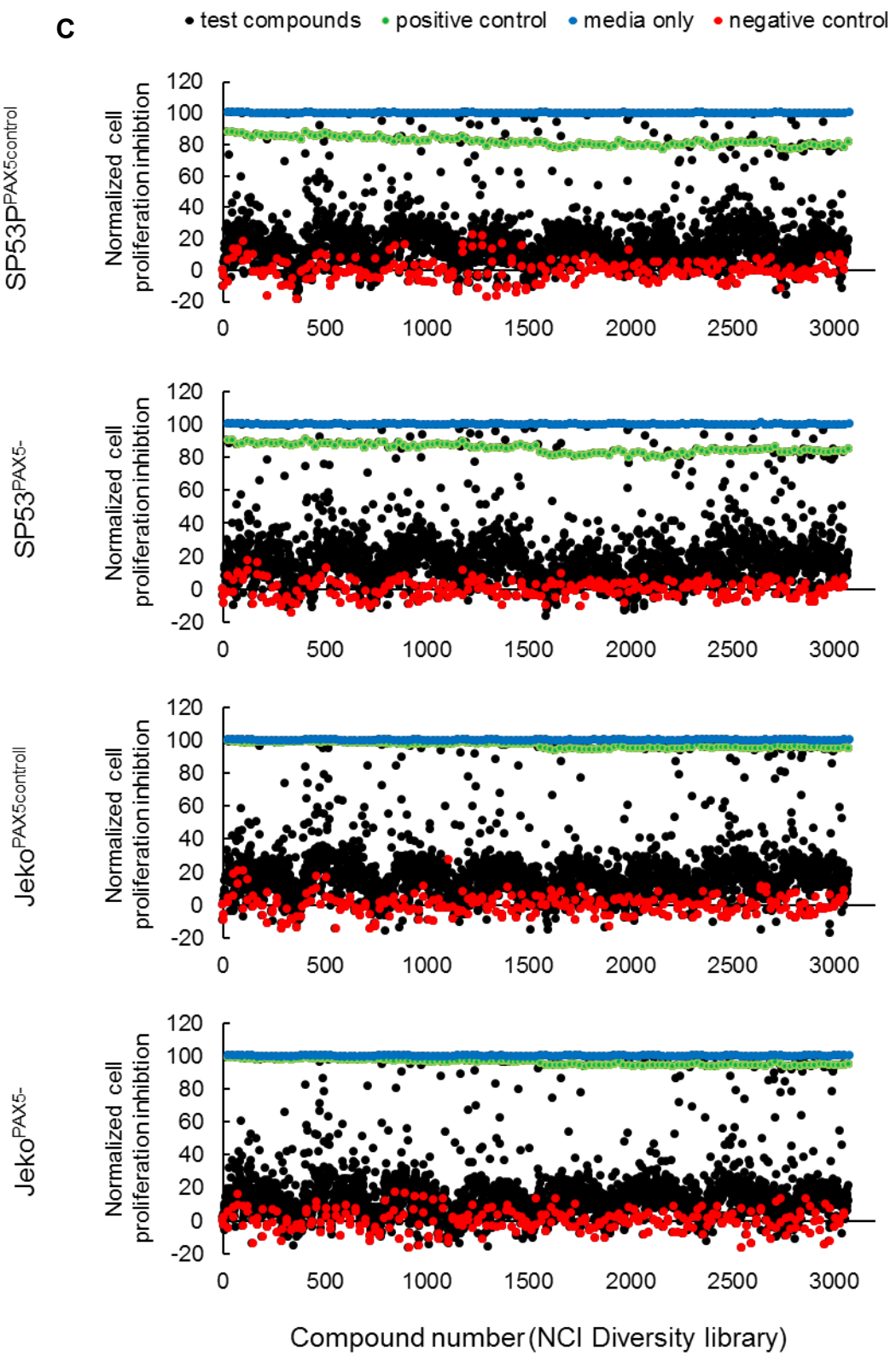
C
test compounds
positive control
media only
negative control
SP53P^PAX5control
SP53^PAX5-
Jeko^PAX5controll
Jeko^PAX5-
Normalized cell proliferation inhibtion
120
100
80
60
40
20
0
-20
0
500
1000
1500
2000
2500
3000
Compound number (NCI Diversity library)

D

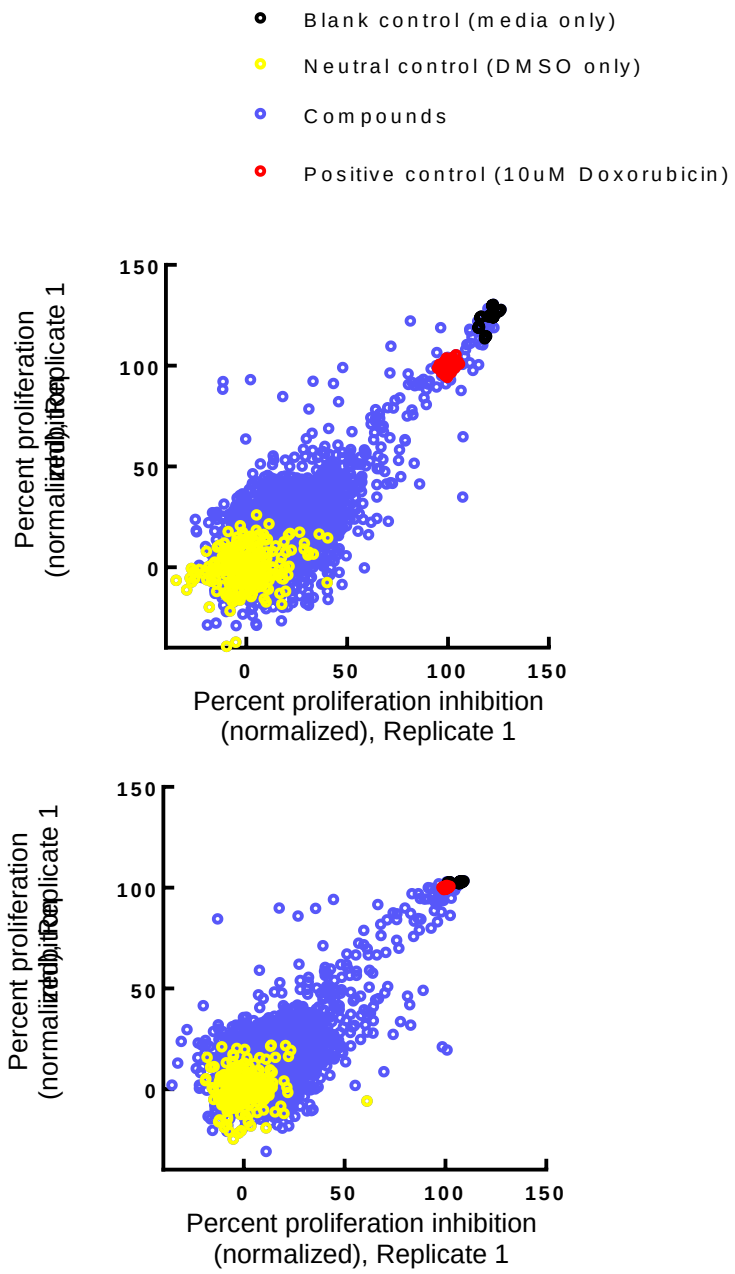

Figure 48: HTS Compound and Internal Control Distribution. (A-C) Signal to noise ratio of HTS screening. Scatter plots represent percent of activity inhibition of positive controls (green), negative controls (red) and test compounds (black) relative to vehicles in four cell types. Custom Clinical library data show in A, Prestwick data show in B and NCI diversity library data show in C.(D) NCI Diversity library normalized data for SP53 (top) and Jeko (bottom) parental cells, Y axis = Replicate #1, X axis = Replicate #2.

PAX5⁻ MCL cells were highly more resistant compared to controls (**Figure 49**). In SP53, only 30-40% of compounds demonstrated effective growth inhibition in PAX5⁻ cells, whereas 60-70% of compounds were effective in controls. In Jeko, only less than 10% compounds were effective in inhibiting PAX5⁻ MCL, whereas 90-100% compounds inhibited growth of controls (**Figure 49**). Further analysis revealed unique compounds that were more resistant in killing PAX5⁻ cells (**Figure 50, Figure 51, Figure 52**), selected for by significance as detailed in Chapter 2.These compounds exhibit a 10% difference cytotoxic inhibition between control and PAX5⁻ cells, and were not screened for a minimum of 40% cell inhibition. As such, identification of unique compounds targeting different pathways can be uncovered to through target validation of our libraries.

To validate such a methodology, we chose to concentrate on the custom clinical library data set. Jeko cells are more resistant to compounds than SP53 cells (**Figure 49**), thus we further evaluated the custom clinical dataset for Jeko cells, and found that there was a similar trend for compound sensitivity over the two independent replicates (**Figure 53**). PAX5⁻ Jeko cells exhibited greater sensitivity to only 7 – 14% of compounds screened from the library, as compared to 29% - 52% of controls. Interestingly, we found that compounds from the Custom Clinical library targeting the PI3K-AKT-mTOR and MEK/ERK signaling cascade were less effective in PAX5⁻Jeko cells compared to control cells (**Figure 54**). Analysis was determined by comparing two independent replicates of the screened library, with overlapping and non-overlapping compounds summarized for pathway activity (**Figure 54**). A similar trend was also observed in PAX5⁻ SP53 cells (**Figure 55**), suggesting PAX5⁻ MCL cells have a higher expression of the common MCL signaling cascade (**Figure 39**), leading to resistance of

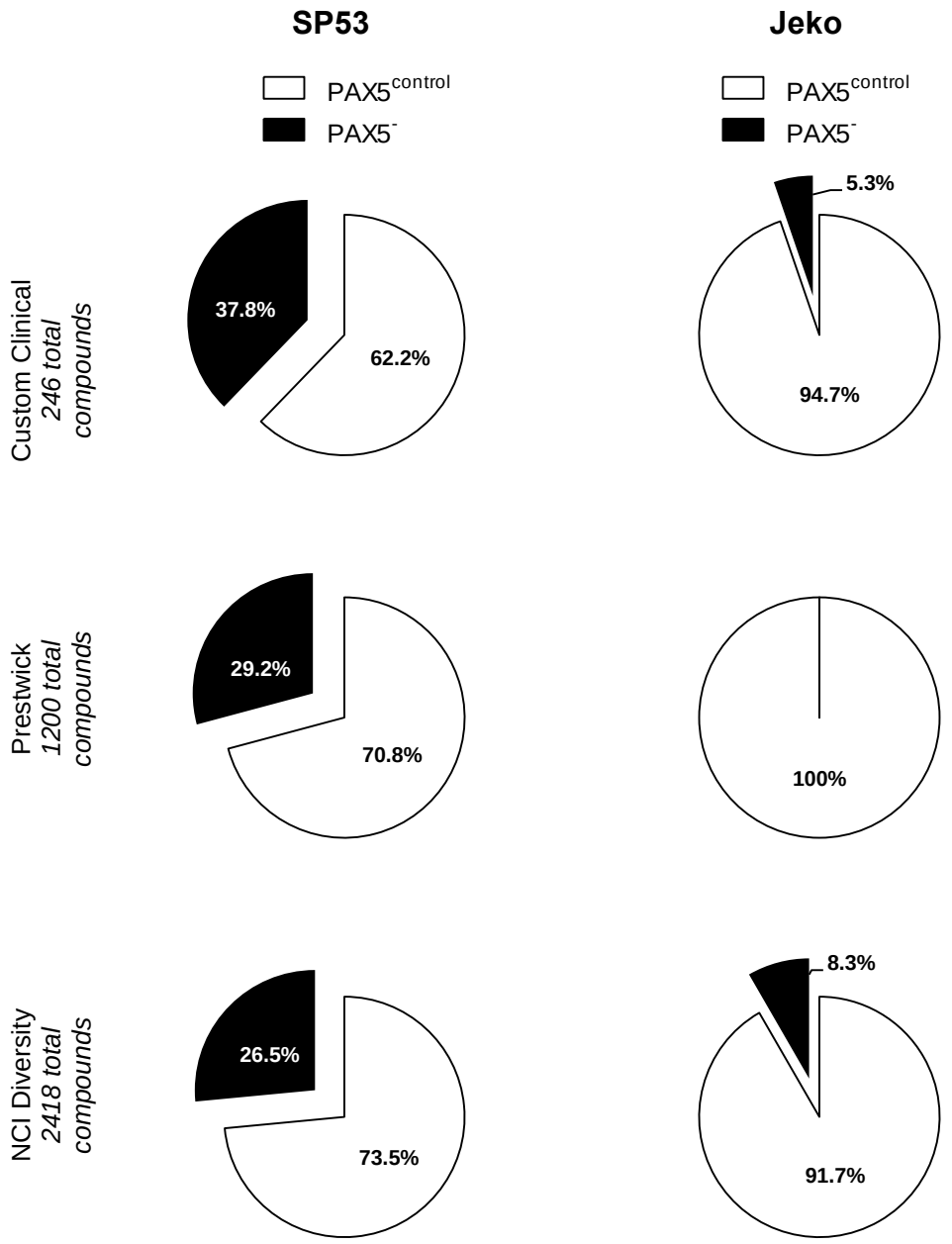

Figure 49: HTS Reveals Drug Resistance Nature of PAX5⁻ MCL Cells. Distribution of the compounds in HTS that are cytotoxic to each cell type. There were significantly more compounds that inhibited proliferation of control cells than PAX5⁻ cells. Compounds that had >40% efficacy were classified as positive hits, and differences between control and PAX5⁻ cells (minimum of 5% cell cytotoxicity) analyzed.

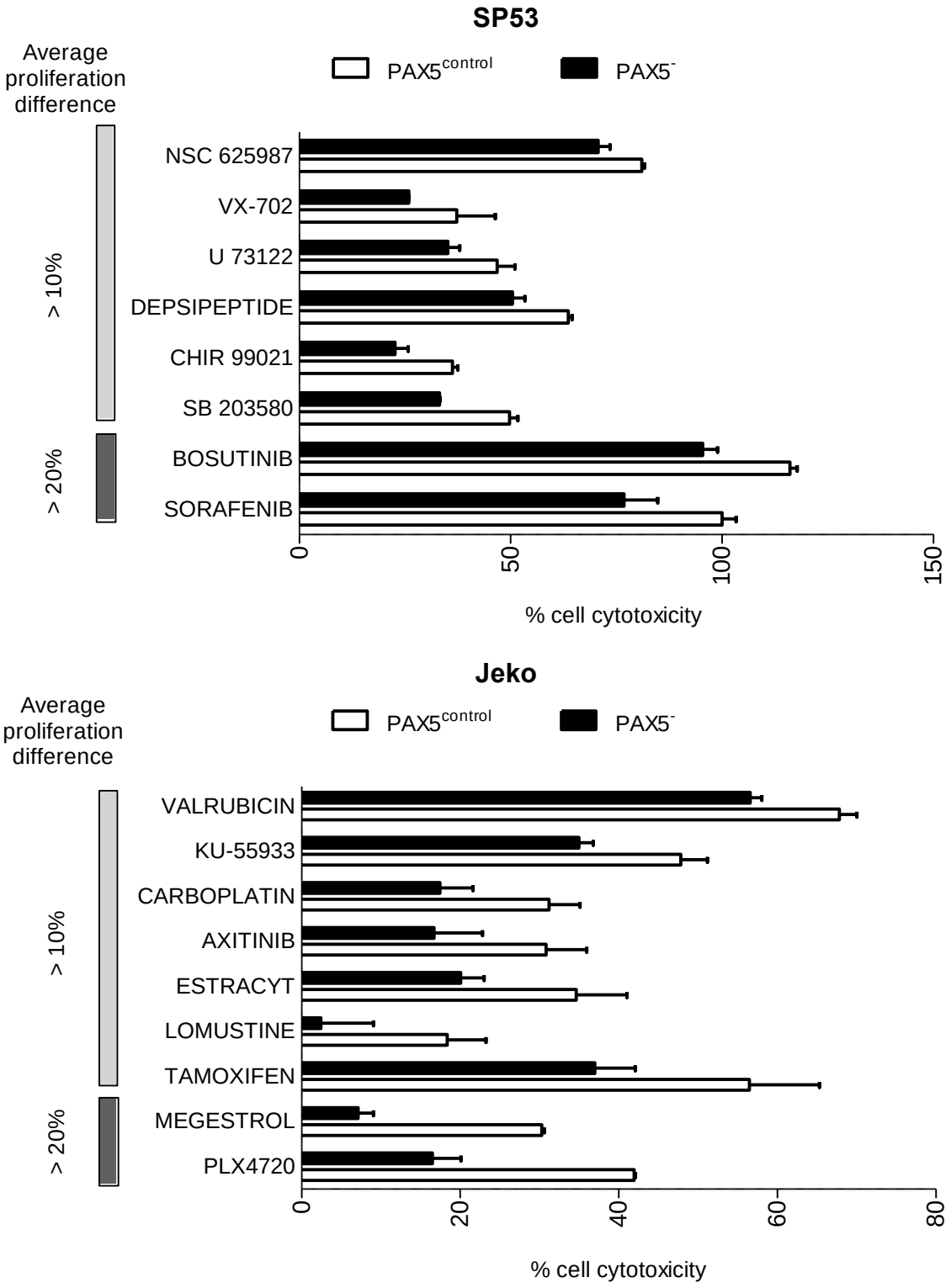

Figure 50: PAX5⁻ Cells Are More Resistant to Compounds from the Custom Clinical Library. Custom clinical library exhibiting compounds with >10% (light gray) and >20% (dark gray) differences between control and PAX5⁻ MCL cells.

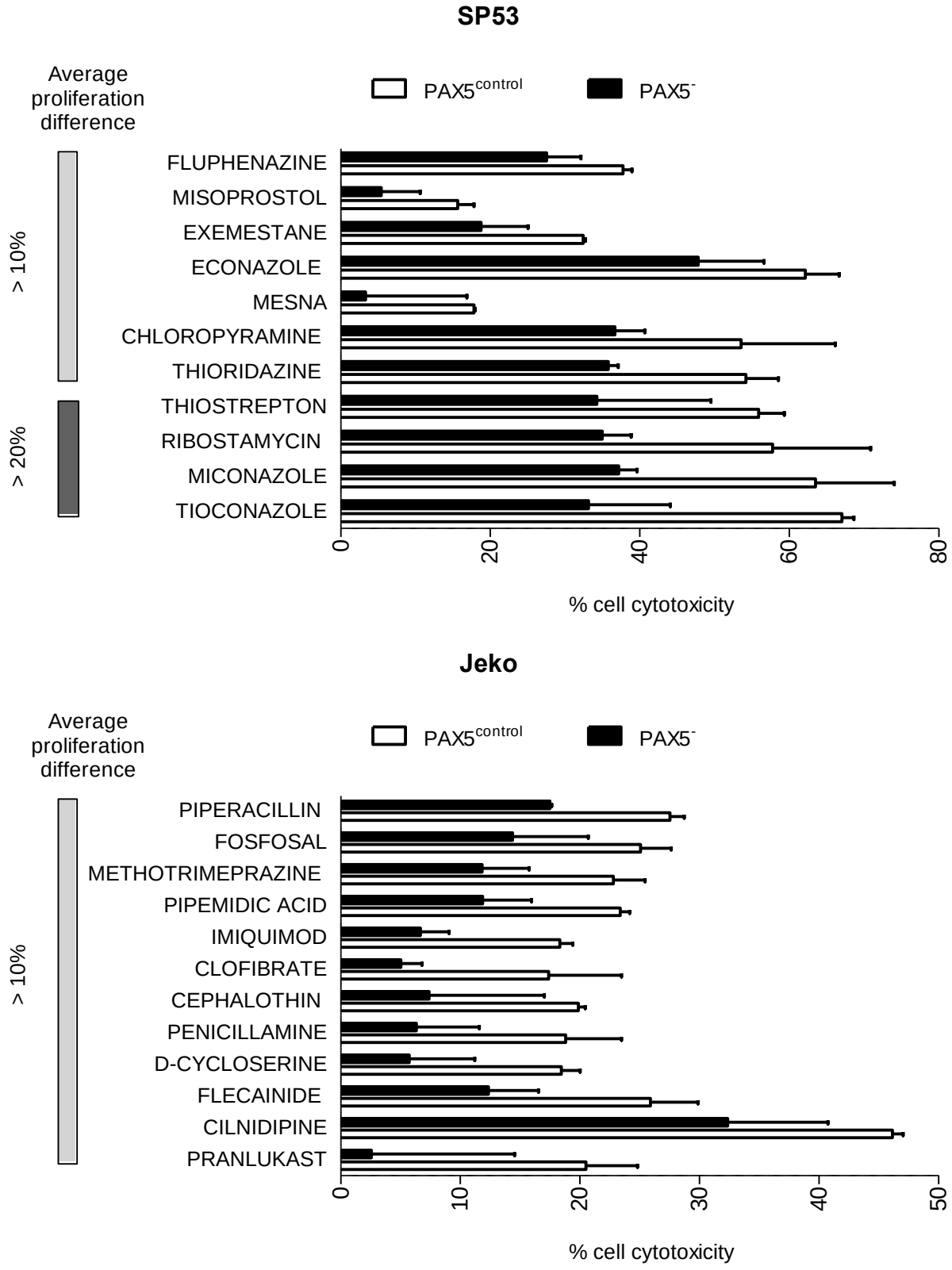

Figure 51: PAX5⁻ Cells Are More Resistant to Compounds from the Prestwick Library. Prestwick library of compounds with >10% (light gray) and >20% (dark gray) differences between control and PAX5⁻ MCL cells.

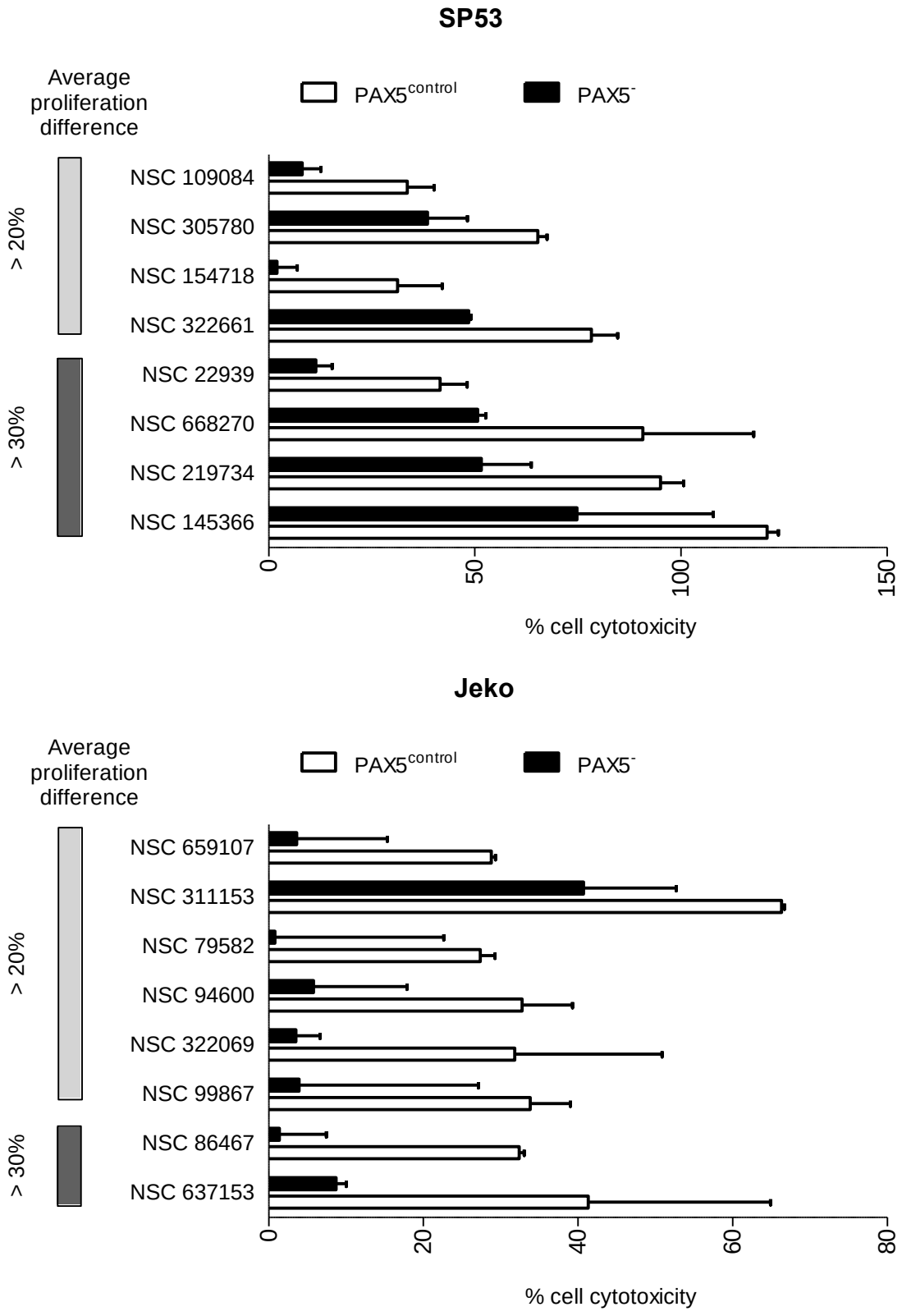

Figure 52: PAX5⁻ Cells Are More Resistant to Compounds from the NCI Diversity Library. NCI Diversity library featuring compounds with >20% (light gray) and >30% (dark gray) differences between control and PAX5⁻ MCL cells.

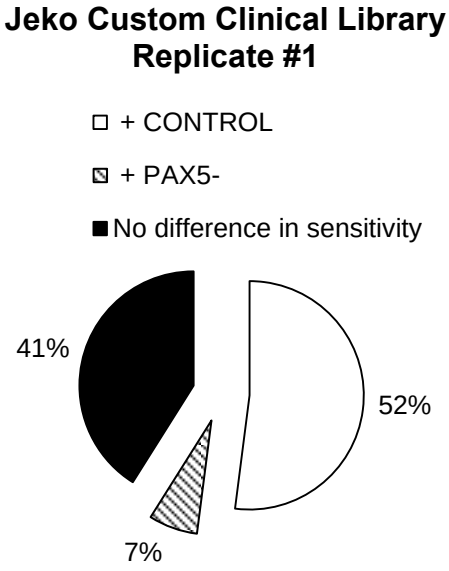

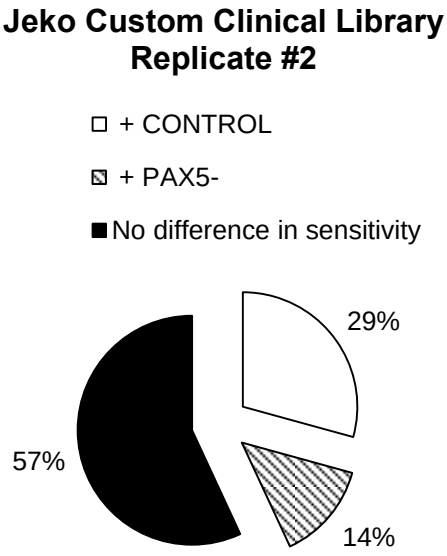

Figure 53: Increased Compound Resistance in Jeko PAX5⁻ Cells. Jeko PAX5⁻ cells were more resistant to compounds screened in the Custom Clinical Library over two replicates (n=2). Reproducibility between independent replicates indicated a drug resistant trend for Jeko PAX5⁻ cells.

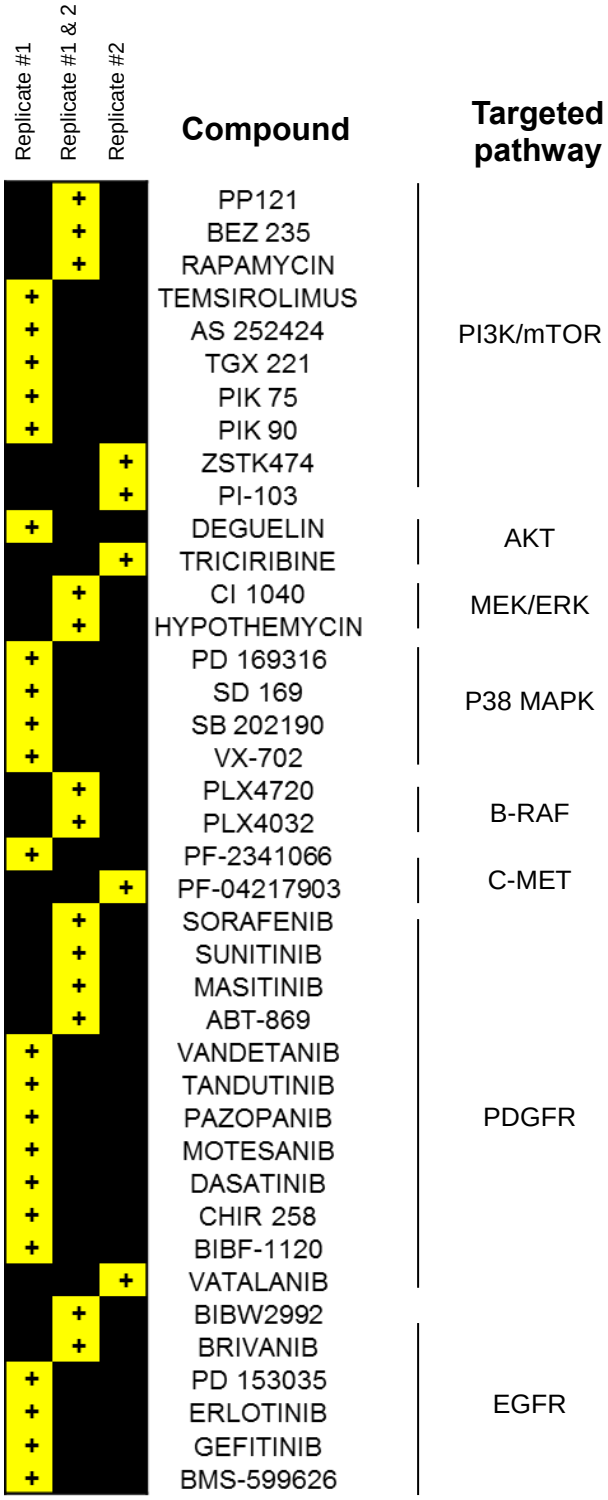

Figure 54: Jeko PAX5⁻ Cells Are More Resistant to PI3K/Mtor and AKT Inhibition.

Jeko PAX5⁻ cells were more resistant to compounds screened in the Custom Clinical Library (n=2). Inhibitors against the PI3K/mTOR and AKT/MEK/MAPK were less sensitive in inducing cytotoxicity in PAX5⁻ MCL cells. Array represents compounds targeting components of aforementioned pathways over two different replicates.

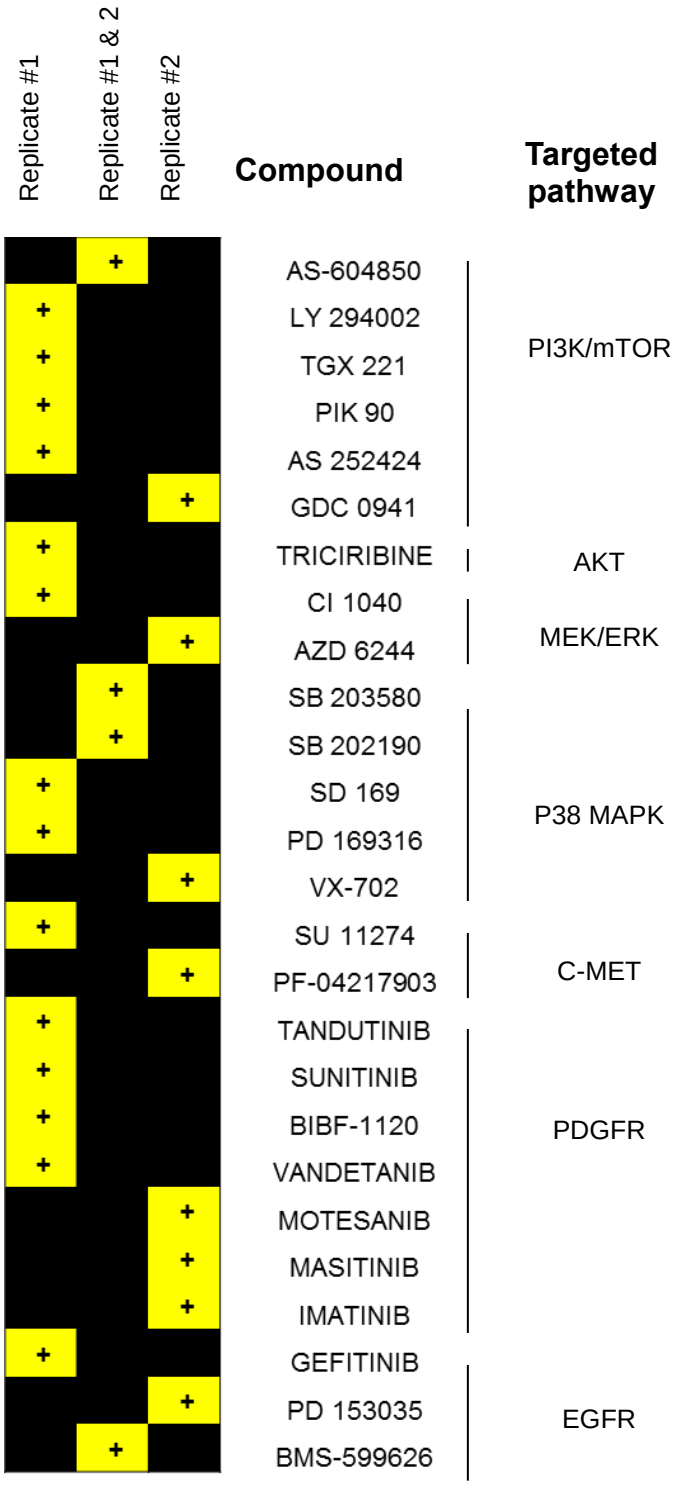

Figure 55: SP53 PAX5⁻ Cells Are More Resistant to PI3K/Mtor and AKT Inhibition.

SP53 PAX5⁻ cells were more resistant to compounds screened in the Custom Clinical Library (n=2). Inhibitors against the PI3K/mTOR and AKT/MEK/MAPK were less sensitive in inducing cytotoxicity in PAX5⁻ MCL cells. Array represents compounds targeting components of aforementioned pathways over two different replicates.

targeting the pathway. Indeed, when averaging both independent replicates, Jeko PAX5^{-} demonstrated an overall increase of resistance against select compounds targeting PI3K, mTOR, MEK and MAPK (**Figure 56**).

MEK has been implicated in tumor cell adhesion (Pals, de Gorter et al. 2007), and we observed an increase in PAX5^{-} MCL cells adhering to bone marrow stromal cells in vitro and in vivo (**Figure 25-29**) . Since we discovered that PAX5^{-} MCL cells were resistant to MEK inhibitors (**Figure 54-56**) and have an upregulation of MEK downstream targets (**Figure 39**), we postulated that MEK inhibition might affect lymphoma cell adhesion. Indeed, we report that Selumetinib (AZD6244) was highly efficient in inhibiting cellular bone marrow adhesion of PAX5^{-} MCL cells (**Figure 57A**), with no adverse effect on cell viability (data not shown). Selumetinib is a MEK1/2 inhibitor, that has been studied in other B cell lymphomas (Bhalla, Evens et al. 2011, Lv, Zhang et al. 2014) as well as other tumor types (Migliardi, Sassi et al. 2012, El Touny, Vieira et al. 2014), however, no studies investigated its effects on adhesion to BMSCs. Various doses of selumetinib was used to compare adhesion of PAX5^{-} MCL and control cells, and we found that selumetinib only affected PAX5^{-} adhesion (**Figure 57B**). Furthermore, it is interesting to point out that selumetinib is ususally used in combination with another compounds to target advanced metastatic diseases (Migliardi, Sassi et al. 2012).

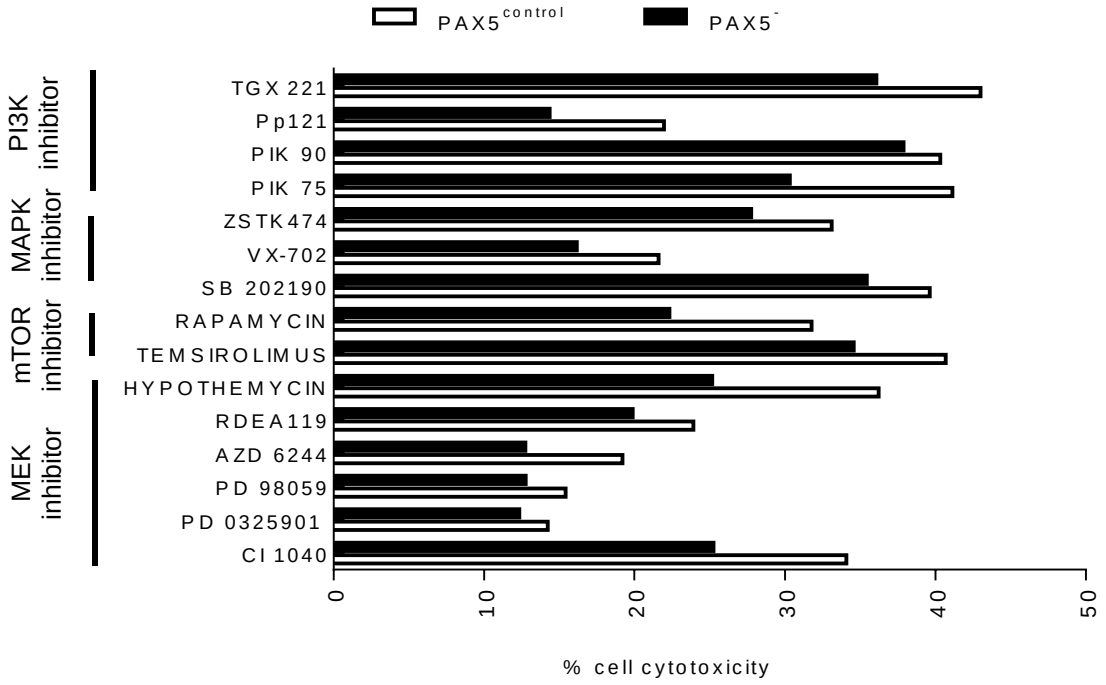

Figure 56: Jeko PAX5¯ Cells Are More Resistant to PI3K, Mtor, MEK and MAPK Inhibitors. PAX5¯ MCL Jeko cells are more resistant to the compounds targeting the PI3K, mTOR, MAPK and MEK pathways over two replicates. Summary of average proliferation inhibition of selected compounds found in the Custom Clinical Library.

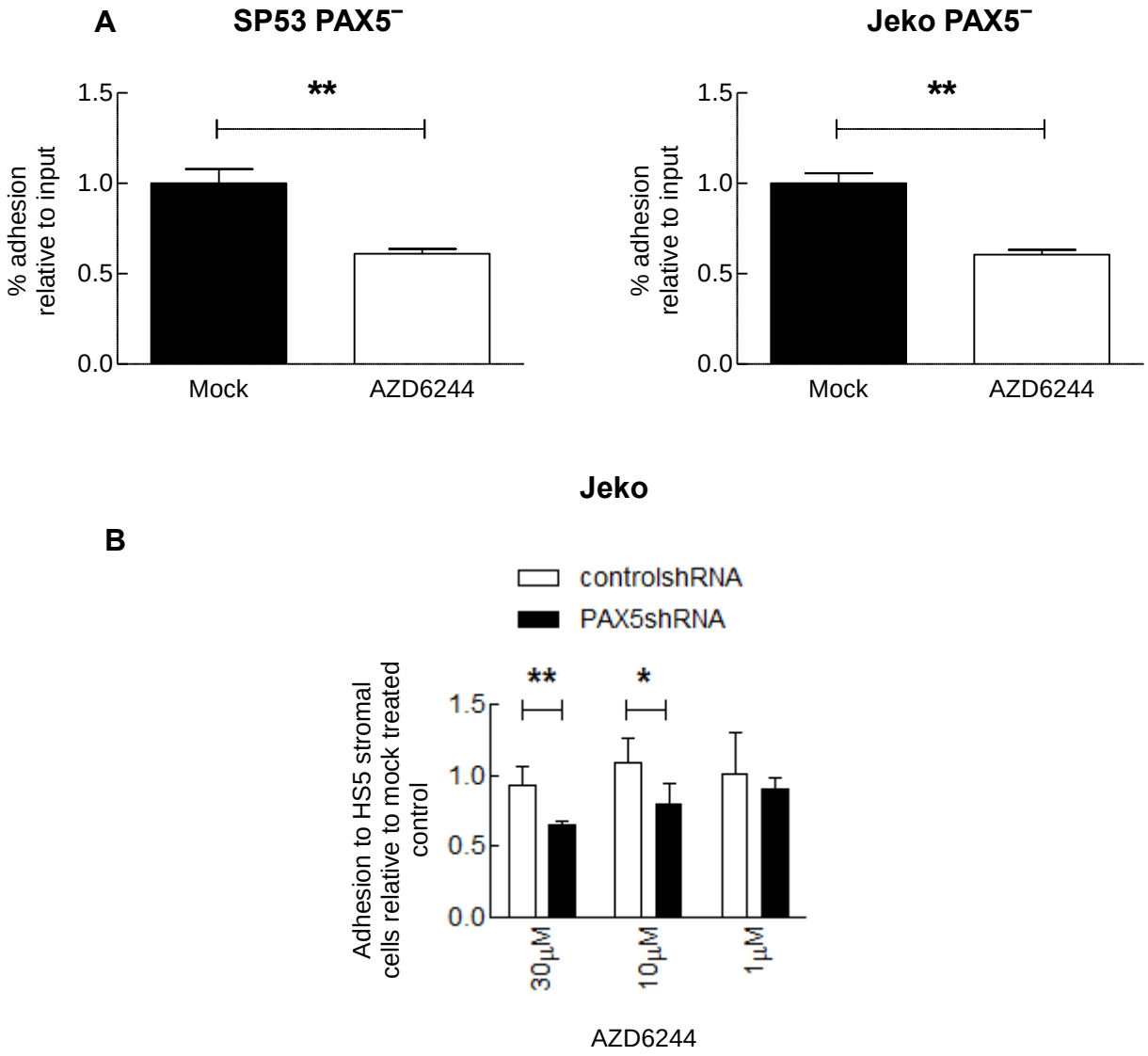

Figure 57: AZD6244 Reduced Bone Marrow Adhesion of PAX5⁻ Cells in vitro. (A) Selumetinib inhibited SP53 and Jeko PAX5⁻ cellular adhesion to HS-5 bone marrow stromal cells. Adhesion of lymphoma cells was calculated by measuring PKH-26 dye intensity relative to fluorescent reading of inputs. Each value represents the mean ±S.D. (n=6 (B) AZD6244 only disrupted adhesion in PAX5⁻ Jeko cells. * $p < 0.05$ (vs. $PAX5^{control}$; Student's t-test); ** $p < 0.005$ (vs. $PAX5^{control}$; Student's t-test).

SUMMARY

PAX5^{-} cells were more resistant to low dose of doxorubicin and bortezomib treatment, and a HTS of 3864 compounds ascertained the drug resistant properties of PAX5^{-} cells compared to control cells, suggesting PAX5 downregulation as an event in MCL drug resistance gain. PAX5^{-} cells exhibited increased compound resistance against PI3K, mTOR, AKT and MEK inhibitors, corroborating our observation of increased signaling of this pathway.

Chapter 6: GENERAL DISCUSSION

PAX5 is a Novel Tumor Suppressor in Mantle Cell Lymphoma

Despite its essential role in determining and maintaining B cell identity in mice (Cobaleda, Schebesta et al. 2007), functions of PAX5 in human B malignancies have been unclear. We discovered that there were quantitative differences of *PAX5* expression among normal B cells and B cells from MCL patients, which displayed decreased levels of PAX5 in MCL (**Figure 1**). Within MCL patients, the *PAX5* levels were decreased in bone marrows compared to blood (**Figure 34**). In xenograft mice, subcutaneous MCL tumors contained higher *PAX5* levels compared to MCL cells from host bone marrow (**Figure 35**). However, *PAX5* expression was not absent in MCL patients, suggesting that even reduced PAX5 levels are sufficient to induce global changes in gene expression for malignant transformation. Our data support downregulation of PAX5 in MCL an important step for conversion to a more aggressive phenotype (**Figure 58**).

PAX5 Affects MCL Cellular Proliferation

In order to mimic *PAX5* levels in MCL patients, we generated MCL cells that are stably knocked down for PAX5. PAX5 levels in Jeko and SP53 were lower than normal B cells (**Figure 1**); we further downregulated PAX5 in these cells to investigate differential expression of PAX5 in MCL. PAX5^{-} MCL cells displayed markedly increased cellular proliferation in vitro and in vivo, whereas overexpression led to delayed growth and cell death (**Figure 12**). Increased cell proliferation was accompanied by changes to the cell cycle and several cell cycle related genes, such as increased cyclin dependent kinases and decreased expression of tumor suppressor

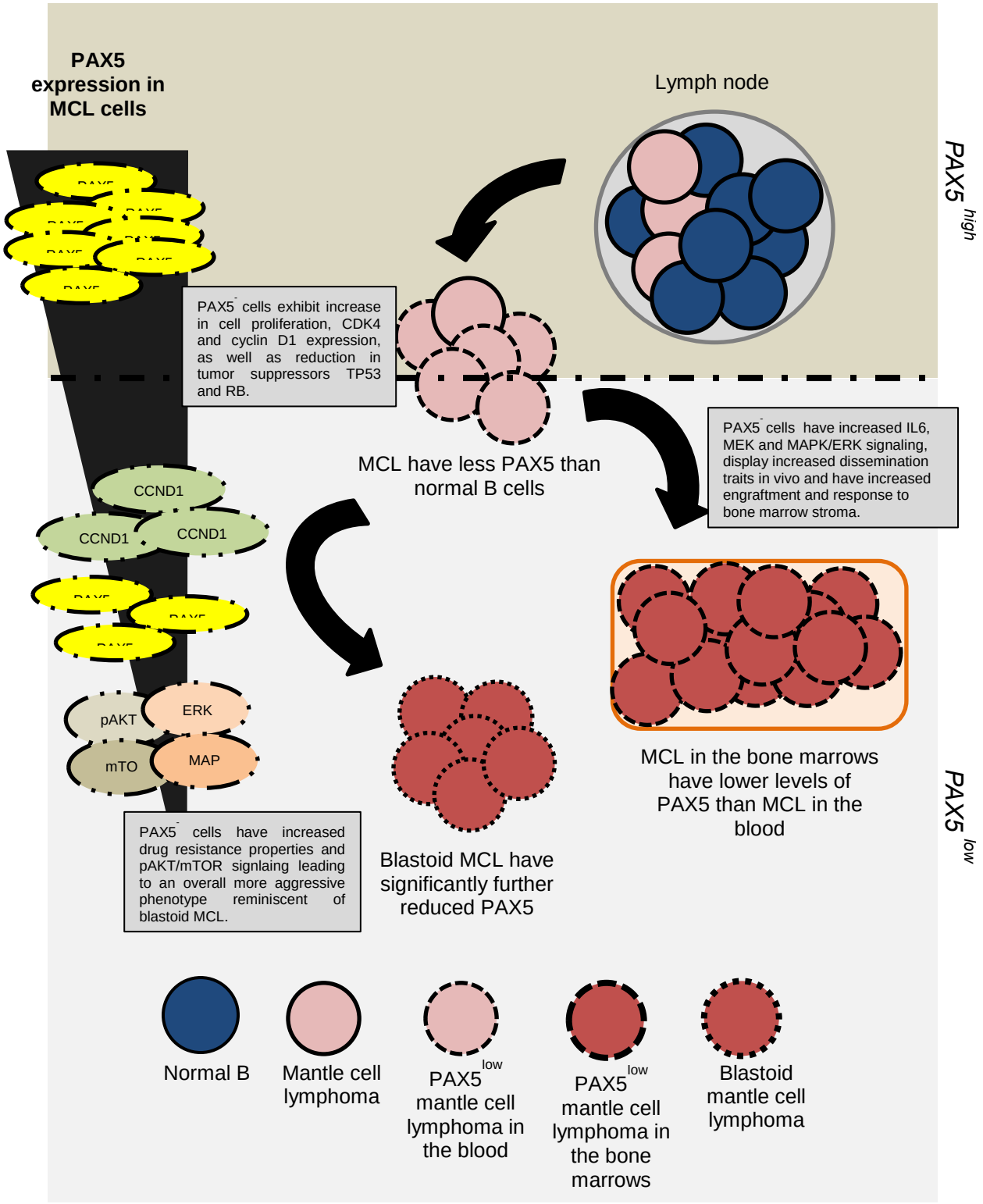

Figure 58: Roles PAX5 Signaling Has in MCL Development and Progression. A model diagram depicting observations made in the study; downregulation of PAX5 leads to increased proliferation, dissemination and drug resistance in MCL.

genes. Expression of cyclin D1, a genetic hallmark for MCL, was also increased upon PAX5 silencing (**Figure 39**). However, given that cyclin D1 is not sufficient to induce lymphomas in mice (Adams, Harris et al. 1999), it is likely that collective changes in upregulation of cell cycle promoting genes and downregulation of cell cycle inhibitory genes such as Rb, p53, p21 and p27 contributed to increased proliferation of PAX5$^-$ MCL cells. Increased cellular proliferation and genomic replication due to loss of PAX5 could potentially lead to increased genomic instability within MCL cells. This further exemplifies the importance of tumor proliferation as prognostic factor in MCL (Rosenwald, Wright et al. 2003, Tiemann, Schrader et al. 2005), as a positive feedback cycle of unchecked replication leading to mutation gains could lead to MCL progression.

PAX5$^-$ MCL cells also utilized existing MCL survival pathways such as AKT/mTOR and MAPK/ERK to promote their growth. It is likely that IL-6 is upstream of these pathways, since PAX5$^-$ SP53 cells produced IL-6 (**Figure 22**). Investigation of the possible role of the platlet-derived growth factor receptor (PDGFR) and epithelial growth factor receptor (EGFR) have on PAX5$^-$ MCL signaling should be further explored, based on the findings of our HTS data (**Figure 54**). We find that PAX5$^-$ MCL cells were more resistant to compounds targeting the PDGFR and EGFR pathway. PDGFR has been implicated in increased AKT and STAT3 signaling (Laimer, Dolznig et al. 2012), and both EGFR and PDGFR have previously been reported to synergize with IL-6 signaling, possibly leading to IL-6 signal sensitivity (Wu, Palmer et al. 2008, Colomiere, Ward et al. 2009, Wang, van Boxel-Dezaire et al. 2013). IL-6 related downstream genes were increased even in Jeko cells which do not produce IL-6, suggesting that PAX5 can influence IL-6 related gene expression. In MM KAS 6/1 cells,

IL-6 addition leads to methylation of TP53 promoter, resulting in decreased TP53 expression levels (Hodge, Peng et al. 2005), an event which we observed in SP53 PAX5^{-} cells as well. Therefore, PAX5 deregulation in MCL could lead to increased sensitivity to survival signals, and provide for increased cellular proliferation that was observed in low serum conditions.

The main source of paracrine IL-6 is likely bone marrow stromal cells. Culturing PAX5^{-} MCL cells with HS-5 conditioned medium led to upregulation of pSTAT3 signaling (**Figure 40**). Advanced MCL patients often present with involvement of extranodal sites such as the bone marrow, hinting that in order for malignant cells to survive in tissues other than the tissue of origin, adaptation to the local microenvironment is necessary. Increased sensitivity to BM growth factors upon PAX5 silencing could provide survival advantages to MCL cells. Therefore, downregulation of PAX5 could be an adaptation process cells to survive in a foreign microenvironment.

Pax5$^{-/-}$ pro-B cells exhibit increased lineage plasticity and ability to differentiate into functional macrophages, granulocytes, dendritic cells, osteoclasts and natural killer cells in vivo (Mikkola, Heavey et al. 2002, Schaniel, Bruno et al. 2002). Adoptive transfer of Pax5$^{-/-}$ B cells into immunodeficient mice led to development of T cells, indicating Pax5 down-regulation confers mature B cells to acquire plasticity similar to early progenitor cells. We did not test direct lineage differentiation of PAX5^{-} MCL due to other oncogenic mutations that were present, however, MCL cells largely increased colony forming ability in PHA-LCM medium upon PAX5 silencing (**Figure 8**). In addition, PAX5^{-} MCL cells had increased PKH26 retention when injected into xenograft hosts, indicating that PAX5 silencing in MCL affects the quiescent cell population that retain the lipophilic dye. This methodology of PKH labelling was utilized to isolate long

term HSCs as well as cancer stem cells (Pece, Tosoni et al. 2010). Our data support PAX5 downregulation promote MCL cells to more stem-like, however, detailed molecular mechanisms should be evaluated by RNA-seq or CHIP-seq.

PAX5 Affects MCL Dissemination and Bone Marrow Adhesion

We observed MCL BM samples had significantly lower amounts of *PAX5* when compared to MCL peripheral blood (**Figure 34**). This is highly interesting as extranodal bone marrow involvement is a common MCL event (Jares, Colomer et al. 2007), and there have been no reports on PAX5's role in lymphoma dissemination. We found that $PAX5^{-}$ cells had increased adhesion to bone marrow stroma in vitro, and we employed two different methodologies for in vivo engraftment and dissemination analysis.

First, we used an intravenous xenograft to better serve as an orthotopic model for MCL engraftment (Klanova, Soukup et al. 2014). Cells were injected into the tail vein, with host bone marrow and spleen tissues analyzed after 8 weeks for tumor cell engraftment. This methodology served to test the ability of MCL cells to engraft and grow in a foreign microenvironment spontaneously. We then investigated on the effects a constant pool of tumor cells entering the circulation would have in MCL dissemination. We employed a second subcutaneous xenograft model, where MCL cells are injected into the skin fold of host mice. This enabled a formation of a primary tumor that is palpable cells to be formed, thus providing for a pool of cells that constantly disseminate into the host's system (Molinsky, Klanova et al. 2013).

^{18}F-FDG have previously been used as a method of monitoring tumor dissemination in patients (Seam, Juweid et al. 2007). We used ^{18}F-FDG to detect infiltrated tumor cells as tumor/neoplastic cells absorb more glucose than normal cells (Levine and Puzio-Kuter 2010). Of note, ^{18}F-FDG has been reported to be highly

absorbed in inflamed tissue as well (Bakheet, Powe et al. 2000). However, the nature of our data suggests that ^{18}F-FDG would be an ideal tracking method, as infiltrating MCL cells would absorb more glucose and also cause a local inflammatory response, thus intensifying on signal recorded. FACS analysis of targets with high glucose absorption should be performed to further improve resolution of tumor cell infiltration.

Interestingly, we found that SP53 PAX5$^-$ xenografts to have higher tumor dissemination than control xenografts (**Figure 32**), higher amount of radioactive ^{18}F-FDG uptake found in the thymus, spleen, bone marrow and lymphnodes of mice. We also noticed an increase of glucose uptake in GIT organs of PAX5$^-$ xenografts compared to control. Dissemination of MCL to components of the gastrointestinal system occurs in MCL and we noticed that MCL patients with GIT-involvement all express significantly low *PAX5* transcript as well (**Figure 33**). This increase in dissemination correlates with our observation that PAX5$^-$ MCL cells have a higher rate of motility in vitro (**Figure 30**). Increased motility and adhesion to the microenvironment have been implicated in increased lymphoma dissemination (Pals, de Gorter et al. 2007) with an upregulation of the p38MAPK signaling pathway (**Figure 39**) reported to play a significant role in tumorigenic B cell motility (Bendall, Baraz et al. 2005). Collectively, our data points to loss of PAX5 as an important event in MCL dissemination, and may be critical for increased engraftment to a foreign microenvironment.

PAX5 Expression Predicts MCL Aggressiveness

When we analyzed for patient survival from a preexisting database (Leukemia-Lymphoma Molecular Profiling Project) as previously reported (Rosenwald, Wright et al. 2003), we could not find a significant correlation between *PAX5* expression and

overall survival. This discrepancy could be explained due to methodology of generating data; the preexisting database used lymph node biopsies form patients, which may contain non-B cells and supporting stromal cells. On the other hand, our data reported is based on purified $CD19^+$ B cells. There is still possibility that B cells we collected contained normal B cells; however, all MCL patient samples analyzed were classified as stage IV with involvement of extranodal sites, indicating minimum amounts of normal B cells in these samples. This is an important distinction between our data set and what has been previously reported, as we only analyzed *PAX5* levels in B cells. Alternatively, further analyses of our sample sets for known MCL prognostic markers such asKi-67, cyclin D1 (Ives Aguilera, Bijwaard et al. 1998) and SOX11 (Mozos, Royo et al. 2009) should be performed to better test the robustness of *PAX5* expression as a prognostic marker.

Through analysis of our clinical data set, we discovered that *PAX5* levels were underexpressed in blastoid MCL. PAX5 levels could be used to predict the prognosis of advanced MCL patients, which correlated with a poorer overall survival (**Figure 37**). When comparing to overall survival of blastoid MCL patients, a similar trend is observed. Increase of blastoid MCL associated pathway signaling pathway members (Rudelius, Pittaluga et al. 2006) as well as compound resistance (such as to bortezomib) suggests that $PAX5^-$ cells display a more aggressive and clinically advanced phenotype compared to control cells. Indeed, it would be interesting to determine if loss of PAX5 expression can force an indolent form of MCL to develop into a more aggressive blastoid phenotype (Pott, Schrader et al. 2005).

Our HTS results further clarified the role PAX5 have in drug resistance. $PAX5^-$ MCL cells are more drug resistant than controls (**Figure 44**). We noticed a global

increase in compound resistance in PAX5¯ MCL (**Figure 49**), with compounds targeting the canonical MCL signaling pathways to be less efficacious over two replicates (Custom Clinical Library) in Jeko PAX5¯ cells and similarly SP53 PAX5¯cells (**Figure 54**). Interestingly, there were fewer drugs that inhibited TP53 deletional mutant Jeko cells than TP53 wild type SP53 cells, suggesting TP53 mutational status could impact drug resistance in MCL. Similarly, Jeko, which is classified as a blastoid variant cell line, also exhibit lower amounts of PAX5, enforcing our observation that loss of PAX5 expression leads to an increase in compound cytotoxic resistance. This overall gain of a more aggressive MCL phenotype upon PAX5 loss could be due to PAX5's role as in regulating a large gene repertoire.

PAX5, MCL and the Novel Frontier

MCL patient blood and bone marrow samples displayed significantly lower levels of *PAX5* transcripts, with the blastoid phenotype particularly low. PAX5^{-} cells had increased proliferation, tumorigenic and drug resistant properties, while displaying greater motility as well as adhesion to the bone marrow microenvironment in vitro and in vivo (**Figure 58**). The downregulation of *PAX5* is seen to occur at a differential level (**Figure 1**), prompting a query on its role in lymhphomagenesis. Since we observed that PAX5 expression decreased in cells from disseminated tissue compared to parental cell tumors, this hints for PAX5 repression to be an epigenetic event for expression regulation (Palmisano, Crume et al. 2003). Analysis of patient genomic DNA for methylation sites within the *PAX5* promoter would better illustrate our point in PAX5 expression control in MCL progression, and to determine if loss of PAX5 in MCL is part of a stepwise tumorigenic machinery to become a more aggressive phenotype.

Our HTS brought about great avenue for future works. There were a myriad of possible ways to analyze and interpret the data; each would bring about a different study on the biology and physiology of mantle cell lymphoma. By generating MCL cells with differential PAX5 expression, we hope to compare control and PAX5^{-} cells in a high throughput manner. The HTS revealed compounds that can potentially target both classical MCL variants and the more drug resistant PAX5^{-} cells, thus possibly paving a way for efficacious MCL drug discovery (**data not shown**). Remarkably, we find that our PAX5^{-} cells were more resistant to bortezomib treatment in vitro, and analysis of our HTS found HSP90 inhibition to be effective in killing PAX5^{-} and normal MCL cells. Previous studies have reported on the use of HSP90 inhibitors to target MCL (Georgakis, Li et al. 2006) though single compound use yielded only moderate clinical activity (Kirschbaum, Frankel et al. 2011, Parekh, Weniger et al. 2011). The possible identification of compounds that could be used in a synergistic concerted manner with current therapeutic regimens could lead to discovery of a more efficacious treatment plan of MCL patients.

Alternatively, we have uncovered compounds that specifically target only PAX5^{-} cells; compounds (**data not shown**) that ultimately are efficient in inhibiting PAX5^{-} cells. Though not therapeutically viable, identification of such compounds can further shed light to the biological and molecular nature of PAX5^{-} MCL cells. Since we also report that Raji and Reh, two non-MCL B cell cell lines, have increased proliferation upon PAX5 loss, it could be extrapolated that PAX5 serves a tumor suppressor in B cell tumors. Thus, PAX5^{-} B cell lymphomas might serve as a functional drug resistant preclinical model for other B cell cancers.

BIBLIOGRAPHY

Adams, B., P. Dorfler, A. Aguzzi, Z. Kozmik, P. Urbanek, I. Maurer-Fogy and M. Busslinger (1992). "Pax-5 encodes the transcription factor BSAP and is expressed in B lymphocytes, the developing CNS, and adult testis." Genes Dev **6**(9): 1589-1607.

Adams, J. M., A. W. Harris, A. Strasser, S. Ogilvy and S. Cory (1999). "Transgenic models of lymphoid neoplasia and development of a pan-hematopoietic vector." Oncogene **18**(38): 5268-5277.

Agarwal, B. and K. N. Naresh (2002). "Bcl-2 family of proteins in indolent B-cell non-Hodgkin's lymphoma: Study of 116 cases." American journal of hematology **70**(4): 278-282.

Alinari, L., V. L. White, C. T. Earl, T. P. Ryan, J. S. Johnston, J. T. Dalton, A. K. Ferketich, R. Lai, D. M. Lucas, P. Porcu, K. A. Blum, J. C. Byrd and R. A. Baiocchi (2009). "Combination bortezomib and rituximab treatment affects multiple survival and death pathways to promote apoptosis in mantle cell lymphoma." MAbs **1**(1): 31-40.

Argatoff, L. H., J. M. Connors, R. J. Klasa, D. E. Horsman and R. D. Gascoyne (1997). "Mantle cell lymphoma: a clinicopathologic study of 80 cases." Blood **89**(6): 2067-2078.

Argatoff, L. H., J. M. Connors, R. J. Klasa, D. E. Horsman and R. D. Gascoyne (1997). "Mantle cell lymphoma: a clinicopathologic study of 80 cases." Blood **89**(6): 2067-2078.

Bakheet, S. M., J. Powe, A. Kandil, A. Ezzat, A. Rostom and J. Amartey (2000). "F-18 FDG uptake in breast infection and inflammation." Clin Nucl Med **25**(2): 100-103.

Banks, P. M., J. Chan, M. L. Cleary, G. Delsol, C. De Wolf-Peeters, K. Gatter, T. M. Grogan, N. L. Harris, P. G. Isaacson, E. S. Jaffe and et al. (1992). "Mantle cell lymphoma. A proposal for unification of morphologic, immunologic, and molecular data." Am J Surg Pathol **16**(7): 637-640.

Barberis, A., K. Widenhorn, L. Vitelli and M. Busslinger (1990). "A novel B-cell lineage-specific transcription factor present at early but not late stages of differentiation." Genes Dev **4**(5): 849-859.

Bea, S., M. Ribas, J. M. Hernandez, F. Bosch, M. Pinyol, L. Hernandez, J. L. Garcia, T. Flores, M. Gonzalez, A. Lopez-Guillermo, M. A. Piris, A. Cardesa, E. Montserrat, R. Miro and E. Campo (1999). "Increased number of chromosomal imbalances and high-level DNA amplifications in mantle cell lymphoma are associated with blastoid variants." Blood **93**(12): 4365-4374.

Bea, S., I. Salaverria, L. Armengol, M. Pinyol, V. Fernandez, E. M. Hartmann, P. Jares, V. Amador, L. Hernandez, A. Navarro, G. Ott, A. Rosenwald, X. Estivill and E. Campo (2009). "Uniparental disomies, homozygous deletions, amplifications, and target genes in mantle cell lymphoma revealed by integrative high-resolution whole-genome profiling." Blood **113**(13): 3059-3069.

Bendall, L. J., R. Baraz, J. Juarez, W. Shen and K. F. Bradstock (2005). "Defective p38 mitogen-activated protein kinase signaling impairs chemotaxic but not proliferative responses to stromal-derived factor-1alpha in acute lymphoblastic leukemia." Cancer Res **65**(8): 3290-3298.

Bernard, M., R. Gressin, F. Lefrere, B. Drenou, B. Branger, S. Caulet-Maugendre, P. Tass, N. Brousse, F. Valensi and N. Milpied (2001). "Blastic variant of mantle cell lymphoma: a rare but highly aggressive subtype." Leukemia **15**(11): 1785-1791.

Bernard, M., R. Gressin, F. Lefrere, B. Drenou, B. Branger, S. Caulet-Maugendre, P. Tass, N. Brousse, F. Valensi, N. Milpied, L. Voilat, A. Sadoun, C. Ghandour, M. Hunault, R. Leloup, L. Mannone, O. Hermine and T. Lamy (2001). "Blastic variant of mantle cell lymphoma: a rare but highly aggressive subtype." Leukemia **15**(11): 1785-1791.

Bhalla, S., A. M. Evens, B. Dai, S. Prachand, L. I. Gordon and R. B. Gartenhaus (2011). "The novel anti-MEK small molecule AZD6244 induces BIM-dependent and AKT-independent apoptosis in diffuse large B-cell lymphoma." Blood **118**(4): 1052-1061.

Bodrug, S. E., B. J. Warner, M. L. Bath, G. J. Lindeman, A. W. Harris and J. M. Adams (1994). "Cyclin D1 transgene impedes lymphocyte maturation and collaborates in lymphomagenesis with the myc gene." EMBO J **13**(9): 2124-2130.

Bosch, F., A. Lopez-Guillermo, E. Campo, J. M. Ribera, E. Conde, M. A. Piris, T. Vallespi, S. Woessner and E. Montserrat (1998). "Mantle cell lymphoma: presenting features, response to therapy, and prognostic factors." Cancer **82**(3): 567-575.

Bosch, F., A. López-Guillermo, E. Campo, J. M. Ribera, E. Conde, M. A. Piris, T. Vallespí, S. Woessner and E. Montserrat (1998). "Mantle cell lymphoma." Cancer **82**(3): 567-575.

Campo, E., M. Raffeld and E. S. Jaffe (1999). "Mantle-cell lymphoma." Semin Hematol **36**(2): 115-127.

Carlo-Stella, C., S. L. Locatelli, A. Giacomini, L. Cleris, E. Saba, M. Righi, A. Guidetti and A. M. Gianni (2013). "Sorafenib inhibits lymphoma xenografts by targeting MAPK/ERK and AKT pathways in tumor and vascular cells." PloS one **8**(4): e61603.

Chao, M. P., A. A. Alizadeh, C. Tang, J. H. Myklebust, B. Varghese, S. Gill, M. Jan, A. C. Cha, C. K. Chan, B. T. Tan, C. Y. Park, F. Zhao, H. E. Kohrt, R. Malumbres, J. Briones, R. D. Gascoyne, I. S. Lossos, R. Levy, I. L. Weissman and R. Majeti (2010). "Anti-CD47 antibody synergizes with rituximab to promote phagocytosis and eradicate non-Hodgkin lymphoma." Cell **142**(5): 699-713.

Chao, M. P., C. Tang, R. K. Pachynski, R. Chin, R. Majeti and I. L. Weissman (2011). "Extranodal dissemination of non-Hodgkin lymphoma requires CD47 and is inhibited by anti-CD47 antibody therapy." Blood **118**(18): 4890-4901.

Chao, M. P., I. L. Weissman and R. Majeti (2012). "The CD47-SIRPalpha pathway in cancer immune evasion and potential therapeutic implications." Curr Opin Immunol **24**(2): 225-232.

Chen, Z., R. Z. Orlowski, M. Wang, L. Kwak and N. McCarty (2014). "Osteoblastic niche supports the growth of quiescent multiple myeloma cells." Blood **123**(14): 2204-2208.

Chi, N. and J. A. Epstein (2002). "Getting your Pax straight: Pax proteins in development and disease." Trends Genet **18**(1): 41-47.

Chilosi, M., C. Doglioni, A. Magalini, G. Inghirami, M. Krampera, G. Nadali, D. Rahal, S. Pedron, A. Benedetti and M. Scardoni (1996). "p21/WAF1 cyclin-kinase inhibitor expression in non-Hodgkin's lymphomas: a potential marker of p53 tumor-suppressor gene function." Blood **88**(10): 4012-4020.

Cho-Vega, J. H., G. Z. Rassidakis, J. H. Admirand, M. Oyarzo, P. Ramalingam, A. Paraguya, T. J. McDonnell, H. M. Amin and L. J. Medeiros (2004). "MCL-1 expression in B-cell non-Hodgkin's lymphomas." Human pathology **35**(9): 1095-1100.

Cobaleda, C., W. Jochum and M. Busslinger (2007). "Conversion of mature B cells into T cells by dedifferentiation to uncommitted progenitors." Nature **449**(7161): 473-477.

Cobaleda, C., W. Jochum and M. Busslinger (2007). "Conversion of mature B cells into T cells by dedifferentiation to uncommitted progenitors." Nature **449**(7161): 473-477.

Cobaleda, C., A. Schebesta, A. Delogu and M. Busslinger (2007). "Pax5: the guardian of B cell identity and function." Nat Immunol **8**(5): 463-470.

Cobaleda, C., A. Schebesta, A. Delogu and M. Busslinger (2007). "Pax5: the guardian of B cell identity and function." Nature immunology **8**(5): 463-470.

Colomiere, M., A. C. Ward, C. Riley, M. K. Trenerry, D. Cameron-Smith, J. Findlay, L. Ackland and N. Ahmed (2009). "Cross talk of signals between EGFR and IL-6R through JAK2/STAT3 mediate epithelial-mesenchymal transition in ovarian carcinomas." Br J Cancer **100**(1): 134-144.

Cooper, A. B., C. M. Sawai, E. Sicinska, S. E. Powers, P. Sicinski, M. R. Clark and I. Aifantis (2006). "A unique function for cyclin D3 in early B cell development." Nat Immunol **7**(5): 489-497.

Czerny, T., G. Schaffner and M. Busslinger (1993). "DNA sequence recognition by Pax proteins: bipartite structure of the paired domain and its binding site." Genes Dev **7**(10): 2048-2061.

Dai, C., Y. Tang, S. Y. Jung, J. Qin, S. A. Aaronson and W. Gu (2011). "Differential effects on p53-mediated cell cycle arrest vs. apoptosis by p90." Proceedings of the National Academy of Sciences **108**(47): 18937-18942.

Dal Col, J., P. Zancai, L. Terrin, M. Guidoboni, M. Ponzoni, A. Pavan, M. Spina, S. Bergamin, S. Rizzo and U. Tirelli (2008). "Distinct functional significance of Akt and mTOR constitutive activation in mantle cell lymphoma." Blood **111**(10): 5142-5151.

Delk, N. A. and M. C. Farach-Carson (2012). "Interleukin-6: a bone marrow stromal cell paracrine signal that induces neuroendocrine differentiation and modulates autophagy in bone metastatic PCa cells." Autophagy **8**(4): 650-663.

Delogu, A., A. Schebesta, Q. Sun, K. Aschenbrenner, T. Perlot and M. Busslinger (2006). "Gene repression by Pax5 in B cells is essential for blood cell homeostasis and is reversed in plasma cells." Immunity **24**(3): 269-281.

Delogu, A., A. Schebesta, Q. Sun, K. Aschenbrenner, T. Perlot and M. Busslinger (2006). "Gene repression by Pax5 in B cells is essential for blood cell homeostasis and is reversed in plasma cells." Immunity **24**(3): 269-281.

Dennison, J. B., M. Shanmugam, M. L. Ayres, J. Qian, N. L. Krett, L. J. Medeiros, S. S. Neelapu, S. T. Rosen and V. Gandhi (2010). "8-Aminoadenosine inhibits Akt/mTOR and Erk signaling in mantle cell lymphoma." Blood **116**(25): 5622-5630.

Ding, B. C., J. R. Whetstine, T. L. Witt, J. D. Schuetz and L. H. Matherly (2001). "Repression of human reduced folate carrier gene expression by wild type p53." Journal of Biological Chemistry **276**(12): 8713-8719.

Dono, M., G. Cerruti and S. Zupo (2004). "The $CD5^+$ B-cell." Int J Biochem Cell Biol **36**(11): 2105-2111.

Dorfler, P. and M. Busslinger (1996). "C-terminal activating and inhibitory domains determine the transactivation potential of BSAP (Pax-5), Pax-2 and Pax-8." EMBO J **15**(8): 1971-1982.

Drakos, E., V. Atsaves, J. Li, V. Leventaki, M. Andreeff, L. J. Medeiros and G. Rassidakis (2009). "Stabilization and activation of p53 downregulates mTOR signaling through AMPK in mantle cell lymphoma." Leukemia **23**(4): 784-790.

Dreyling, M. (2011). "Therapy of mantle cell lymphoma: new treatment options in an old disease or vice versa?" Semin Hematol **48**(3): 145-147.

El Touny, L. H., A. Vieira, A. Mendoza, C. Khanna, M. J. Hoenerhoff and J. E. Green (2014). "Combined SFK/MEK inhibition prevents metastatic outgrowth of dormant tumor cells." J Clin Invest **124**(1): 156-168.

Espinet, B., F. Sole, C. Pedro, M. Garcia, B. Bellosillo, M. Salido, L. Florensa, F. I. Camacho, T. Baro, J. Lloreta and S. Serrano (2005). "Clonal proliferation of cyclin D1-

positive mantle lymphocytes in an asymptomatic patient: an early-stage event in the development or an indolent form of a mantle cell lymphoma?" Hum Pathol **36**(11): 1232-1237.

Euhus, D. M., C. Hudd, M. C. LaRegina and F. E. Johnson (1986). "Tumor measurement in the nude mouse." J Surg Oncol **31**(4): 229-234.

Familiades, J., M. Bousquet, M. Lafage-Pochitaloff, M. C. Bene, K. Beldjord, J. De Vos, N. Dastugue, E. Coyaud, S. Struski, C. Quelen, N. Prade-Houdellier, S. Dobbelstein, J. M. Cayuela, J. Soulier, N. Grardel, C. Preudhomme, H. Cave, O. Blanchet, V. Lheritier, A. Delannoy, Y. Chalandon, N. Ifrah, A. Pigneux, P. Brousset, E. A. Macintyre, F. Huguet, H. Dombret, C. Broccardo and E. Delabesse (2009). "PAX5 mutations occur frequently in adult B-cell progenitor acute lymphoblastic leukemia and PAX5 haploinsufficiency is associated with BCR-ABL1 and TCF3-PBX1 fusion genes: a GRAALL study." Leukemia **23**(11): 1989-1998.

Fernandez, V., E. Hartmann, G. Ott, E. Campo and A. Rosenwald (2005). "Pathogenesis of mantle-cell lymphoma: all oncogenic roads lead to dysregulation of cell cycle and DNA damage response pathways." J Clin Oncol **23**(26): 6364-6369.

Fortschegger, K., S. Anderl, D. Denk and S. Strehl (2014). "Functional heterogeneity of PAX5 chimeras reveals insight for leukemia development." Mol Cancer Res **12**(4): 595-606.

Haberkorn, U., L. G. Strauss, C. Reisser, D. Haag, A. Dimitrakopoulou, S. Ziegler, F. Oberdorfer, V. Rudat and G. van Kaick (1991). "Glucose uptake, perfusion, and cell

proliferation in head and neck tumors: relation of positron emission tomography to flow cytometry." J Nucl Med **32**(8): 1548-1555.

Hagman, J. and K. Lukin (2006). "Transcription factors drive B cell development." Current opinion in immunology **18**(2): 127-134.

Hanna, J., S. Markoulaki, P. Schorderet, B. W. Carey, C. Beard, M. Wernig, M. P. Creyghton, E. J. Steine, J. P. Cassady, R. Foreman, C. J. Lengner, J. A. Dausman and R. Jaenisch (2008). "Direct reprogramming of terminally differentiated mature B lymphocytes to pluripotency." Cell **133**(2): 250-264.

Herrmann, A., E. Hoster, T. Zwingers, G. Brittinger, M. Engelhard, P. Meusers, M. Reiser, R. Forstpointner, B. Metzner, N. Peter, B. Wormann, L. Trumper, M. Pfreundschuh, H. Einsele, W. Hiddemann, M. Unterhalt and M. Dreyling (2009). "Improvement of overall survival in advanced stage mantle cell lymphoma." J Clin Oncol **27**(4): 511-518.

Hodge, D. R., B. Peng, J. C. Cherry, E. M. Hurt, S. D. Fox, J. A. Kelley, D. J. Munroe and W. L. Farrar (2005). "Interleukin 6 supports the maintenance of p53 tumor suppressor gene promoter methylation." Cancer Res **65**(11): 4673-4682.

Hoflinger, S., K. Kesavan, M. Fuxa, C. Hutter, B. Heavey, F. Radtke and M. Busslinger (2004). "Analysis of Notch1 function by in vitro T cell differentiation of Pax5 mutant lymphoid progenitors." J Immunol **173**(6): 3935-3944.

Hong, H., K. Takahashi, T. Ichisaka, T. Aoi, O. Kanagawa, M. Nakagawa, K. Okita and S. Yamanaka (2009). "Suppression of induced pluripotent stem cell generation by the p53-p21 pathway." Nature **460**(7259): 1132-1135.

Ives Aguilera, N. S., K. E. Bijwaard, B. Duncan, A. E. Krafft, W. S. Chu, S. L. Abbondanzo, J. H. Lichy and J. K. Taubenberger (1998). "Differential Expression of Cyclin D1 in Mantle Cell Lymphoma and Other Non-Hodgkin's Lymphomas." Am J Pathol **153**(6): 1969-1976.

Jares, P., D. Colomer and E. Campo (2007). "Genetic and molecular pathogenesis of mantle cell lymphoma: perspectives for new targeted therapeutics." Nat Rev Cancer **7**(10): 750-762.

Johnson, K., M. Shapiro-Shelef, C. Tunyaplin and K. Calame (2005). "Regulatory events in early and late B-cell differentiation." Molecular immunology **42**(7): 749-761.

Jung, H. J., Z. Chen and N. McCarty (2011). "Stem-like tumor cells confer drug resistant properties to mantle cell lymphoma." Leuk Lymphoma **52**(6): 1066-1079.

Kane, R. C., R. Dagher, A. Farrell, C. W. Ko, R. Sridhara, R. Justice and R. Pazdur (2007). "Bortezomib for the treatment of mantle cell lymphoma." Clin Cancer Res **13**(18 Pt 1): 5291-5294.

Karpinich, N. O., M. Tafani, R. J. Rothman, M. A. Russo and J. L. Farber (2002). "The Course of Etoposide-induced Apoptosis from Damage to DNA and p53 Activation to Mitochondrial Release of Cytochromec." Journal of Biological Chemistry **277**(19): 16547-16552.

Kastan, M. B. and J. Bartek (2004). "Cell-cycle checkpoints and cancer." Nature **432**(7015): 316-323.

Kawamata, N., M. A. Pennella, J. L. Woo, A. J. Berk and H. P. Koeffler (2012). "Dominant-negative mechanism of leukemogenic PAX5 fusions." Oncogene **31**(8): 966-977.

Kikuchi, Y., S. Uno, Y. Kinoshita, Y. Yoshimura, S. Iida, Y. Wakahara, M. Tsuchiya, H. Yamada-Okabe and N. Fukushima (2005). "Apoptosis inducing bivalent single-chain antibody fragments against CD47 showed antitumor potency for multiple myeloma." Leuk Res **29**(4): 445-450.

Kim, J. K. and J. A. Diehl (2009). "Nuclear cyclin D1: an oncogenic driver in human cancer." J Cell Physiol **220**(2): 292-296.

Klanova, M., T. Soukup, R. Jaksa, J. Molinsky, L. Lateckova, B. C. Maswabi, D. Prukova, J. Brezinova, K. Michalova, P. Vockova, F. Hernandez-Ilizaliturri, V. Kulvait, J. Zivny, M. Vokurka, E. Necas, M. Trneny and P. Klener (2014). "Mouse models of mantle cell lymphoma, complex changes in gene expression and phenotype of engrafted MCL cells: implications for preclinical research." Lab Invest **94**(7): 806-817.

Kolch, W. (2005). "Coordinating ERK/MAPK signalling through scaffolds and inhibitors." Nature reviews Molecular cell biology **6**(11): 827-837.

Kuppers, R. (2005). "Mechanisms of B-cell lymphoma pathogenesis." Nat Rev Cancer **5**(4): 251-262.

Laimer, D., H. Dolznig, K. Kollmann, P. W. Vesely, M. Schlederer, O. Merkel, A. I. Schiefer, M. R. Hassler, S. Heider, L. Amenitsch, C. Thallinger, P. B. Staber, I. Simonitsch-Klupp, M. Artaker, S. Lagger, S. D. Turner, S. Pileri, P. P. Piccaluga, P. Valent, K. Messana, I. Landra, T. Weichhart, S. Knapp, M. Shehata, M. Todaro, V. Sexl, G. Hofler, R. Piva, E. Medico, B. A. Ruggeri, M. Cheng, R. Eferl, G. Egger, J. M. Penninger, U. Jaeger, R. Moriggl, G. Inghirami and L. Kenner (2012). "PDGFR blockade is a rational and effective therapy for NPM-ALK-driven lymphomas." Nat Med **18**(11): 1699-1704.

Lanzkron, S. M., M. I. Collector and S. J. Sharkis (1999). "Hematopoietic stem cell tracking in vivo: a comparison of short-term and long-term repopulating cells." Blood **93**(6): 1916-1921.

Lanzkron, S. M., M. I. Collector and S. J. Sharkis (1999). "Homing of Long-Term and Short-Term Engrafting Cells In Vivoa." Annals of the New York Academy of Sciences **872**(1): 48-56.

Lee, E. Y., H. Cam, U. Ziebold, J. B. Rayman, J. A. Lees and B. D. Dynlacht (2002). "E2F4 loss suppresses tumorigenesis in< i> Rb</i> mutant mice." Cancer cell **2**(6): 463-472.

Lee, H., J. Deng, M. Kujawski, C. Yang, Y. Liu, A. Herrmann, M. Kortylewski, D. Horne, G. Somlo and S. Forman (2010). "STAT3-induced S1PR1 expression is crucial for persistent STAT3 activation in tumors." Nature medicine **16**(12): 1421-1428.

Levine, A. J. and A. M. Puzio-Kuter (2010). "The Control of the Metabolic Switch in Cancers by Oncogenes and Tumor Suppressor Genes." Science **330**(6009): 1340-1344.

Lv, X. B., X. Zhang, L. Deng, L. Jiang, W. Meng, Z. Lu and X. Wang (2014). "MiR-92a mediates AZD6244 induced apoptosis and G1-phase arrest of lymphoma cells by targeting Bim." Cell Biol Int **38**(4): 435-443.

Malumbres, M. and M. Barbacid (2005). "Mammalian cyclin-dependent kinases." Trends in biochemical sciences **30**(11): 630-641.

Mangioni, C., R. Fruscio, M. Signorelli, M. Broggini and G. Damia (2012). "Ovarian carcinoma tumor-initiating cells have a mesenchymal phenotype." Cell Cycle **11**(10): 1966-1976.

Manna, S. K., C. Gangadharan, D. Edupalli, N. Raviprakash, T. Navneetha, S. Mahali and M. Thoh (2012). "Ras puts the brake on doxorubicin-mediated cell death in p53-expressing cells." Journal of Biological Chemistry **287**(15): 12157-12157.

Martin, P., A. Chadburn, P. Christos, R. Furman, J. Ruan, M. A. Joyce, E. Fusco, P. Glynn, R. Elstrom, R. Niesvizky, E. J. Feldman, T. B. Shore, M. W. Schuster, S. Ely, D. M. Knowles, S. Chen-Kiang, M. Coleman and J. P. Leonard (2008). "Intensive treatment strategies may not provide superior outcomes in mantle cell lymphoma: overall survival exceeding 7 years with standard therapies." Ann Oncol **19**(7): 1327-1330.

Massagué, J. (2004). "G1 cell-cycle control and cancer." Nature **432**(7015): 298-306.

Matsui, W., C. A. Huff, Q. Wang, M. T. Malehorn, J. Barber, Y. Tanhehco, B. D. Smith, C. I. Civin and R. J. Jones (2004). "Characterization of clonogenic multiple myeloma cells." Blood **103**(6): 2332-2336.

McManus, S., A. Ebert, G. Salvagiotto, J. Medvedovic, Q. Sun, I. Tamir, M. Jaritz, H. Tagoh and M. Busslinger (2011). "The transcription factor Pax5 regulates its target genes by recruiting chromatin-modifying proteins in committed B cells." Embo j **30**(12): 2388-2404.

Migliardi, G., F. Sassi, D. Torti, F. Galimi, E. R. Zanella, M. Buscarino, D. Ribero, A. Muratore, P. Massucco, A. Pisacane, M. Risio, L. Capussotti, S. Marsoni, F. Di Nicolantonio, A. Bardelli, P. M. Comoglio, L. Trusolino and A. Bertotti (2012). "Inhibition of MEK and PI3K/mTOR suppresses tumor growth but does not cause tumor regression in patient-derived xenografts of RAS-mutant colorectal carcinomas." Clin Cancer Res **18**(9): 2515-2525.

Mikkola, I., B. Heavey, M. Horcher and M. Busslinger (2002). "Reversion of B cell commitment upon loss of Pax5 expression." Science **297**(5578): 110-113.

Molineaux, S. M. (2012). "Molecular pathways: targeting proteasomal protein degradation in cancer." Clin Cancer Res **18**(1): 15-20.

Molinsky, J., M. Klanova, B. Maswabi, T. Soukup, M. Trneny, E. Necas, J. Zivny and P. Klener (2013). "In vivo growth of mantle cell lymphoma xenografts in immunodeficient mice is positively regulated by VEGF and associated with significant up-regulation of CD31/PECAM1." Folia Biol (Praha) **59**(1): 26-31.

Morrison, A. M., U. Jager, A. Chott, M. Schebesta, O. A. Haas and M. Busslinger (1998). "Deregulated PAX-5 transcription from a translocated IgH promoter in marginal zone lymphoma." Blood **92**(10): 3865-3878.

Mozos, A., C. Royo, E. Hartmann, D. De Jong, C. Baró, A. Valera, K. Fu, D. D. Weisenburger, J. Delabie, S.-S. Chuang, E. S. Jaffe, C. Ruiz-Marcellan, S. Dave, L. Rimsza, R. Braziel, R. D. Gascoyne, F. Solé, A. López-Guillermo, D. Colomer, L. M. Staudt, A. Rosenwald, G. Ott, P. Jares and E. Campo (2009). SOX11 expression is highly specific for mantle cell lymphoma and identifies the cyclin D1-negative subtype.

Mullighan, C. G., S. Goorha, I. Radtke, C. B. Miller, E. Coustan-Smith, J. D. Dalton, K. Girtman, S. Mathew, J. Ma and S. B. Pounds (2007). "Genome-wide analysis of genetic alterations in acute lymphoblastic leukaemia." Nature **446**(7137): 758-764.

Mullighan, C. G., S. Goorha, I. Radtke, C. B. Miller, E. Coustan-Smith, J. D. Dalton, K. Girtman, S. Mathew, J. Ma, S. B. Pounds, X. Su, C. H. Pui, M. V. Relling, W. E. Evans, S. A. Shurtleff and J. R. Downing (2007). "Genome-wide analysis of genetic alterations in acute lymphoblastic leukaemia." Nature **446**(7137): 758-764.

Nebral, K., D. Denk, A. Attarbaschi, M. Konig, G. Mann, O. A. Haas and S. Strehl (2008). "Incidence and diversity of PAX5 fusion genes in childhood acute lymphoblastic leukemia." Leukemia **23**(1): 134-143.

Nera, K. P., P. Kohonen, E. Narvi, A. Peippo, L. Mustonen, P. Terho, K. Koskela, J. M. Buerstedde and O. Lassila (2006). "Loss of Pax5 promotes plasma cell differentiation." Immunity **24**(3): 283-293.

Nishimura, H., T. Akiyama, Y. Monobe, K. Matsubara, Y. Igarashi, M. Abe, T. Sugihara and Y. Sadahira (2010). "Expression of sphingosine-1-phosphate receptor 1 in mantle cell lymphoma." Modern Pathology **23**(3): 439-449.

Nodit, L., D. W. Bahler, S. A. Jacobs, J. Locker and S. H. Swerdlow (2003). "Indolent mantle cell lymphoma with nodal involvement and mutated immunoglobulin heavy chain genes." Hum Pathol **34**(10): 1030-1034.

Nutt, S. L., B. Heavey, A. G. Rolink and M. Busslinger (1999). "Commitment to the B-lymphoid lineage depends on the transcription factor Pax5." Nature **401**(6753): 556-562.

O'Connor, O. A., C. Moskowitz, C. Portlock, P. Hamlin, D. Straus, O. Dumitrescu, D. Sarasohn, M. Gonen, J. Butos, E. Neylon, R. Hamelers, B. Mac-Gregor Cortelli, S. Blumel, A. D. Zelenetz, L. Gordon, J. J. Wright, J. Vose, B. Cooper and J. Winter (2009). "Patients with chemotherapy-refractory mantle cell lymphoma experience high response rates and identical progression-free survivals compared with patients with relapsed disease following treatment with single agent bortezomib: results of a multicentre Phase 2 clinical trial." Br J Haematol **145**(1): 34-39.

Orchard, J., R. Garand, Z. Davis, G. Babbage, S. Sahota, E. Matutes, D. Catovsky, P. W. Thomas, H. Avet-Loiseau and D. Oscier (2003). "A subset of t(11;14) lymphoma with mantle cell features displays mutated IgVH genes and includes patients with good prognosis, nonnodal disease." Blood **101**(12): 4975-4981.

Ott, G., J. Kalla, A. Hanke, J. G. Muller, A. Rosenwald, T. Katzenberger, R. Kretschmar, H. Kreipe and H. K. Muller-Hermelink (1998). "The cytomorphological

spectrum of mantle cell lymphoma is reflected by distinct biological features." Leuk Lymphoma **32**(1-2): 55-63.

Palmisano, W. A., K. P. Crume, M. J. Grimes, S. A. Winters, M. Toyota, M. Esteller, N. Joste, S. B. Baylin and S. A. Belinsky (2003). "Aberrant Promoter Methylation of the Transcription Factor Genes PAX5 α and β in Human Cancers." Cancer Research **63**(15): 4620-4625.

Pals, S. T., D. J. de Gorter and M. Spaargaren (2007). "Lymphoma dissemination: the other face of lymphocyte homing." Blood **110**(9): 3102-3111.

Parish, C. R. (1999). "Fluorescent dyes for lymphocyte migration and proliferation studies." Immunology and cell biology **77**(6): 499-508.

Pece, S., D. Tosoni, S. Confalonieri, G. Mazzarol, M. Vecchi, S. Ronzoni, L. Bernard, G. Viale, P. G. Pelicci and P. P. Di Fiore (2010). "Biological and molecular heterogeneity of breast cancers correlates with their cancer stem cell content." Cell **140**(1): 62-73.

Perez-Galan, P., M. Dreyling and A. Wiestner (2011). "Mantle cell lymphoma: biology, pathogenesis, and the molecular basis of treatment in the genomic era." Blood **117**(1): 26-38.

Pérez-Galán, P., H. Mora-Jensen, M. A. Weniger, A. L. Shaffer, E. G. Rizzatti, C. M. Chapman, C. C. Mo, L. S. Stennett, C. Rader and P. Liu (2011). "Bortezomib resistance in mantle cell lymphoma is associated with plasmacytic differentiation." Blood **117**(2): 542-552.

Perez-Galan, P., G. Roue, N. Villamor, E. Montserrat, E. Campo and D. Colomer (2006). "The proteasome inhibitor bortezomib induces apoptosis in mantle-cell lymphoma through generation of ROS and Noxa activation independent of p53 status." Blood **107**(1): 257-264.

Pinyol, M., L. Hernandez, M. Cazorla, M. Balbin, P. Jares, P. L. Fernandez, E. Montserrat, A. Cardesa, C. Lopez-Otin and E. Campo (1997). "Deletions and loss of expression of p16INK4a and p21Waf1 genes are associated with aggressive variants of mantle cell lymphomas." Blood **89**(1): 272-280.

Pott, C., C. Schrader, M. Bruggemann, M. Ritgen, L. Harder, T. Raff, M. Tiemann, P. Dreger and M. Kneba (2005). "Blastoid variant of mantle cell lymphoma: late progression from classical mantle cell lymphoma and quantitation of minimal residual disease." Eur J Haematol **74**(4): 353-358.

Pridans, C., M. L. Holmes, M. Polli, J. M. Wettenhall, A. Dakic, L. M. Corcoran, G. K. Smyth and S. L. Nutt (2008). "Identification of Pax5 target genes in early B cell differentiation." The Journal of Immunology **180**(3): 1719-1728.

Psyrri, A., S. Papageorgiou, E. Liakata, A. Scorilas, D. Rontogianni, C. K. Kontos, P. Argyriou, D. Pectasides, N. Harhalakis and V. Pappa (2009). "Phosphatidylinositol 3′-kinase catalytic subunit α gene amplification contributes to the pathogenesis of mantle cell lymphoma." Clinical Cancer Research **15**(18): 5724-5732.

Puthier, D., R. Bataille and M. Amiot (1999). "IL-6 up-regulates Mcl-1 in human myeloma cells through JAK/STAT rather than Ras/MAP kinase pathway." European journal of immunology **29**(12): 3945-3950.

Revilla, I. D. R., I. Bilic, B. Vilagos, H. Tagoh, A. Ebert, I. M. Tamir, L. Smeenk, J. Trupke, A. Sommer, M. Jaritz and M. Busslinger (2012). "The B-cell identity factor Pax5 regulates distinct transcriptional programmes in early and late B lymphopoiesis." Embo j **31**(14): 3130-3146.

Rizzatti, E. G., R. P. Falcao, R. A. Panepucci, R. Proto-Siqueira, W. T. Anselmo-Lima, O. K. Okamoto and M. A. Zago (2005). "Gene expression profiling of mantle cell lymphoma cells reveals aberrant expression of genes from the PI3K-AKT, WNT and TGFbeta signalling pathways." Br J Haematol **130**(4): 516-526.

Rosenwald, A., G. Wright, A. Wiestner, W. C. Chan, J. M. Connors, E. Campo, R. D. Gascoyne, T. M. Grogan, H. K. Muller-Hermelink, E. B. Smeland, M. Chiorazzi, J. M. Giltnane, E. M. Hurt, H. Zhao, L. Averett, S. Henrickson, L. Yang, J. Powell, W. H. Wilson, E. S. Jaffe, R. Simon, R. D. Klausner, E. Montserrat, F. Bosch, T. C. Greiner, D. D. Weisenburger, W. G. Sanger, B. J. Dave, J. C. Lynch, J. Vose, J. O. Armitage, R. I. Fisher, T. P. Miller, M. LeBlanc, G. Ott, S. Kvaloy, H. Holte, J. Delabie and L. M. Staudt (2003). "The proliferation gene expression signature is a quantitative integrator of oncogenic events that predicts survival in mantle cell lymphoma." Cancer Cell **3**(2): 185-197.

Rudelius, M., S. Pittaluga, S. Nishizuka, T. H. T. Pham, F. Fend, E. S. Jaffe, L. Quintanilla-Martinez and M. Raffeld (2006). "Constitutive activation of Akt contributes to the pathogenesis and survival of mantle cell lymphoma." Blood **108**(5): 1668-1676.

Salaverria, I., P. Perez-Galan, D. Colomer and E. Campo (2006). "Mantle cell lymphoma: from pathology and molecular pathogenesis to new therapeutic perspectives." Haematologica **91**(1): 11-16.

Salaverria, I., P. Perez-Galan, D. Colomer and E. Campo (2006). "Mantle cell lymphoma: from pathology and molecular pathogenesis to new therapeutic perspectives." haematologica **91**(1): 11-16.

Sant, M., C. Allemani, C. Tereanu, R. De Angelis, R. Capocaccia, O. Visser, R. Marcos-Gragera, M. Maynadie, A. Simonetti, J. M. Lutz and F. Berrino (2010). "Incidence of hematologic malignancies in Europe by morphologic subtype: results of the HAEMACARE project." Blood **116**(19): 3724-3734.

Schaniel, C., L. Bruno, F. Melchers and A. G. Rolink (2002). "Multiple hematopoietic cell lineages develop in vivo from transplanted Pax5-deficient pre-B I-cell clones." Blood **99**(2): 472-478.

Seam, P., M. E. Juweid and B. D. Cheson (2007). "The role of FDG-PET scans in patients with lymphoma." Blood **110**(10): 3507-3516.

Shapiro-Shelef, M. and K. Calame (2004). "Plasma cell differentiation and multiple myeloma." Current opinion in immunology **16**(2): 226-234.

Smedby, K. E. and H. Hjalgrim (2011). "Epidemiology and etiology of mantle cell lymphoma and other non-Hodgkin lymphoma subtypes." Semin Cancer Biol **21**(5): 293-298.

Smith, M. R. (2011). "Should there be a standard therapy for mantle cell lymphoma?" Future Oncol **7**(2): 227-237.

Suh, K. S. and A. Goy (2008). "Bortezomib in mantle cell lymphoma."

Tavaluc, R. T., L. S. Hart, D. T. Dicker and W. S. El-Deiry (2007). "Effects of low confluency, serum starvation and hypoxia on the side population of cancer cell lines." Cell Cycle **6**(20): 2554-2562.

Tiemann, M., C. Schrader, W. Klapper, M. H. Dreyling, E. Campo, A. Norton, F. Berger, P. Kluin, G. Ott, S. Pileri, E. Pedrinis, A. C. Feller, H. Merz, D. Janssen, M. L. Hansmann, H. Krieken, P. Moller, H. Stein, M. Unterhalt, W. Hiddemann and R. Parwaresch (2005). "Histopathology, cell proliferation indices and clinical outcome in 304 patients with mantle cell lymphoma (MCL): a clinicopathological study from the European MCL Network." Br J Haematol **131**(1): 29-38.

Tomayko, M. M. and C. P. Reynolds (1989). "Determination of subcutaneous tumor size in athymic (nude) mice." Cancer Chemother Pharmacol **24**(3): 148-154.

Vater, I., F. Wagner, M. Kreuz, H. Berger, J. I. Martin-Subero, C. Pott, J. A. Martinez-Climent, W. Klapper, K. Krause, M. J. Dyer, S. Gesk, L. Harder, A. Zamo, M. Dreyling, D. Hasenclever, N. Arnold and R. Siebert (2009). "GeneChip analyses point to novel pathogenetic mechanisms in mantle cell lymphoma." Br J Haematol **144**(3): 317-331.

Vose, J. M. (2012). "Mantle cell lymphoma: 2012 update on diagnosis, risk-stratification, and clinical management." Am J Hematol **87**(6): 604-609.

Wang, M., Ç. Atayar, S. Rosati, A. Bosga-Bouwer, P. Kluin and L. Visser (2009). "JNK is constitutively active in mantle cell lymphoma: cell cycle deregulation and polyploidy by JNK inhibitor SP600125." The Journal of pathology **218**(1): 95-103.

Wang, M., L. Zhang, X. Han, J. Yang, J. Qian, S. Hong, P. Lin, Y. Shi, J. Romaguera, L. W. Kwak and Q. Yi (2008). "A severe combined immunodeficient-hu in vivo mouse model of human primary mantle cell lymphoma." Clin Cancer Res **14**(7): 2154-2160.

Wang, M. L., S. Rule, P. Martin, A. Goy, R. Auer, B. S. Kahl, W. Jurczak, R. H. Advani, J. E. Romaguera, M. E. Williams, J. C. Barrientos, E. Chmielowska, J. Radford, S. Stilgenbauer, M. Dreyling, W. W. Jedrzejczak, P. Johnson, S. E. Spurgeon, L. Li, L. Zhang, K. Newberry, Z. Ou, N. Cheng, B. Fang, J. McGreivy, F. Clow, J. J. Buggy, B. Y. Chang, D. M. Beaupre, L. A. Kunkel and K. A. Blum (2013). "Targeting BTK with Ibrutinib in Relapsed or Refractory Mantle-Cell Lymphoma." New England Journal of Medicine **369**(6): 507-516.

Wang, Y., A. H. van Boxel-Dezaire, H. Cheon, J. Yang and G. R. Stark (2013). "STAT3 activation in response to IL-6 is prolonged by the binding of IL-6 receptor to EGF receptor." Proc Natl Acad Sci U S A **110**(42): 16975-16980.

Weisenburger, D. D. and J. O. Armitage (1996). "Mantle cell lymphoma-- an entity comes of age." Blood **87**(11): 4483-4494.

Wu, E., N. Palmer, Z. Tian, A. P. Moseman, M. Galdzicki, X. Wang, B. Berger, H. Zhang and I. S. Kohane (2008). "Comprehensive dissection of PDGF-PDGFR signaling pathways in PDGFR genetically defined cells." PLoS One **3**(11): e3794.

Xue, Z., H. Yan, J. Li, S. Liang, X. Cai, X. Chen, Q. Wu, L. Gao, K. Wu and Y. Nie (2012). "Identification of cancer stem cells in vincristine preconditioned SGC7901 gastric cancer cell line." Journal of cellular biochemistry **113**(1): 302-312.

Young, R. M. and L. M. Staudt (2014). "Ibrutinib treatment of CLL: the cancer fights back." Cancer Cell **26**(1): 11-13.

Zhang, L., J. Yang, J. Qian, H. Li, J. E. Romaguera, L. W. Kwak, M. Wang and Q. Yi (2012). "Role of the microenvironment in mantle cell lymphoma: IL-6 is an important survival factor for the tumor cells." Blood **120**(18): 3783-3792.

Zhou, Y., H. Wang, W. Fang, J. E. Romaguer, Y. Zhang, K. B. Delasalle, L. Kwak, Q. Yi, X. L. Du and M. Wang (2008). "Incidence trends of mantle cell lymphoma in the United States between 1992 and 2004." Cancer **113**(4): 791-798.

Zushi, S., Y. Shinomura, T. Kiyohara, Y. Miyazaki, S. Kondo, M. Sugimachi, Y. Higashimoto, S. Kanayama and Y. Matsuzawa (1998). "STAT3 mediates the survival signal in oncogenic ras-transfected intestinal epithelial cells." International journal of cancer **78**(3): 326-330.

VITA

Albert Eng Keong Teo was born in Penang, Malaysia on July 1st, 1987, the son of Beng Im Ch'ng and Christopher Kheng Hoe Teo. After completing his work at Penang Free School, Penang, Malaysia in 2004, he entered Winona State University in Winona, Minnesota. He received the degree of Bachelor of Science with a major in molecular and cellular biology from Winona State in May, 2008. In August of 2008 he entered The University of Texas Graduate School of Biomedical Sciences at Houston.